

Characterizing the Molecular Signaling Pathways in the  
Cerebral Arteries of Stroke-Prone Spontaneously Hypertensive  
Rats (SHRsp) Before and After Stroke

---

© Killol Chokshi

A thesis submitted to the School of Graduate Studies in partial fulfillment of the requirements for  
the degree of Master of Science, Pharmacy

School of Pharmacy

Memorial University of Newfoundland

St. John's, NL

October 2018

## Abstract

**Background:** Hemorrhagic stroke (HS) is associated with loss of middle cerebral artery (MCA) autoregulation in the stroke-prone spontaneously hypertensive rat (SHRsp). We believe the MCA dysfunction may be due to increased inflammatory signalling (p38MAPK and ERK) and decreased contractile signalling (MLC and PKC) in the MCA during stroke, altered calcium (TRPV4) channel expression, accompanied with increased neuro-inflammation (astrocyte and microglia) and neuronal damage in brain after stroke. **Methods:** SHRsp were fed a high salt (4%NaCl) diet and sacrificed at nine weeks of age for pre-stroke and after evidence of stroke (~15 weeks) for post-stroke samples. The MCAs were isolated to measure protein levels and expression using immunofluorescence (IF), and western blot (WB) for inflammatory and contractile proteins. Tissues were analyzed for activation of neuro-inflammation, neuronal damage, for total and activated inflammatory proteins (ERK1/2 and p38MAPK), cerebrovascular contraction (PKC and MLC), and changes involved in transient receptor potential V4 (TRPV4) activation. **Results:** Results from both WB and IF indicate an increase in activated inflammatory proteins post-stroke, with an associated decrease in expression of activated contractile proteins and TRPV4 channel compared to pre-stroke SHRsp. The post-stroke samples also show significant increase in neuro-inflammation and neuronal damage compared to pre-stroke samples. **Conclusion:** The results show an increase in ratio of activated/total (p38 MAPK and ERK1/2) accompanied with a decrease in activated/total PKC and TRPV4 channel expression in post-stroke which may relate to a decrease in vessel structural integrity and alter vascular tone in the MCAs effecting its ability to contract in response to pressure. Significant neuro-inflammation and neuronal damage in the brain tissue surrounding the MCA in post-stroke samples confirm MCA dysfunction accompanies brain damage during stroke.

## **Acknowledgements**

I would like to thank almighty for blessing me with this opportunity, and providing me with the courage and support which kept me going throughout my masters.

I would like to thank my mother, whose steadfast dedication towards seeing me succeed at each and every step of life, keeps me strong and motivated. It was because of her powerful and unequivocal support I took on the challenge of pursuing as well as completing my MSc despite of facing numerous challenges throughout. She was so patient and loving that she heard my rants daily, but comforted and encouraged me to keep on going. I would like to dedicate my thesis and accomplishments to her, who unfortunately passed away before I could fulfill her wish of seeing me graduate with MSc. But today and forever, I dedicate everything to you for giving me everything you had!

Many thanks to my dad for being the financial backbone so I could focus my entire concentration on the lab work instead of looking for work, and also for understanding why many things in my MSc took a lot of time. I would also like to thank my brother, who always encouraged me and provided me with practical advice, which is what I needed the most throughout my MSc. Thanks to my sister in law who took the position of handling the trickiest situation and guiding me whenever required.

Special thanks to my best friend and my loving wife Shweta, for being rock solid throughout past many years and supporting me through thick and thin. The constant motivation and charismatic talk always pushed me back on track. A huge thanks to my buddies Divyesh, Jay, Jaimin and Ovesh for providing a phenomenal support throughout.

I owe a very special thank you to my supervisor, Dr. Noriko Daneshtalab, who taught me skills that could have only be learnt through her guidance and experience only. I have honed my organizational, thinking, logical flow and methodological skills under her supervision which have proved to be immensely helpful. I am deeply grateful to her for providing me with a chance to fulfill my mom's wish (pursuing grad school), granting me a long leave during normal academic session to spend last few months with mom (which I will cherish lifetime) and for providing me with part time research assistant work opportunity when I was completing my thesis.

I would also like extend my gratitude to Dr. Jules Doré for teaching me western blot from scratch and guiding me throughout my masters. A warm thanks to him for always answering my one minute queries which always turned in to hour long discussions. Thank you for helping me troubleshoot protocols, and providing numerous lab supplies throughout my masters. His practical and wittiest way of dealing with issues in and out of the lab have taught me a lot. Special thanks to Dr. John Weber for his timely guidance and advice throughout my masters.

Special thanks to Dr. Smeda for always explaining me complex systems in a simplified way and comforting me during hard times. Many thanks to my lab mates, Marwan, Hilary, Kayla, Bruna, Brittany, Amy and Mercy. It has been pleasure working with the team and their help has helped me a lot. I would also like to thank Karen Mearow, Karen Stapelton, Iliana Dimitrov, Animal care staff and histology staff for always helping. Special thanks to everyone who played a part in my masters. ☺

## Table of Contents

Abstract	i
Acknowledgements	ii
Table of Contents	iv
List of Figures	vii
List of Tables	viii
List of abbreviations and symbols	ix
Chapter One: Introduction	1
1.1. Stroke: Definition and Prevalence	1
1.2. Risk Factors for hemorrhagic stroke	2
1.2.1. General Hypertension	4
1.2.2. Hypertension in hemorrhagic stroke	5
1.3. Pathophysiology of hemorrhagic stroke	7
1.4. Cerebral Autoregulation	8
1.5. Smooth muscle cells and endothelium in regulating vascular tone	10
1.5.1. Role of MLC in vascular contraction	12
1.5.2. Role of PKC in vascular contraction	15
1.5.3. TRP Channels (calcium channel) in vasculature	17
1.6. Vascular “endothelial” dysfunction	21
1.6.1. Role of ROS in vascular dysfunction	22
1.7. Inflammation in vascular dysfunction	23

1.7.1. Role of MAPK and ERK in vascular dysfunction	24
1.8. Neuro-inflammation	28
1.8.1. Microglia in Neuro-inflammation	28
1.8.2. Astrocytes in neuro-inflammation	30
1.9. Neuronal damage	31
1.10. Animal models of hemorrhagic stroke	32
1.10.1. Animal models with artificially induced stroke	32
1.10.2. Animal models for spontaneously occurring stroke (SHRsp)	33
1.11. Objectives and Hypothesis	35
Chapter Two - Materials and Methods	37
2.1. Animals	37
2.2. General Experimental Design	37
2.3. Sample isolation and tissue processing	39
2.4. Immunofluorescence	39
2.4.1. Sectioning and standard process of immune-fluorescence	439
2.4.2. Quantification of immunofluorescent images	43
2.5. Neurological degeneration	45
2.5.1. Sampling and processing of H and E Stain	45
2.5.2. Quantification of the neural damage	45
2.6. Western blot	48
2.6.1. Sample Lysis and Aliquot preparation	48
2.6.2. BCA Protein Assay	48
2.6.3. SDS-PAGE and immunoblotting	54

2.6.4. Quantification of bands	56
2.7. Statistical Analysis	56
Chapter Three – Results	57
3.1. Detection of phosphorylated and total MLC in MCA by immunofluorescence	57
3.2. Detection of phosphorylated and total MLC in MCA by western blot	60
3.3. Detection of phosphorylated and total PKC in MCA by immunofluorescence	61
3.4. Detection of phosphorylated and total PKC in MCA by western blot	64
3.5. TRPV4 Expression in MCA by immunofluorescence	66
3.6. Analysis of phosphorylated and total P38MAPK by immunofluorescence	68
3.7. Analysis of phosphorylated and total P38MAPK by western blot	71
3.8. Analysis of phosphorylated and total ERK1 and 2 by immunofluorescence	73
3.9. Analysis of phosphorylated and total ERK1 and 2 by western blot	76
3.10. Neuro-inflammation: Astrocyte and Microglia Analysis by immunofluorescence	78
3.11. Neural damage: H and E Stain	80
Chapter Four – Discussion	84
4.1. Limitations and future directions	97
4.2. Conclusion	99
References	100

## List of Figures

<b>Figure 1.1:</b> Schematic diagram of signal transduction pathway of MLC for SMC contraction and relaxation.	14
<b>Figure 1.2:</b> Schematic diagram for the TRPV4 mediated vasodilation.	20
<b>Figure 1.3:</b> Schematic diagram of two main MAP Kinases: ERK and p38 MAPK.	27
<b>Figure 2.1:</b> Experimental Timeline for sampling of pre-stroke and post-stroke samples when SHRsp rats are on High Salt Diet.	38
<b>Figure 2.2:</b> Representation of the semi-quantification process for measuring immunofluorescent staining of protein of interest in the MCA by Image J.	44
<b>Figure 3.1:</b> Representative images for phosphorylated MLC Staining.	58
<b>Figure 3.2:</b> Representative images for Total MLC Staining.	59
<b>Figure 3.3:</b> Representative images for Phosphorylated PKC Staining.	62
<b>Figure 3.4:</b> Representative images for Total PKC Staining.	63
<b>Figure 3.5:</b> Representative image for Phosphorylated and Total PKC bands.	65
<b>Figure 3.6:</b> Representative images for TRPV4 Staining.	67
<b>Figure 3.7:</b> Representative images for Phosphorylated P38 MAPK Staining.	69
<b>Figure 3.8:</b> Representative images for Total P38 MAPK Staining.	70
<b>Figure 3.9:</b> Representative image for Phosphorylated and Total P38MAPK bands.	72
<b>Figure 3.10:</b> Representative images for Phosphorylated ERK1/2 Staining.	74
<b>Figure 3.11:</b> Representative images for Total ERK1/2 Staining.	75
<b>Figure 3.12:</b> Representative image for Phosphorylated and Total ERK1/2 bands.	77
<b>Figure 3.13:</b> Representative images for Astrocytes and Microglia staining.	79
<b>Figure 3.14:</b> Representative images of H and E stains of brain slices.	81
<b>Figure 3.15:</b> Total Neural Damage Scoring by H and E staining of brains.	83

## List of Tables

<b>Table 2.1.:</b> Specific details for the blocking solution, antibodies and reagents used in protocols for immunofluorescence.	41
<b>Table 2.2.:</b> Scoring system for four semi-quantifiable parameters (Cell vacuolation, degenerating neurons, area of cell oedema and area of cell infiltration)	47
<b>Table 2.3.:</b> List of solutions used in western blot and immunofluorescence	49
<b>Table 2.4.:</b> Specific details for the blocking solution, antibodies and reagents used in protocols for western blot.	55

### List of abbreviations and symbols

<b>A</b>		<b>G</b>	
ACE	Angiotensin-Converting Enzyme	GAPDH	Glyceraldehyde 3-phosphate dehydrogenase
ADMA	Asymmetric dimethylarginine	GFAP	Glial fibrillary acidic protein
AVM	Arteriovenous Malformations	GMP	Guanosine Monophosphate
<b>B</b>		GPCR	G-Protein coupled receptors
BBB	Blood Brain Barrier	<b>H</b>	
BCA	Bicinchoninic acid	HBCEs	Human Brain Capillary Endothelial Cells
BDNF	Brain derived neurotrophic factor	HRP	Horseradish Peroxidase
BP	Blood Pressure	<b>I</b>	
BSA	Bovine Serum Albumin	Iba1	Ionized calcium binding adaptor molecule 1
<b>C</b>		ICAM-1	Intracellular Adhesion Molecule-1
CAM	Calmodulin	ICH	Intracerebral Hemorrhage
COX-2	Cyclooxygenase-2	iNOS	inducible nitric oxide synthase
CNS	Central Nervous System	IP3	Inositol 1,4,5-triphosphate
CRP	C-reactive protein	<b>M</b>	
<b>D</b>		MAPK	Mitogen Activated Protein Kinase
DAG	Diacylglycerol	MBS	Myosin binding site
DAMPS	Danger associated molecular patterns	MCA	Middle Cerebral Artery
DAPI	4',6-diamidino-2-phenylindole	MGV	Mean Gray Value
<b>E</b>		MLC	Myosin Light Chain
ECM	Extracellular Matrix	MLCK	Myosin Light Chain Kinase
EDHF	Endothelium Derived Hyperpolarizing Factors	MLCP	Myosin Light Chain Phosphatase
EET	Epoxyeicosatrienoic acid	MMP	Matrix metalloproteinases
ERK	Extracellular signal regulated kinase		

<b>N</b>		RPM	Revolutions per Minute
NBF	Neutral Buffered Formalin	RT	Room Temperature
NGS	Normal Goat Serum	<b>S</b>	
NO	Nitric Oxide	SDS	Sodium Dodecyl Sulfate
<b>P</b>		SHR	Spontaneously Hypertensive Rats
PAI-1	Plasminogen activator inhibitor-1	SHRsp	stroke-prone Spontaneous Hypertensive Rats
PAGE	Polyacrylamide Gel	SOD	Superoxide Dismutase
PAMPS	Pathogens associated molecular patterns	SMC	Smooth Muscle Cells
PAR	Protease-activated receptor	<b>T</b>	
PBS	Phosphate Buffered Saline	TBS	Tris-buffered saline
PDC	Pressure Dependent Constriction	TBST	Tris-buffered Saline and Tween 20
PLC	Phospholipase C	TNFR	tumour necrosis factor receptor
<b>R</b>		TRP	Transient Receptor Potential
RAS	Renin-Angiotensin System	TRPV4	Transient Receptor Potential Cation Channel, Subfamily Vanilloid, member 4
RIPA	Radioimmunoprecipitation assay	<b>V</b>	
ROCK	Rho-associated kinase	VCAM-1	Vascular cell adhesion molecule-1
ROS	Reactive Oxygen Species	VSMC	Vascular Smooth Muscle Cells

## **1. Introduction**

### ***1.1. Stroke: Definition and Prevalence***

Stroke is one of the major cardiovascular diseases and a leading cause of functional impairment (partial paralysis, lapse in motor-coordination and instability) in North America (1,2). Approximately 795, 000 people in the United States have a stroke each year, out of which 610, 000 experience their first attack and 185, 000 are recurrent stroke events, resulting in 6.8 million stroke survivors above 19 years of age (2,3). For patients who are above 65 years of age, 26% become dependent on others for their daily activities and 46% have cognitive deficits six months after stroke (2,3).

Stroke is classically defined as a neurological deficit attributed to focal injury of the central nervous system (CNS) by a vascular cause; which mostly includes intracerebral hemorrhage (ICH), cerebral infarction and subarachnoid hemorrhage (SAH) (4). Stroke can be broadly classified as being ischemic or hemorrhagic. Ischemic stroke or cerebral infarcts are the result of development of emboli and/or thrombi leading to vessel blockages, resulting in deficiency of oxygen and nutrients in vital brain tissues (5). On other hand hemorrhagic stroke occurs mainly due to rupture of cerebral vessels, often as a result of high blood pressure exerting excessive pressure on the arterial walls already damaged by aneurysm, atherosclerosis or arteriovenous malformations (AVM) (6). The incidence of hemorrhagic stroke is approximately 20% of all strokes, however it is associated with having a high mortality and morbidity in adults (7), with the five year mortality rate being around 50% in patients older than 45 years (8).

Intracerebral hemorrhage (ICH), a type of hemorrhagic stroke, encompasses 10% to 15% of all strokes (9). Epidemiologically, there is no definitive age at which one suffers ICH, but a trend towards growing incidence of ICH at younger age has been seen globally, which is a great cause of

concern (10). The only treatment option available for ICH is surgery, with long term hospitalization and rehabilitation being required upon surgical interventions as patients often suffer varying degrees of neurological dysfunction (11). Many factors play a vital role in contributing to hemorrhagic stroke development which are considered significant risk factors.

### ***1.2. Risk factors for hemorrhagic stroke***

In a major systematic review of cohort and case-control studies, the “REGARDS” study, the risk factors for ICH in African-American and Caucasian people in the United States was investigated. Out of many potential risk factors; age, male sex, high alcohol intake and hypertension were identified to be the most significant (12). “INTERSTROKE” Study, another major international case-control study performed in 22 countries highlighted the same major risk factors, accounting for around 80% of all risk factors for stroke (13). The study also included smoking, waist-to-hip ratio and diet as modifiable risk factors for hemorrhagic stroke (13). Interestingly, age was one of the main non-modifiable risk factors for ICH, with race also playing a significant factor in the development of hemorrhagic stroke.

The “REGARDS” study indicated the risk of stroke increases five fold after the age of 45 in African-American and declines slightly around the age of 65-75 (12). Broderick and colleagues, who also studied the risk of ICH in various populations indicated ICH risk in African-Americans was 1.8 times higher than Caucasians in the age group of 55-74 years (14). However after the age of 75 years, the risk of stroke in African-Americans was decreased to 0.23 times that of Caucasians. The reason for this extreme change in ratio is believed to be due to the early occurrence of ICH in most African-Americans at risk, leaving those who survive into their 70s and 80s at lower risk ((14)). Age-related increase in ICH risk was attributed to many internal changes occurring in the

body as we age: the stiffening of the vessels (15), the slowing down of the repairing process and the weakening of the immune system (16), which diminish the ability of the body to tackle any stress. Thus aging provides an environment for structural and functional cerebrovascular changes, leading to increase in ICH. Along with age, another non-modifiable risk factor involved in increasing the risk of ICH is sex.

Males have been associated with nearly three times higher risk of ICH compared to females, particularly when it concerns age-specific stroke occurrence (12). Although age-specific stroke rates are higher in males, due to longer life expectancy females have been shown to have more stroke events, particularly at an old age. This phenomenon might be attributed to the loss of the protective role of estrogen on the healthy functioning of the vessels, which is lost after menopause (17). In females, estrogen affects the vascular functions greatly via increased endothelial nitric oxide (NO) leading to increase in required NO dependent-mechanisms such as regulation of appropriate myogenic tone possibly resulting in normal functioning of the vessels (18). Neuroprotective mechanisms attributed to estrogen and progesterone would be less in men compared to women due to their lower circulating hormone levels (17). Overall, the proper balance of estrogen and progesterone seems to have a beneficial effect and a vital role in delaying the occurrence of stroke until later in life of females compared to males. Interestingly it also appears that the age and sex-related difference in the risk of ICH between males and females can be supplemented to the difference in alcohol intake; Young and middle-aged men have been deemed to be more vulnerable to stroke than women possibly as men are more often heavy drinkers compared to women (19).

Heavy alcohol use has been identified as a risk factor for ICH in case-control studies (20). The criteria of high alcohol intake differed across regions, with the heavy alcohol intake

mainly classified to be 0.5 oz of pure alcohol per day (21). The maintenance of high blood pressure by heavy drinking might promote degeneration of cerebral arterial vasculature, but the effect on aneurysm is unknown (19). Alcohol intoxication accompanied with acute increase in systolic blood pressure and/or alterations in cerebral arterial tone might serve as a mechanism triggering hemorrhagic stroke (19,22). Increased systolic blood pressure (hypertension) on its own is one of the main risk factors for stroke, especially in people aged 45 years or younger (13). Hypertension (raised blood pressure) is the biggest single contributor to many cardiovascular and cerebrovascular diseases (23).

### *1.2.1. General Hypertension*

Hypertension is mainly classified into two: primary (essential) and secondary hypertension. Essential hypertension is defined as elevated blood pressure where secondary causes, such as renal disorder, are ruled out (24). The cause for essential hypertension is not clearly known, but many studies have shown different possible causes, such as high intake of salt leading to hypervolemia (25) and increased sodium retention, causing an increased total peripheral resistance leading to an overall increased cardiac index (cardiac output/body surface area) (26). Other possible causes of essential hypertension may be aging, African descent and low-potassium diet (24).

Alternatively, secondary hypertension commonly has an earlier onset age, no family history and a clear cause such as renal or endocrine disorders (23). In association with kidneys, the renin-angiotensin system (RAS) is a powerful modulator of blood pressure, and its own activation causes hypertension (27). The RAS system includes renin, an enzyme catalyzing the conversion of angiotensinogen to angiotensin (Ang) I, followed by angiotensin-converting enzyme (ACE) cleavage of Ang I to II and activation of AT1 receptors. This receptors are responsible for RAS

biological actions, leading to increased blood pressure (28). Ang II under condition of high salt intake is known to produce renal damage, and Ang II effects are partly mediated by aldosterone, whose secretions is also increased by Ang II (29). Aldosterone has shown to increase renal profibrotic factors and produce renal injury (29). Aldosterone activates the mineralocorticoid receptor in the distal renal tubule of the kidney to increase sodium and water retention, and potassium excretion, leading to an increase in blood volume and thus blood pressure (30). The RAS system in conjunction with aldosterone controls the changes in the systemic blood pressure.

In the past few decades pharmacological blockade of RAS with renin inhibitors, angiotensin receptor blockers, or angiotensin-converting enzyme (ACE) inhibitors have been used to effectively lower blood pressure in a significant proportion of patients with hypertension (31), demonstrating the important role of RAS activation as a cause of human hypertension. Chronic kidney disease has also been linked with hypertension as it leads to impaired volume excretion and increased retention of sodium due to reduced renal function and mass (32). Kidney's impaired capacity to excrete sodium in response to elevated blood pressure is a major contributor to sustained hypertension, irrespective of the initial cause (27). Dysfunctional kidneys, vascular changes and altered cardiac index are known to be associated with the hypertension leading to ICH development (33).

### *1.2.2. Hypertension in Hemorrhagic Stroke*

Hypertensive patients with underlying vascular disease are at higher risk of ICH (34). The extent to which hypertension contributes to ICH is different in males and females, as females are known to have a significant degree of intracerebral bleeding at a lower blood pressure, compared to males (35). This vulnerability of high bleeding in females can be linked to vascular

reactivity and sex hormone dependent functioning mechanism (35). Hypertension is seen in almost half of the elderly population and systemic arterial hypertension is considered to be an age-dependent disorder (15). Increase in blood pressure (BP) trajectories are also closely associated with increased risk of stroke. A study measuring the rise in blood pressure (systolic BP range) over 10 years found pre-hypertensive group (120-140 mm Hg) had significantly higher stroke risk relative to normotensive group (<120mm Hg); after adjusting for possible confounders, the highest risk of ICH and cerebral infarction was seen in individuals in the stage 2 hypertensive group (175-179mm Hg) (36). Hypertension is a systemic phenomenon, often associated with vessel wall thickening and stiffening in the major arteries in the systemic circulation. A strong and significant association between changes in vascular function and wall thickening were seen in the vasculature during hypertension (37). High blood volume in the body due to increased sodium retention and the kidney's impaired capacity may have a direct effect on the vasculature, as isolated human endothelial cells have been shown to stiffen during minor increases in sodium concentration (38). The extent of alterations in vascular functions due to vascular wall thickening is being researched extensively. High risk hypertensive patients have vessels that lose their ability to vasodilate and regulate vascular function (39). The vasculature in the cerebral arterial system is extremely susceptible to high blood pressure and any drastic changes would affect its functioning and prove to be detrimental (40).

Sustained elevation in blood pressure affects the structural integrity of cerebral blood vessels, causing adaptive changes (artery stiffening, changes in pulse wave velocity and resistance to mean flow) targeted at reducing the mechanical stress on the arterial wall and protecting the micro-vessels from the pulsatile stress of cardiac output (41). The cerebral circulation is innervated with neurovascular sensing control mechanism (neurons, astrocyte end-feet processes, etc.) that

assure the blood supply in the brain is proportionate to the energy and metabolic needs of its cellular constituents (42). In pathological conditions like hypertension, neurovascular coupling is disrupted and hence cerebral blood flow is no longer sufficient to maintain the metabolic demands of the brain tissue (42).

### ***1.3. Pathophysiology of hemorrhagic stroke***

In hemorrhagic stroke a ruptured or leaking artery occurs, likely due to the structural changes in the artery, due to high blood pressure (4) as discussed in section 1.2.2. The weakened vessels associated with ICHs are generally categorized as aneurysms, where the weak area of an artery bulges due to high blood pressure until it ruptures and bleeds. Arteriovenous malformations (AVM), another type of weakened cerebral vessel that tends to rupture or leak easily. AVMs are a bundle of dysplastic vessels fed by arteries and drained by veins without intervening capillaries, forming a high-flow, low resistance system between the arterials and venules (43). Once ruptured, the damage increases up to five-fold depending on the location, drainage and association with aneurysm (44). The ruptured vessels disrupt the flow of blood causing insufficient supply of oxygen and nutrients to other vital parts of the brain.

Hemorrhagic stroke can most often develop spontaneously (due to the weakened vessels), but sometimes it can be instigated by different factors such as hypertension, angiopathy, tumours or head trauma. Intracerebral hemorrhage, the most common form of cerebral hemorrhage, is the most fatal and least treatable type of hemorrhagic stroke resulting in long term neurological deficiency and notable brain injury (45). The 30 day mortality for ICH is reported to be 30-55% (46). Because of underlying small vessel disease, ICH location is associated with the risk of future ICH recurrence (47). ICH in deeper brain region is fatal as accumulation of blood in the brain upon ICH causes

deposition of fibrous tissues, cholesterol clefts, macrophages and calcified tissue (48). This is followed by increase in oncotic pressure and tension inside the vasculature (49), contributing directly to a decline in clinical conditions (50). Significant deleterious effects of ICH may be directly associated with cytotoxicity, excitotoxicity and inflammation caused by the accumulation of blood and its components (51). Changes in vascular integrity might also affect the extent of damage and its implications when an ICH occurs.

ICH can also arise due to underlying vascular dysfunction, which may be caused due to the presence of oxidative stress, reduction in nitric oxide (NO) bioavailability, imbalance in production of vasoconstrictor/vasodilator factors, pro-inflammatory environment, senescence of endothelial cells and impaired angiogenesis (15). Vascular injury is usually accompanied with vascular smooth muscle cells displaying plasticity leading to vascular remodelling (52), potentially causing the vessels to stiffen over time. Arterial stiffening of the large cerebral arteries is a major risk factor as the pulsatile component of cardiac output is transmitted directly to capillaries, increasing the risk of ICH, as the major cerebral vessels fail to auto-regulate blood flow to the brain.

#### ***1.4.Cerebral Autoregulation***

Certain cerebral blood vessels are highly susceptible to changes in blood flow and pressure, hence they are always auto-regulated to provide consistent blood flow. Cerebral blood flow autoregulation is the ability of the brain to maintain relatively constant blood flow despite changes in the perfusion blood pressure (53). Autoregulation in the brain is distinct from the systemic components as it maintains relatively steady blood flow during fluctuating systemic blood pressure via metabolic, myogenic and neurogenic mechanisms (54). The most vital

objective of autoregulation is to maintain an optimum level of brain perfusion to suffice metabolic demands (55).

The brain is very sensitive to over or under perfusion and the resistance provided by large arteries help protect the downstream vessels during changes in the systemic blood pressure. The cerebral endothelium in the blood vessels play a vital role in proper functioning of the cerebral arteries as it has specialized tight junctions that do not allow ions to pass easily, very low hydraulic conductivity and relatively low transcellular transport, all of which help retain ions in the vascular bed opposing outwards water movement (55). This strict water regulation is of prime importance as the brain has limited capacity for expansion within the skull. Sudden and sharp increase in blood pressure can cause ICH and lead to accumulation of blood causing serious damage to the brain.

Alternatively, low blood flow or pressure may lead to a decrease in availability of oxygen (56), causing the brain tissues to experience hypoxia.. Although there is decrease in oxygen availability due to decreased blood flow. No clinical signs or symptoms of hypoxia are seen until the decrease in perfusion exceeds the ability of increased oxygen to meet metabolic demands. Once past the threshold, signs of hypo-perfusion such as dizziness and altered mental status are evident (56). The decrease in blood flow also stimulates release of vasoactive substances which help in increasing blood flow. Compared to reduced blood flow, unsuppressed high blood flow causes significant deleterious effects at a much faster rate on the brain, making it very important to control the higher end of blood pressure.

When the cerebral blood flow fluctuates at the higher end of the auto-regulatory curve, the myogenic tone of the cerebral smooth muscle causes constriction in response to elevated pressure, known as pressure dependent constriction (PDC) (57). The larger diameter cerebral

vessels extending from the circle of Willis to pial arteries have been shown to play a crucial role in adjusting blood flow above the normal range of blood pressures (58). A further increase in pressure causes the vessels to undergo some instability, typically after few rapid dilations with only partial re-constriction. If the pressure is not decreased, complete loss of tone (forced dilatation) occurs (57). This loss of tone decreases cerebrovascular resistance producing a sudden, large increase in cerebral blood flow (300-400%), known as auto-regulatory breakthrough (58). In the cerebral circulation an impaired myogenic response results in impaired cerebral autoregulation and higher susceptibility to hypertension-induced cerebral hemorrhage (59). The MCA (Middle cerebral Artery), one of the main cerebral arteries, is directly associated with the pulsatile component of systemic blood circulation, making it highly vulnerable to any fluctuation in blood pressure (60). The signalling mechanism in smooth muscle cells and endothelium work in tandem to regulate the vascular tone and protect the middle cerebral artery during major fluctuations in blood pressure.

### ***1.5. Smooth muscle cells and endothelium in regulating vascular tone***

Vascular tone is regulated by two mechanisms, vasoconstriction and vasodilation, occurring through interactions between endothelial and smooth muscle cells. The endothelial layer plays an important role in regulating signalling mechanisms dependent on stimuli from the vascular lumen. Normal functioning of endothelium prevents abnormal blood clotting and bleeding, suppresses SMC proliferation and limits inflammation of the vascular body (39). Endothelial cells produce compounds such as nitric oxide (NO), endothelin, prostaglandin, angiotensin II and more, vital to regulating vascular homeostasis (39). Endothelial nitric oxide synthase (eNOS) produces NO from l-arginine, NO then diffuses to underlying smooth muscle

cells and catalyzes the activation of guanylate cyclase (**Figure 1.2**). Activated guanylate cyclase signals the conversion of guanosine triphosphate to 3,5-cyclic guanosine monophosphate (cGMP), stimulating soluble guanylate cyclase leading to an increase in cyclic GMP levels and eventually leading to smooth muscle relaxation and dilatation of blood vessels (61,62). This vasodilation helps in increasing the lumen diameter and allowing optimal amount of blood to pass through the vasculature and reach distant cellular sites, which is vital during hypotension.

Vasoconstriction of a vessel requires free intracellular calcium levels to regulate smooth muscle cell (SMC) contractility (62). Calcium levels in SMC are mainly regulated in two ways: calcium entry through voltage dependent calcium channels (like TRPV4) and by involvement of intracellular calcium stores (52). Activation of G-Protein coupled receptors (GPCR) generates phospholipase C which then converts phosphatidylinositol 4,5-diphosphate (PIP<sub>2</sub>) to inositol 1,4,5-triphosphate (IP<sub>3</sub>) and diacyl glycerol (DAG). Intracellular IP<sub>3</sub> directing releases calcium from cellular stores causing calcium dependent constriction of vessels (52). The homeostatic balance between vasodilation and vasoconstriction helps maintain constant blood flow to the brain in the event of systemic high blood pressure.

Sometimes vasoconstriction is also seen as a result of abnormally functioning endothelium in disease state like hypertension, where endothelial degradation due to shear stress may lead to hypertrophy of the SMC, promote thrombosis and increase vascular inflammation (39). Endothelial dysfunction predicts poor outcome in patients as it increases vascular reactivity and aggravates macrovascular disease (39). Any changes in the signalling mechanism regulated by endothelial and smooth muscle layer has a direct impact on functioning of the vessel. Changes in signalling pathways of protein kinase C (PKC), myosin light chain (MLC), mitogen activated

protein kinase (MAPK) and Rho-kinase have also been shown to affect the vascular smooth muscle cell contraction directly as well as indirectly (33).

#### *1.5.1. Role of Myosin Light Chain (MLC) in vascular contraction*

Vascular smooth muscle contraction is triggered by an increase in calcium release from the sarcoplasmic reticulum and/or entry of calcium from the extracellular space through calcium channels. The released calcium binds to calmodulin (CAM) to form calcium-calmodulin complex, which in turn activates myosin light chain kinase (MLCK) causing phosphorylation of MLC, actin-myosin interaction and vascular smooth muscle contraction (63,64). **Figure 1.1** shows a schematic representation of the signalling mechanisms potentiating smooth muscle contraction through the MLC pathway. Stimulation (activation) of MLC initiates the assembly of cytoskeletal/extracellular matrix adhesion complex proteins at the membrane orchestrating the polymerization and organization of sub-membranous actin filaments, leading to SMC contraction (65). The cytoskeletal network may serve to strengthen the membrane for the transmission of force generated by the contractile apparatus to the extracellular matrix enabling the SMC to adapt to mechanical stress (like high blood pressure) in the initial stages of the disease (65).

The stage of MLC phosphorylation in vascular smooth muscle cell (VSMC) determines whether the cross-bridges are cycling, turned off, or in a semi-activated state. The extent of MLC phosphorylation is balanced by MLCK and MLC phosphatase (MLCP). Vasoconstriction is mostly evoked by myosin regulatory light chain phosphorylation at Ser 19 by MLCK, which is enhanced by Rho-associated kinase (ROCK) - mediated inhibition of myosin light chain phosphatase (MLCP) (66). In simplified terms, MLCK is responsible for activating

(phosphorylating) MLC leading to formation of actin-myosin bonds and eventually causing contraction, whereas MLCP is associated with recycling, as well as deactivating the phosphorylated myosin, resulting in relaxation (67). The relaxation of VSMC is initiated by a decrease in free calcium levels due to increased calcium uptake by sarcoplasmic reticulum and extrusion of calcium by the plasmalemmal calcium pump and sodium-calcium exchanger. The decrease in intracellular calcium is followed by dissociation of the calcium-calmodulin complex and the dephosphorylation of MLC by MLCP, causing vascular relaxation (68).

MLCP enzyme can also be inhibited, to induce prolonged vascular constriction, by blocking the targeting site of MLCP termed the myosin binding site (MBS). When phosphorylated, the serine and threonine residues of MBS inhibit the activation of the catalytic domain, which in turn reduce MLCP enzyme activity, leading to prolonged contraction (64). Another mechanism by which MLCP is inhibited is through activation of GPCR, resulting in releasing of arachidonic acid leading to activation of Rho-kinase pathway (69). Protein Kinase C activated by phorbol esters and/or DAG may also inhibit MLCP activity by phosphorylating and activating CPI-17 (an inhibitor of the subunit), resulting in a delayed phosphorylation-dephosphorylation cycle of MLC and prolonged constriction (69).

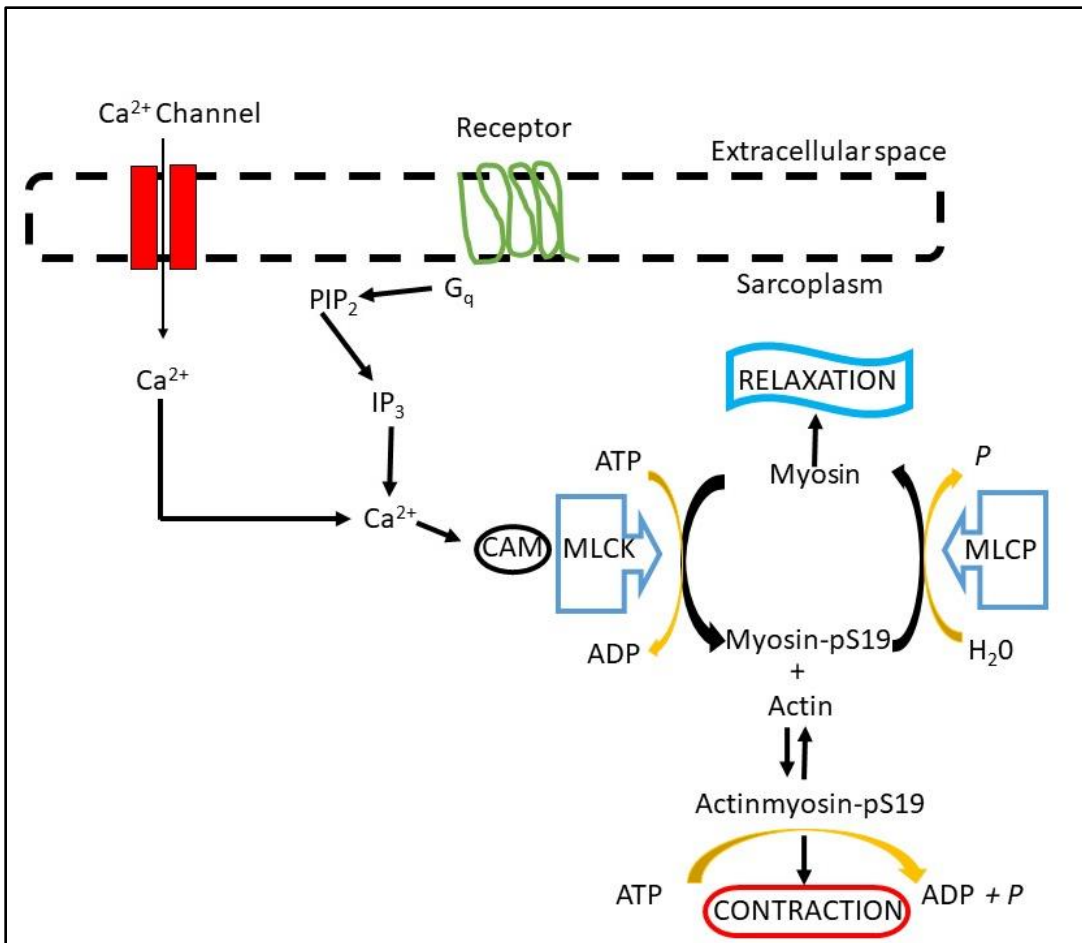


**Figure 1.1.:** Schematic diagram of signal transduction pathway of MLC for SMC contraction and relaxation. Availability of calcium in the cell forms a calcium-calmodulin complex which activated MLCK to phosphorylate Myosin. Phosphorylated myosin binds to activated actin to produce SMC contraction. MLCP dephosphorylated myosin to initiate SMC relaxation. [Figure (copyright clearance obtained) adapted from *IUMBM Life, Walsh M.P., 2011*]

ADP – Adenosine Diphosphate, ATP – Adenosine Triphosphate, CAM – Calmodulin, MLCK – Myosin Light Chain Kinase, MLCP – Myosin Light Chain Phosphatase,  $\text{PIP}_2$  - Phosphatidylinositol 4,5-diphosphate,  $\text{IP}_3$ - Inositol 1,4,5-triphosphate

### 1.5.2. Role of Protein Kinase C (PKC) in Vascular contraction

Protein Kinase C (PKC) is also one of the important signalling proteins which mediates vascular contraction and is activated partly through release of calcium. Activated Gq/11 proteins within the GPCR (G-protein coupled receptor) signalling system induce calcium activation and sensitization of Phospholipase C (PLC) mediated conversion of phosphatidylinositol 4,5-bisphosphate (PIP<sub>2</sub>) to inositol 1,4,5-triphosphate (IP<sub>3</sub>) and DAG, to cause release of calcium and activation of PKC (70). PKC can also be activated independent of calcium release as a study by Goyal et.al demonstrated calcium independent PKC-mediated contractility in ovine cerebral arteries (71). Most PKC isoforms are regulated either by calcium or DAG or by both, depending on the isoform.

PKC isoforms are classified into sub-groups based on cofactor requirements, structural properties and specific *in vivo* activity, and spatial organization in the cell (72). The conventional PKC isoforms ( $\alpha$ ,  $\beta$ I,  $\beta$ II, and  $\gamma$ ) are regulated by calcium and DAG, whereas the novel PKC isoforms ( $\delta$ ,  $\epsilon$ ,  $\eta$ , and  $\theta$ ) are regulated by DAG, but not calcium (73,74). Different PKC isoforms are expressed in smooth muscle of different vascular beds, for example:  $\alpha$ ,  $\beta$  and  $\gamma$  isoforms of PKC are mainly localized in the cytosolic component of unstimulated smooth muscle cells and are translocated to the cell membrane when cells are activated through stimuli (63). Brain tissues of spontaneously hypertensive rats (SHR) have shown PKC isoenzymes well distributed and expressed throughout the brain region (75), hence demonstrating a role of PKC in vital functions of the brain. PKC signalling pathways activated in the SMC also affect the functioning of the endothelial layer as changes to the PKC function and activation have been shown to affect endothelial and SMC function that lead to vascular dysfunction.

PKC activity in the endothelium is known to contribute towards the regulation of blood pressure and vascular function, as PKC has been associated with the endothelial dysfunction in blood vessels of SHR and deoxycorticosterone acetate (DOCA) hypertensive rats (76). A study by Schiffrin *et al.*, showed that stimulation of ET-1 by angiotensin II increases vascular PKC activity to a large extent in blood vessels of SHR, compared to normotensive rats, indicating higher levels of PKC during hypertension (77). Studies in SHR rats have shown angiotensin II infusion causes endothelial dysfunction and hypertension, and increases production of free oxygen radicals in the vascular tissue (77), contributing to vascular changes such as vascular remodelling. Some PKC isoforms are known to induce signal transduction events mediating long term cellular functions such as cell differentiation (78), further causing vascular changes such as vascular remodelling. Additionally, upregulation of PKC has seen to be crucial in several comorbidities such as arterogenesis, hypertension and cancer prognosis (79). In diseases such as diabetes and hypertension, PKC has shown to aggravate inflammation of the vasculature (80) affecting the normal vascular tone.

Defective PKC signalling contributes to abnormal vascular contraction as activation of PKC increases the myofilament force sensitivity to calcium, thus maintaining contraction (81). As mentioned earlier, the activation of PKC requires either calcium or DAG or both, irrespective of it being upregulated in disease states or functioning during normal conditions. The calcium needed for the PKC isoforms to be activated is mostly transported into the cell through different calcium channels, such as transient receptor potential cation channel - vanilloid, member 4 (TRPV4). Conversely, the PKC alpha isoform has also been shown to mediate TRPV4 activation in the endothelial cells (82). Activation of TRPV4 channel in vasculature plays a significant role

in regulating calcium influx into the cell and influences the vascular contractile mechanism to a large extent.

### *1.5.3. Transient Receptor Potential (TRP) Channels in vasculature*

The transient receptor potential (TRP) channels are a family of nonselective cation channels with a diverse degree of calcium permeability, which do not have a voltage sensor, but are susceptible to other stimuli including shear stress, mechanical stretch, pressure, oxidative stress and inflammatory proteins (83). TRP channels can be grouped into six subfamilies: Ankyrin (TRPA), canonical (TRPC), melastatin (TRPM), mucolipin (TRPML), polycystic (TRPP) and vanilloid (TRPV) TRP channels (84). Entry of calcium occurs through TRPA, TRPC and TRPV4 channels and studies have shown TRPA1, TRPC3, TRPV3 and TRPV4 are significantly involved in endothelium dependent vasodilatory response (85). TRP channels are known to regulate vascular tone by changing calcium levels in endothelial cells releasing mediators [nitric oxide and endothelium derived hyperpolarizing factors (EDHF)] causing vasodilation (86). TRP channels are found in both smooth muscle cells and the endothelial layer of the vasculature.

Many TRP channels like the TRPV4 channel, have been detected in smooth muscle cells of different vascular beds, such as aorta and rat cerebral arteries (87), but is predominantly expressed in the endothelial cells compared to smooth muscle cells (88,89). TRPV4 channel is a shear stress sensing channel, mostly found in endothelial cells. During high blood flow TRPV4 senses shear stress and causes a rapid influx of calcium, leading to release of EDHF (vasodilatory mediators) from the endothelium, leading to vasodilation (90). TRPV4 channels

are also activated by numerous other stimuli, such as heat and cell swelling (91). One of the EDHF, epoxyeicosatrienoic acid (EET), a potent vasodilator produced by endothelial cells via cytochrome P-450 enzymes, is known to activate the TRPV4 channels (89,92) causing a vasodilatory response in the vasculature.

A study by Earley and colleagues showed an absence of EET-induced vasodilatory response in the isolated mesenteric artery of TRPV4 knockout mice, suggesting the importance of the channel and significance of the pathway in vasodilation (89). Activation of TRPV4 in cerebral myocytes by EET has been shown to elevate calcium level and transient potassium channel activity (89), resulting in vasodilation. The same group also showed that suppression of TRPV4 expression in intact cerebral arteries prevents EET induced hyperpolarization of smooth muscle cell and hence limits vasodilation (89). The role of TRPV4 channels in vasodilation was studied by Sonkusare and colleagues where they demonstrated endothelial TRPV4 channel activation led to hyperpolarization of the smooth muscle cell, establishing TRPV4 channel activation as a vital component in cerebral vascular vasodilation (93). TRPV4 channels have also been shown to activate calcium dependent potassium channels (BKca: big conductance potassium calcium channels and SKca: small conductance potassium calcium channels), leading to TRPV4 induced hyperpolarization in EC and eventually causing vasodilation (89). **Figure 1.2** demonstrates a schematic representation of TRPV4 activated vasodilation. TRPV4 when activated, hyperpolarizes the SMC resulting in vascular relaxation (vasodilation). TRPV4 channels, like other TRP channels, perform several other supplementary functions in the vasculature.

TRP channels play an important role in pathophysiology of many cardiovascular diseases by regulating fundamental cell functions like proliferation, differentiation, contraction,

relaxation and cell death (84). TRPV4 has also been implicated in partially regulating cell proliferation of human brain capillary endothelial cells (HBCEs) (94), affecting the vasculature morphology. Hyper-activation of TRPV4 is also known to cause calcium overload leading to oscillating blood vessel diameters (93), potentially leading to vascular dysfunction during disease states such as hypertension.

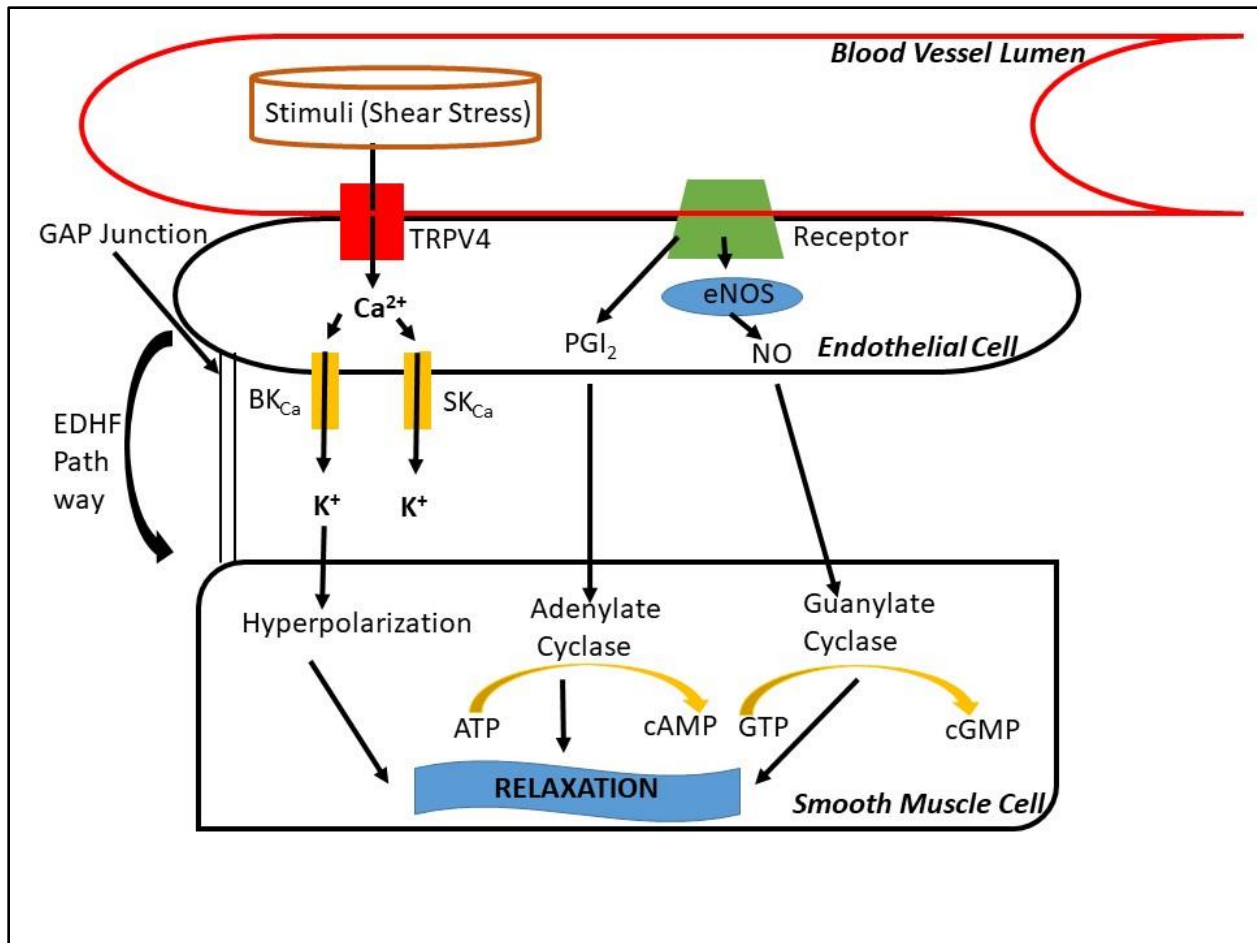


**Figure 1.2.:** Schematic diagram for TRPV4 mediated vasodilation. TRPV4 channel is activated by stimuli (shear stress) during hypertension causing calcium influx and activating potassium channels resulting in hyperpolarization of SMC causing vasodilation. NO and PGI are known to activate downstream leading to vasodilation of the SMC. [Figure (copyright clearance obtained) adapted from *Pharmacological Research, Sukumaran et al., 2013*]

TRPV4 - Transient Receptor Potential Cation Channel (Vanilloid, member 4), eNOS – endothelial Nitric Oxide Synthase, GTP – Guanosine Triphosphate, ATP- Adenosine Triphosphate, BK<sub>Ca</sub> and SK<sub>Ca</sub> – Big and Small conductance potassium channels, EDHF - Endothelium Derived Hyperpolarizing Factors, cGMP - cyclic Guanosine Monophosphate, cAMP –cyclic adenosine monophosphate

### ***1.6. Vascular “endothelial” dysfunction***

Vascular changes play a crucial role in cerebrovascular and neurodegenerative diseases. Vascular endothelial cells line the entire circulatory system and perform diverse functions which include fluid filtration, such as in the glomeruli of the kidneys, maintain blood vessel tone, hormone trafficking and neutrophil recruitment (95), making the endothelium a key player in vascular dysfunction. Endothelial cells are well known as a source of growth inhibitors and promoters, such as heparin and heparin sulphates (96), platelet-derived growth factor (97), and thrombospondin (98). Several vasoactive substances produced by the endothelium, such as nitric oxide, endothelin, and angiotensin II may also play a role in the regulation of vascular growth (96). Alterations of endothelial cells directly affect the vascular functioning, as the endothelium is directly involved in the maintenance of functional capillaries and vessels (96). Dysfunction of the endothelium is implicated in several diseases such as peripheral vascular disease, stroke and heart disease among others (96).

Hence, dysfunction of endothelium dependent regulatory systems play a huge role in pathogenesis of cardiovascular diseases such as hypertension and diabetes (99). Concurrent to endothelial cells, chronic hypertension has also been shown to cause changes in smooth muscle cells, such as pressure-induced deformation of extracellular matrix (ECM) proteins and their cell surface receptors. This may initiate rapid contraction and cytoskeletal remodelling through modulation of ion channels, membrane depolarization and generation of reactive oxygen species (ROS) (100).

### *1.6.1. Role of Reactive Oxygen Species (ROS) in vascular dysfunction*

It is known that vascular cell homeostasis depends on regulated levels of ROS (101). The imbalance in production of ROS likely promotes vascular inflammation, increased reactivity, endothelial dysfunction and structural remodelling, leading to elevated peripheral resistance and increased blood pressure (102). The presence of pro-hypertensive factors amplify blood pressure elevation during generation of ROS that not only affect the vasculature, but also affect vital organs such as heart, kidneys, nervous system and immune system (102). Thus, ROS have been expressed in different disease types and throughout the progression of a disease.

The imbalance in ROS leads to free radical transformation of surrounding chemical metabolites and deterioration of nitric oxide (NO) signalling cascade and promotes oxidative post-translational protein changes that hinder cell and vascular signalling pathways, potentially resulting in cerebrovascular dysfunction (103). Endothelial dysfunction, demonstrated by decreased NO bioavailability, is a familiar feature of many vascular diseases (61). Gradual loss of vascular homeostasis occurs due to molecular and morphological changes, such as reduction in NO, and increased vascular thickening, due to the increasing age, disease-induced oxidative stress, and the presence of inflammatory stimuli (103).

During ICH, neutrophils are stimulated and release a large amount of ROS. This in turn causes excessive uptake of superoxide dismutase (SOD) followed by lipid peroxidation resulting in damage to the surrounding tissues (104,105). Free ROS damage nerve cells by injuring cell membranes, causing cell necrosis. As the brain tissue and vasculature is very sensitive to ROS, this can lead to increased cell membrane permeability and calcium influx into the vessels causing vascular dysfunction (7). Increased calcium ion concentration due to increased calcium influx activates phospholipase, leading to phospholipid “decomposition” and structural damage to

organelle membranes in the vasculature (106). Most ROS are well known to directly induce the production of acute pro-inflammatory cytokines such as interleukin-10 (IL-10), tumor necrosis factor (TNF- $\alpha$ ) and also stimulate nuclear factor (NF- $\kappa$ B) all crucial in inflammation (107).

### ***1.7. Inflammation in vascular dysfunction***

Inflammation is a reaction to injury in living tissues induced by oxidative stress and can further exacerbate damage through an increasing oxidative stress (108). Inflammatory responses in the vasculature involves a complex interaction between the extracellular matrix (ECM), vascular smooth muscle cells (VSMC), endothelial cells (EC) and inflammatory cells (neutrophils, lymphocytes, monocytes and macrophages) (109). Acute inflammation in blood vessels most often results in increased vasodilation, blood stasis and increased vascular permeability due to cytoskeletal changes in EC leading to disruptions of EC junctions (109). ECs when stimulated by inflammation, cause an increase in expression of adhesion molecules such as intracellular adhesion molecule-1 (ICAM-1), vascular cell adhesion molecule-1 (VCAM-1), integrin and selectins which promote the adherence of inflammatory cells and recruit cytokines, matrix metalloproteinases (MMPs) and growth factors (62).

In a few chronic diseases, a delayed inflammatory response involves upregulation of inflammatory factors such as C-reactive protein (CRP), plasminogen activator inhibitor-1 (PAI-1), and protease-activated receptor (PAR) signalling (110). Cytokines, a diverse group of mostly soluble short acting proteins, peptides and glycoproteins. They activate specific receptors of different cell types activating JAK-STAT, NF- $\kappa$ B and Smad signalling pathways leading to an inflammatory response in the form of increased cell permeability, adhesion and/or apoptosis

(109). Activation of cytokines (such as interleukins, tumor necrosis factor and interferon) leads to ECM deposition and changes in morphology of the vessel (110). Their interaction with mitochondria also result in increased production of ROS (111).

Interestingly, activation of cytokine induced pathways in ECs modify the production of vasodilatory mediators such as NO, EDHF, prostacyclin, and bradykinin, as well as vasoconstrictive mediators such as endothelin and angiotensin II (112). Cytokines also interact with VSMC to activate calcium transport and regulate protein kinase C (PKC) and mitogen activated protein kinase (MAPK) pathways, which lead to cell growth, proliferation and migration (109), and have been associated with vascular inflammation (113) in diseases like hypertension and atherosclerosis.

#### *1.7.1. Role of MAPK and Extracellular Signal-Regulated Kinase (ERK) in vascular dysfunction*

MAPKs are known to transduce stress related signals through chains of interlinked pathways that lead to induction of inflammation (114). The MAPK signalling pathway is composed of a triple kinase cascade: a MAPK, a MAPK activator (MAPK kinase), and a MAPKK activator (MAPKK kinase, MEKK). Small G proteins can activate MAPKK kinase, causing phosphorylation and this in turn activate the downstream MAPK Kinase (115,116). Activated MAPKK phosphorylates the third member of the sequence, MAPK (Figure 1.3). This activation of MAPK leads to phosphorylation and activation of the transcription factors present in the cytoplasm or nucleus, leading to expression of target genes, resulting in biological

responses linking extracellular signals and fundamental cellular processes such as growth, proliferation, migration, apoptosis and metabolism (115,117).

Activation of p38 MAPK requires dual phosphorylation of specific threonine (Thr) and tyrosine (Tyr) residues simultaneously (115) and is activated downstream from toll like receptors (TLR). MAPK pathway activation promotes production of various pro-inflammatory cytokines such as TNF- $\alpha$ , IL-1 $\beta$ , IL-6, and IFN- $\gamma$  (118). TNF- $\alpha$  in VSMC has been shown to stimulate TNFR1 and activate MAPK, aiding in the process of VSMC migration. Migration and proliferation of VSMC promote their accumulation in vascular lesions (119). p38 MAPK is also involved in the stabilization and translation of multiple pro-inflammatory mRNAs, generating a larger inflammatory response. Phosphorylated p38 MAPK has been detected in neurons and microglia following ischemic brain injury suggesting it plays a role in the inflammatory response (120). Both MAPK and ERK have been implicated in many vascular diseases as they control a broad spectrum of cellular processes, stress and inflammatory responses.

MAPKK1 and MAPKK2 activate ERK1 and ERK2, respectively, by catalyzing the phosphorylation at Thr185 and Tyr187. Once activated, ERK translocates to the nucleus where it phosphorylates and regulates different transcription factors ultimately resulting in changes to gene expression (121). ERK 1/2 can be activated by growth factors such as brain derived neurotrophic factor (BDNF), platelet derived growth factor (PDGF) and by pro-inflammatory stimuli (for example: IL-1 $\beta$ ) (122). ERK is also activated by sensing patterns such as pathogens associated molecular patterns (PAMPS) and danger associated molecular patterns (DAMPS) during an inflammatory reaction in the vasculature and tissue surrounding the vessel (115).

The ERK1/2 cascade is a central signal transduction pathway in the cell, but the same stimuli can also activate other cascades, such as PI3K-AKT, NF- $\kappa$ B, and others. These cascades

may interact with each other and hence modulate the signaling output by cross-phosphorylation between the cascades, by combinatorial effects on their downstream targets, or by modulation of activity (123). The final outcome of the activation of ERK1/2 also depends on many factors such as presence of scaffold proteins, substrate competition, temporal regulation, and subcellular localization by anchoring proteins (118). ERK1 and ERK2 are therefore crucial regulators of proliferation, differentiation and survival; hence dysregulation of ERK1/2 cascade is known to result in various pathologies, inducing neurodegenerative, vascular, developmental diseases, and cancer and diabetes (123). PKC dependent activation of MEK results in activation of ERK resulting in multiple downstream effects such as phosphorylation of actin binding caldesmon (124). The phosphorylation of caldesmon on Ser789 can reverse the caldesmon-mediated inhibition of myosin ATPase activity, resulting in the contraction of the smooth muscle cells in the vasculature (124). Cell culture studies have also shown that MAP kinase (ERK1 and ERK2) influences the cells' motility machinery by phosphorylating and, thereby, enhancing MLCK activity leading to phosphorylation of MLC (125). Thus, the activation of ERK1/2 is able to influence the phosphorylation of caldesmon, actin, and MLCK, in turn affecting the overall contractile mechanism of the vasculature in the disease state.

Studies have shown phosphorylated p38 MAPK and ERK to be localized in reactive microglia, indicating reactive microglia to be responsible for thrombin induced neuronal death (120,126). This recruitment of activated microglia is accompanied with phosphorylation of MAPK family contributing to ICH-associated neuronal loss (127). MAPK pathways and microglial signalling have been thought of as a potential target for pathogenic conditions related to hemorrhagic stroke (126), suggesting a crucial role of neuro-inflammation in diseases such as stroke.

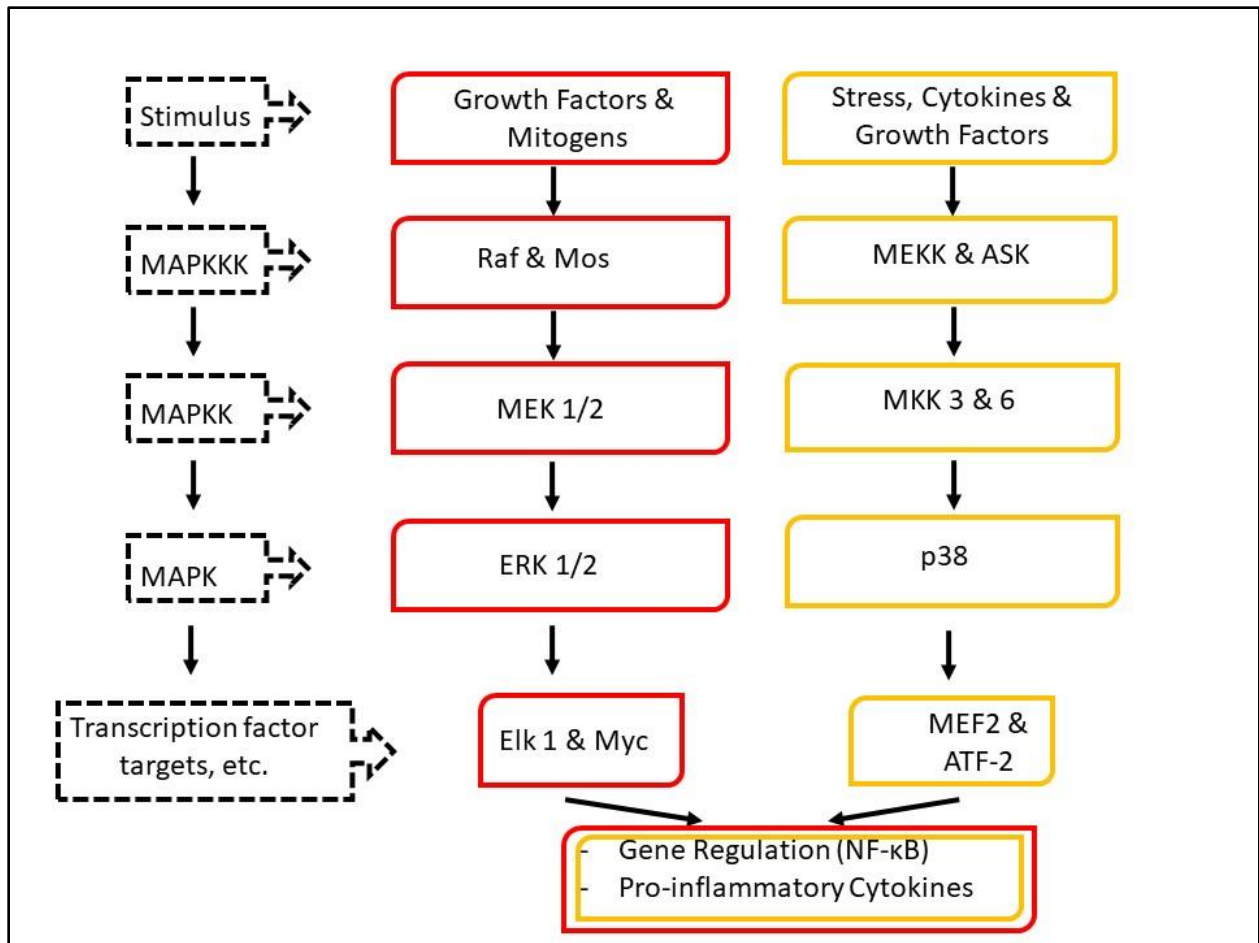


**Figure 1.3.:** Schematic diagram of two main MAP Kinases: ERK and p38 MAPK. p38 and ERK require different stimuli to activate and once activated they signal downstream through similar but separate cascades ultimately activating transcription factors leading to release of pro-inflammatory cytokines and gene regulation. [Figure (copyright clearance obtained) adapted from *GUT (BMJ Journals), Hommes et al., 2003*]

ATF-2 - Activating transcription factor 2, ERK - Extracellular signal regulated kinase, MAPK - MAP kinase, MAPKK - MAP kinase kinase, MAPKKK - MAP kinase kinase kinase, MEF - Myocyte enhance factor, MKK - MAP kinase kinase, ASK - Apoptosis signal regulating kinase.

### ***1.8.Neuro-inflammation***

Neuro-inflammation is generally the result of acute focal injury. The Central Nervous System (CNS) response to acute focal damage can be categorized into three distinct phases: 1) inflammation and cell death, 2) cell proliferation for tissue replacement and 3) tissue remodelling (128). The CNS response includes a rapid inflammatory response from intrinsic tissue cells by recruitment of inflammatory and immune cells, macrophage and leukocyte infiltration followed by death of parenchymal cells and debris removal, accompanied by platelet influx and aggregation of local cells (128).

The inflammatory response in the brain differs from rest of the body, as the blood brain barrier (BBB) protects the brain by limiting what enters and leaves the brain (129). During damage to the CNS, select group of cells, namely microglial cells, astrocytes and mast cells serve as part of the primary immune response (129). Mast cells are important for attracting and potentially activating other immune cells by secreting pro-inflammatory cytokines and chemo-attractants (130). Astrocytes and microglia contribute to the local immune response within the brain through production of cytokines, complement components and chemokines (131).

#### ***1.8.1. Microglia in Neuro-inflammation***

Microglial cells are one of the major immune cells involved in the defence against brain damage. When activated by damage and pro-inflammatory cytokines, microglia have the capacity to disrupt neural cells and the BBB and aggravate damage. A study in mice after ICH showed significant expression of inflammatory factors (IL-17A) and microglial activation in the peri-hematoma region with impaired neurological function, suggesting a role of microglia in

ICH (132). The same study also demonstrated that inhibition of IL-17A prevented ICH induced cytokine expression and downstream signalling molecules resulting in diminished activation of microglia (132), stating a role of pro-inflammatory factors in activating microglia.

Microglia have a modifiable and adaptable nature based on the situation. Beneficial for brain repair due to their neuro-protective role, or destructive, when they are activated by pro-inflammatory stimuli (105). Microglia undergo morphologic transformation from resting state to an amoeboid state during distress, where they become indistinguishable from the circulating macrophages (133). They are myeloid derived cell, which can polarize into two distinct macrophages, M1 (pro-inflammatory) and M2 (anti-inflammatory). The polarization of microglia (also classified as M1 or M2) is mostly guided by the microenvironment of the site of injury and it serves as a deciding factor for the effect of neuro-inflammatory responses to the brain damage (134). The M1 phenotype is related with inflammatory responses increasing production of inflammatory cytokines and oxidative/nitrative compounds, such as TNF, interleukins and chemokine ligands (CCL2 and 3), and activating astrocytes, whereas M2 phenotype releases anti-inflammatory factors to promote tissue repair (134). The microglial M1 phenotype activation with a given stimulus plays an important role in determining the effect on neuronal survival and astrocyte activation and proliferation. It is the phenotype of microglial cells that dictates the cross-communication between astrocytes and microglia following brain injury (134).

### *1.8.2. Astrocytes in neuro-inflammation*

Astrocytes regulate neuro-inflammatory responses in neurological diseases, as they are known to maintain the immune system at baseline by keeping a check on the permeability of

BBB and microglial activation (135). Astrocytic processes connect each synapse and they are an integral part of the internal layer of the BBB, which allow astrocytes to react to local changes as well as respond to systemic changes in the body. They are also known to provide functional and trophic support to neurons by transporting glucose, neurotransmitters (such as glutamate) and neurotrophic factors (136).

Astrocytes regulate neuro-inflammatory responses by two mechanisms: 1) astrocytes have the ability to form physical barriers that can seal the site of injury and localize the inflammatory response; 2) they can indirectly regulate the response of neuronal injury by affecting neuronal health and axonal regrowth (135). Astrocytes are found to be highly activated after stroke and can form a scar around the area of damage (137). Astrocyte scars consist of narrow zones of newly generated astrocytes with elongated processes that intertwine and immediately surround the sides of the lesion core, and are generally devoid of other neural lineage cells (neurons or oligodendrocytes). The density of astrocytes in scar tissue is often twice that of healthy tissue (138).

Inflammation is an integral component of the glial (astrocyte) scar. In the CNS, CD 36, an inflammatory mediator, occurs in the subset of astrocytes in the scar. It is suspected of being a novel mediator for injury induced astrogliosis and can serve as a target to reduce glial scar in stroke (137). Astrocytes are also known to uptake glutamate in the CNS and they regulate activity of glutamatergic synapses, making them crucial in neuronal survival during diseased conditions (136). Glutamate-mediated excitotoxicity is believed to contribute to neurological issues in many neuro-degenerative diseases (139). The changes in expression of astrocytes and microglia in brain regions during the damage are accompanied by morphological changes in the neurons and cells surrounding the site of damage (140,141).

### ***1.9. Neuronal damage***

Neurological disorder pathogenesis most often includes vascular damage, neuro-inflammation, neuronal injury and neurodegeneration (142). After damage, two events characterize a brain injury: 1) primary, or immediate, damage that induces degeneration and cell death directly, and 2) secondary, or delayed, damage that effects cell death and degeneration through independent active mechanisms (143). The secondary neural damage is proportional to the extent of the initial injury, hence a more extensive and longer-lasting primary injury results in higher secondary neuronal degeneration (143).

Axonal damage (another type of neuronal damage) spread along the anatomical and functional connections and can be either anterograde or retrograde depending on the level of damage (144). During injury, the axons undergo shrinkage and neurons undergo series of changes such as reduction in cytoplasmic substances, nuclear eccentricity, nuclear and nucleolar enlargement, dendrite shrinkage and changes in morphology (145,146). Neural degeneration in the brain is accompanied by apoptotic processes that are regulated by mitochondria (147).

The apoptotic process is responsible for degrading the degenerated cells and neurons surrounding the damage site. During ICH, the loss of blood flow leads to decreased availability of vital nutrients causing dysregulated autophagy, which often occurs through degradation of cytoplasm and organelles of the cell (148). The dysregulation of autophagic machinery is implicated in neuronal cell fate in several diseases such as cancer and neurodegenerative diseases (143). Brain damage is also accompanied by necrosis of neighbouring cells, including vacuolation of the cytoplasm, breakdown of the plasma membrane and induction of inflammation around the dying cell by release of cellular contents such as pro-inflammatory mediators and lysosomes (149). The damage during ICH results in a pool of blood at the site of

injury. This causes the surrounding cells to degrade due to the presence of inflammatory mediators as a result of blood decomposition (150-152). Thus, mechanisms of neuronal degeneration, cell vacuolation, edema, necrosis, apoptosis and axotomy are widely observed during damage in the brain in various diseases including stroke (49,153,154). For studying and identifying the morphological changes accompanied with the cellular changes during brain diseases (such as stroke) animal models have been used for the past few decades.

### ***1.10. Animal models of hemorrhagic stroke***

Animal models have contributed to a large extent in our understanding of the pathology of various diseases and assisted in the development of potential therapeutic treatment strategies (155). A greater understanding of the underlying etiology of different subtypes of stroke have been possible only due to studies with animal models. Although the animal models have been very helpful in scientific studies, it is important to understand that the models do not attempt to demonstrate or replicate the whole disease process but aim to target details of specific aspects in carefully controlled and monitored conditions (156). Most studies use rodents as their animal model. The rodent models used for stroke can be divided into two broad classes: 1) models where stroke is artificially induced and 2) stroke that occurs spontaneously in the animal model (157).

#### ***1.10.1. Animal models with artificially induced stroke***

The consequences of spontaneous ICH are mimicked in mice and rats by enzymatically inducing vessel rupture by intra-parenchymal injection of blood or blood products (158,159).

The pathological mechanisms of hemorrhagic brain damage and edema formation have been studied by “blood injection” surgical models (160). The collagenase injection model, one of the blood injection models, disrupts the basal lamina of vessels, causing spontaneous bleeding into the brain tissue. This then generates long-term neuro-functional deficits and hence this model has been an extensively used model for studying stroke (159,161,162). Other models of artificially induced stroke include the balloon inflation model and the cerebral avulsion method (163).

The blood avulsion method (model for cortical injury) involves stripping the cortical surface of blood vessels, where avulsion creates cortical hemorrhages (164). The cortical avulsion by pial stripping might lead to a mixed form of injury with hemorrhage and non-perfused ischemia occurring at the same time. Whereas balloon inflation models are a better fit compared to avulsion, they allow study of the effect of hematoma and its removal on brain injury in a more direct manner (165). The essential features of the artificially induced stroke models are the consequences or different types of vascular insult through acute vessel injury, but it does not mimic the entire vascular pathology itself which leads to irregular onset of ICH with variability in size and location (157). Hence spontaneously induced stroke animal models are a preferred choice for study by our research group and other researchers throughout the world.

#### *1.10.2. Animal models for spontaneously occurring stroke*

The spontaneously hypertensive stroke-prone rat is a rat model in which stroke occurrence is spontaneous (166). SHRsp is widely used model for essential hypertension and cerebrovascular dysfunction. SHRsp rats have shown genetic susceptibility to stroke, independent of its severe hypertension (167). SHRsp was selectively bred from a sub-strain of

the spontaneously hypertensive rat (SHR), which were developed by selective cross-breeding of outbred Wistar Kyoto rats (156).

SHRsp develops high blood pressure at eight to nine weeks of age, leading to increase in cerebral blood vessel luminal pressure, increasing the chance of stroke development.

Hemorrhagic stroke development in SHRsp is also accompanied by stroke like symptoms (limb weakness, motor incoordination, drooling, dehydration, twitching and seizures) which are seen by 11-15 weeks when fed high salt diet (156,166). Middle cerebral artery (MCA) of SHRsp rats have been shown to lose their ability to constrict in response to elevations in transmural pressure (168) and show denervation of cerebral vessels increasing susceptibility of vessels to rupture (169), as experiments in SHRsp have demonstrated loss of pressure dependent constriction (PDC) in the MCA following hemorrhagic stroke (168).

Smeda and colleagues observed that the MCAs of post-stroke SHRsp depolarized but did not constrict to elevated potassium levels, suggesting a dysfunctional voltage gated calcium channels (170). The ability to respond to endothelial mediated responses to endogenous mediators such as bradykinin and NOS inhibitors was lost in post-stroke MCA accompanied with diminished response on the post-stroke MCA to protein kinase C (PKC) activation and intracellular calcium release with vasopressin stimulation (171). Smeda and colleagues also showed a loss of cerebral blood flow auto-regulation prior to stroke in SHRsp and observed that the loss of cerebral auto-regulation led to enhanced cerebral perfusion and facilitated development of hemorrhage (172).

SHRsp on a high salt diet, have increased vascular permeability up to two weeks before ICH, predicting hemorrhage, suggesting hypertensive ICH is preceded by vasculopathy (173). The development of endothelial dysfunction, inflammation, increased blood brain barrier leakage

and permeability are evident before the appearance of any stroke lesions (174,175). As mentioned earlier, vascular dysfunction and inflammation have been implicated in many diseases such as hypertension and stroke (39,102,114), and loss of cerebral autoregulation (and PDC) in the MCA of SHRsp suggest underlying signalling changes are taking place within the MCA as stroke develops indicating a need to investigate the progression to stroke. Previous studies on isolated post-stroke MCAs have shown diminished response to PKC activators (phorbol esters) indicating functional deterioration of the MCA, suggesting an underlying mechanism affecting the functioning of the vessel during stroke.

### ***1.11. Objectives and Hypothesis***

The major objective of this study is to determine cellular signalling changes (inflammatory and contractile) that occur before and after stroke in the vessel (MCA). The signalling changes may be responsible for loss of vascular tone and PDC in MCAs of SHRsp rats. The middle cerebral artery of pre-stroke and post-stroke SHRsp will be isolated after sacrifice, and flash frozen for use in either western blot or immunofluorescence. The expression and activation (phosphorylated and total) of both inflammatory (p38MAPK and ERK) and contractile (MLC and PKC) signalling pathways in the MCA before and after stroke will be determined using both western blot and immunofluorescence techniques. The study will also determine TRPV4 channel expression before and after stroke to identify the role of calcium channel signalling in MCA dysfunction.

This study will also try to determine the extent of neuro-inflammation and neuronal damage in the surrounding brain tissue of MCAs in SHRsp before and after stroke, and to

evaluate corresponding brain damage in the enclosing area of MCAs. The degree of neuro-inflammation will be compared between pre-stroke and post-stroke samples by immunofluorescent analysis of astrocyte and microglia activation in the brain region surrounding the MCAs. Similarly but independently, neuronal damage will be determined by hematoxylin and eosin staining analysis of cell vacuolation, neuron degeneration, cell infiltration and cell edema, in the pre-stroke and post-stroke samples.

Specific hypotheses of the study:

1. There will be a significant increase in the expression, as well as activation, of inflammatory signalling mechanisms (p38MAPK and ERK) in post-stroke MCAs, compared to pre-stroke MCAs.
2. The post-stroke MCAs will show a significant decrease in the expression, as well as activation, of signalling pathway (MLC and PKC) involved in vascular contraction compared to pre-stroke MCAs.
3. TRPV4 calcium channel expression will be higher in the post-stroke MCAs compared to pre-stroke MCAs.
4. The degree of astrocyte spread and microglial activation (neuro-inflammation) will be significantly higher in the post-stroke SHRsp compared to pre-stroke SHRsp.
5. Neuronal damage in the surrounding area of the MCA will be significantly higher in the post-stroke SHRsp compared to pre-stroke SHRsp.

## **2. Materials and Methods:**

### ***2.1. Animals***

All experimental procedures and animal breeding were carried out in compliance with the guidelines and recommendations set forth by the Animal Care ethics committee (Protocol Number: 15-30 ND) and the Canadian Council of Animal Care (Guide to care and Use of Experimental Animals, Vol 1, 2<sup>nd</sup> Edition) at the Animal Care Facility situated in the Health Science Centre of Memorial University of Newfoundland and Labrador. Stroke prone spontaneously hypertensive male rats (SHRsp; Charles River Laboratories, Quebec, Canada) were housed two per cage and bred in-house in ventilated cages under standard light cycle (12 hour light followed by 12 hour dark), controlled humidity and temperature condition. The SHRsp used in the study were fed Japanese style stroke-prone high salt diet containing 4% NaCl (Zeigler Bros., Inc., Pennsylvania, USA) from 5 weeks of age. Ad libitum access to food and water was permitted.

### ***2.2. General Experimental Design***

The rats were divided into two experimental groups and sampled based on the timeline of stroke (Figure 1). SHRsp rats were sacrificed before 10 weeks of age (at 9.3 weeks of age) for obtaining pre-stroke samples (n=24 per group) (166). To obtain the post-stroke samples, rats were monitored for external signs of behavioural distress. This consisted of weakness, lethargy, non-responsive to stimuli, pilo-erection, redness around eyes, hunched back, sluggish movement, twitching, immobility and full and continuous seizures. The appearance of any or a combination of the mentioned distress signs were the determining factors for post-stroke samples (generally around 15 weeks of age; n=24) (166). Animals were sacrificed for obtaining samples of MCA for immunofluorescence and western blot analysis.

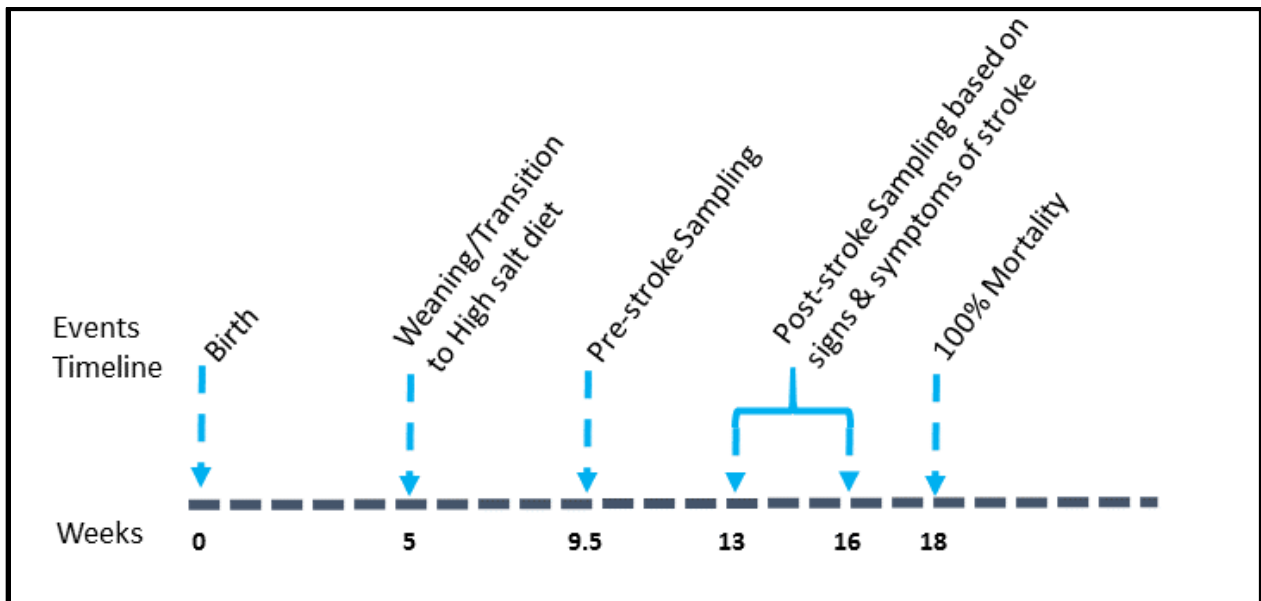


**Figure 2.1:** Experimental Timeline for sampling of pre-stroke and post-stroke samples when SHRsp rats are on High Salt Diet. [Figure (copyright clearance obtained) adapted from Dr. Noriko Daneshtalab research presentation].

### ***2.3. Sample isolation and tissue processing:***

At the time of sacrifice, rats were anaesthetized with an intraperitoneal injection of 50 mg: 10 mg/kg of ketamine:xylazine (Ketamine: Ketalean, Bimeda MIC, Animal Health Inc., Ontario, Canada and xylazine: Rompun, Bayer Inc., Ontario, Canada). The animals were then exsanguinated by cardiac puncture in the left ventricle, using a heparinized 10 mL syringe and 22 G needle. The blood samples were centrifuged at 45000 rpm for 10 minutes at 4°C within 30 minutes of sampling. The plasma was collected and stored at a -80° C until further analysis of pro-inflammatory cytokines. The brain was removed carefully and placed in 1x Phosphate Buffered Saline (PBS) for isolating MCA. For western blot experiments, both MCA's were peeled, flash frozen in liquid nitrogen and stored until analysis at -80° C. For immunofluorescence analysis, MCA's were cut alongside surrounding brain tissue, placed in a chip, and embedding medium (Tissue Tek : Sakura Finetech Inc. , California, USA) added. The chip was then placed on a small dish, flash frozen using liquid nitrogen, and stored in -80° C until experimentation. The rest of the brain was fixed in 10% neutral buffered formalin (NBF) for future histological examination of neurological damage.

### ***2.4. Immunofluorescence:***

#### ***2.4.1. Sectioning and standard process of immunofluorescence:***

The flash frozen MCA's with surrounding brain tissue were brought to -20° C in a cryotome (Fisher Scientific, Pittsburgh, PA, USA) and 8 micrometer ( $\mu\text{m}$ ) sections were cut and placed on charged slides (4 slices/slide) and then stored at -20° C until processed for immunofluorescence (IF) studies. The MCA were analysed for the expression of various receptors and proteins. These consisted of the calcium channel receptor Transient Receptor Potential Cation Channel (TRPV4), Phosphorylated and total Extracellular signal regulated kinases (ERK1/2) and p38 Mitogen Activated Protein Kinase (p38MAPK), the activated and total Protein Kinase C (PKC) and Myosin Light Chain (MLC). The brain tissue surrounding the MCA was analysed for activation of astrocytes and microglia to determine extent of neuro-inflammatory activation.

Slides containing sections of MCA were thawed [10 minutes at room temperature (RT)] and washed in 1x PBS. The slides then underwent different processing based on the primary antibody of interest, shown in **Table 2.1**. In general, the sections were fixed either with 4% paraformaldehyde (PFA) for 20 minutes at RT or acetone for 15 minutes at -20° C, then were rinsed with 1x PBS. Some samples underwent 3% hydrogen peroxide treatment for 15 minutes at RT to prevent oxidation. Antigen retrieval process was required by some antibodies, with either citrate buffer at 100° C for 30 minutes or 0.5% or 1% sodium dodecyl sulfate (SDS). The sections were then blocked [with 5% or 10% normal goat serum (NGS)] at room temperature for one hour. Primary antibody was then added, reconstituted in 2% NGS in 1x PBS, overnight at 4° C.

The next day, the sections were washed with Tris-buffered saline (TBS) 5 times for 10 minute intervals, followed by incubation with the secondary antibody specific against the species used to generate the primary antibody (made up in 2% NGS in TBS) for 30 minutes at room temperature. After further washing with TBS (5 times at 10 minute intervals), the sections were finally coated with 50/50 Glycerol: distilled water solution, coverslipped and sealed with clear nailpolish. Samples were imaged within two hours of the staining process using an Olympus FV1000 confocal microscope (Olympus Inc., Miami, FL, USA). The Sections were imaged using FV10-ASW (Version 1.7) Software at either 40x (zoomed in 1.4 times) or 20x (zoomed in 2.8 times). Parameters were kept constant among all samples being analyzed for quantification comparison.

**Table 2.1.:** Specific details for the blocking solution, antibodies and reagents used in protocols for immunofluorescence.

<b>Protein of interest</b>	<b>Blocking Solution composition (length of incubation)</b>	<b>Antigen Retrieval Procedure (length of incubation)</b>	<b>Primary Antibody and Dilution (Day 1) (<u>Overnight at 4° C</u>) [company of purchase]</b>	<b>Dilution of Secondary Antibody (Day 2) (<u>30 minutes at RT</u>) [Jackson Immunoresearch unless otherwise indicated]</b>
P-p38MAPK	10% Normal Goat Serum +0.1% Triton-X in 1X PBS (1 Hour at RT)	1% SDS (4 minutes at RT)	P-p38MAPK (1:100) Rabbit mAb. [Cell Signalling (4511S)]	Goat anti-rabbit Cy5 (1:400) + DAPI (1:1000).
T-p38MAPK	5% Normal Goat Serum +0.1% Triton-X in 1X PBS (1 Hour at RT)	1% SDS (3 minutes at RT)	T-p38MAPK (1:100) Rabbit mAb. [Cell Signalling (9212S)]	Goat anti-rabbit Cy5 (1:150) + DAPI (1:1000).
P-ERK1/2	10% Normal Goat Serum +0.1% Triton-X in 1X PBS (1 Hour at RT)	1% SDS (4 minutes at RT)	P-ERK1/2 (1:100) Rabbit mAb. [Cell Signalling (4370S)]	Goat anti-rabbit Cy5 (1:200) + DAPI (1:1000).
T-ERK1/2	10% Normal Goat Serum +0.1% Triton-X in 1X PBS (1 Hour at RT)	1% SDS (5 minutes at RT)	T-ERK1/2 (1:75) Rabbit mAb. [Cell Signalling (4695S)]	Goat anti-rabbit Cy2 (1:300) + DAPI (1:1000).
P-PKC	10% Normal Goat Serum +0.1% Triton-X in 1X PBS (1 Hour at RT)	1% SDS (4 minutes at RT)	P-PKC (1:75) Rabbit mAb. [Cell Signalling (9371S)]	Goat anti-rabbit Cy5 (1:400) + DAPI (1:1000).
T-PKC	10% Normal Goat Serum +0.1% Triton-X in 1X PBS (1 Hour at RT)	0.5% SDS (3 minutes at RT)	T-PKC (1:50) Mouse mAb. [Santa Cruz (SC-17804)]	Goat Anti-mouse Rhodamine Red-X (1:400) + DAPI (1:1000).

<b>Protein of interest</b>	<b>Blocking Solution composition (length of incubation)</b>	<b>Antigen Retrieval Procedure (length of incubation)</b>	<b>Primary Antibody and Dilution (Day 1) (<u>Overnight at 4° C</u>) [company of purchase]</b>	<b>Dilution of Secondary Antibody (Day 2) (<u>30 minutes at RT</u>) [Jackson Immunoresearch unless otherwise indicated]</b>
P-MLC	2.5% Bovine Serum Albumin +0.1% Triton-X in 1X PBS (1 Hour at RT)	NA	P-MLC2 (1:75) Rabbit mAb. [Cell Signalling (3671S)]	Goat anti-rabbit Cy5 (1:400) + DAPI (1:1000).
T-MLC	2.5% Bovine Serum Albumin +0.1% Triton-X in 1X PBS (1 Hour at RT)	0.5% SDS (4 minutes at RT)	T-MLC2 (1:250) Rabbit mAb. [Cell Signalling (3672S)]	Goat anti-rabbit Cy2 (1:400) + DAPI (1:1000).
TRPV4	10% Normal Goat Serum +0.1% Triton-X in 1X PBS (1 Hour at RT)	NA	Anti-TRPV4 (1:100) Rabbit pAb. [Abcam (ab39260)]	Goat anti-rabbit Cy5 (1:300) + DAPI (1:1000).
Astrocytes	10% Normal Goat Serum +0.1% Triton-X in 1X PBS (2 Hour at RT)	NA	GFAP-Cy3 (1:1000). [Sigma Aldrich (C9205)]	DAPI (1:1000)
Microglia	10% Normal Goat Serum +0.1% Triton-X in 1X PBS (2 Hour at RT)	NA	Iba 1 (1:1000). [Wako Chemical: (019-19741)]	Goat anti-rabbit Cy5 (1:150) + DAPI (1:1000).

#### *2.4.2. Quantification of immunofluorescent images:*

Each sample was imaged for a Z stack of 8 slices of 1  $\mu\text{m}$  each followed by global calibration and conversion to grayscale in Fiji software (ImageJ, U. S. National Institutes of Health, Bethesda, Maryland, USA). The vessel area (V) was determined in a precise manner with freehand selection tool and the mean gray value (MGV) of the vessel was measured. Mean gray value is the total pixel intensity of the measured area divided by the total measured area. MGV is expressed as pixel intensity per square millimetre. Three random readings from the image background (B1, B2 and B3) were obtained and the mean gray value of the background was subtracted from the mean gray value of the vessel to get the actual optical fluorescence density of the vessel (M2), as shown in **Figure 2.2**.

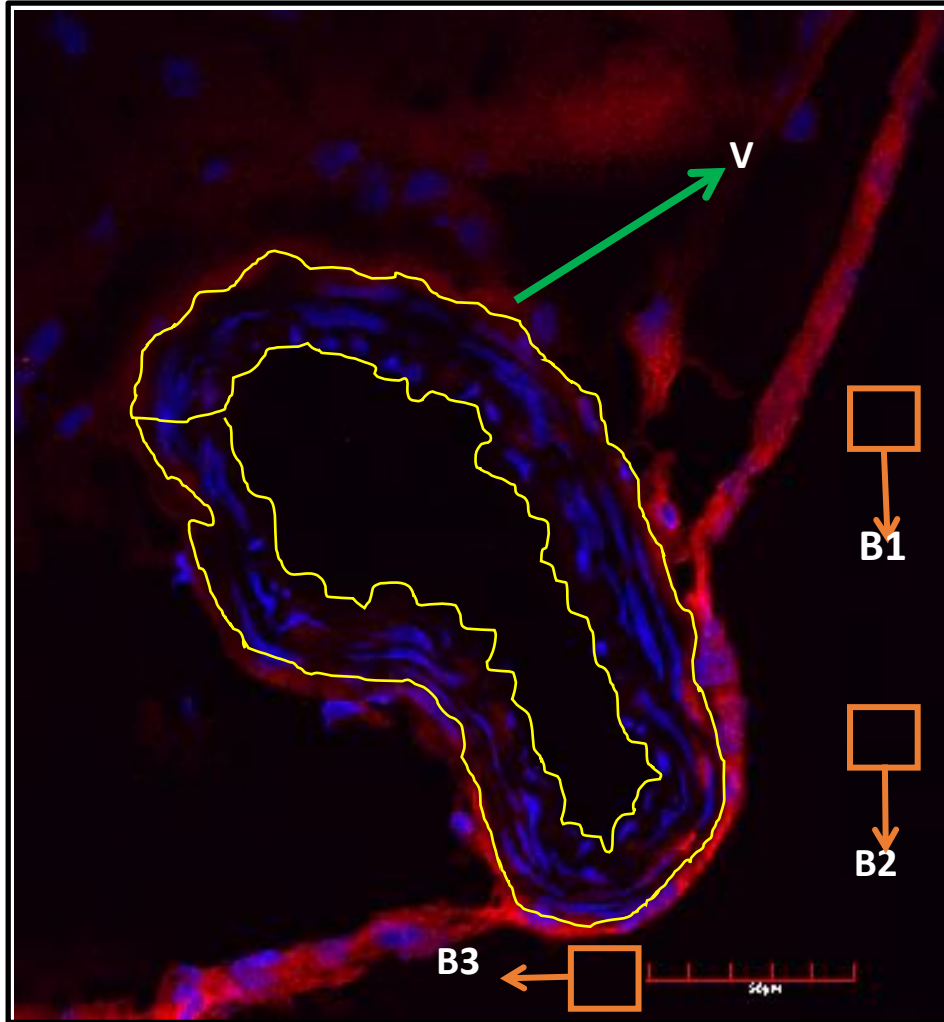


**Figure 2.2:** Representation of the semi-quantification process for measuring immunofluorescent staining of protein of interest in the MCA by Image J. V is the Vessel Area used for determination of mean gray value for protein of interest. B1, B2 and B3 are background area measurements used for determination of mean gray value (MGV) for the background.

$$\text{Fluorescence for protein of interest} = \text{MGV (V)} - \text{MGV} \left\{ \frac{\text{B1} + \text{B2} + \text{B3}}{3} \right\}$$

## ***2.5. Neurological Degeneration:***

### *2.5.1 Sampling and processing for H and E Stain*

The brain samples, fixed in 10% NBF were embedded in paraffin before slicing and 6  $\mu\text{m}$  coronal sections where MCAs feed into the M2 section [anterior region extending from insula with the opercular segments [parietal and temporal] included]. The paraffin embedded sections were de-paraffinized in xylene for 35 minutes, and rehydrated by placing in decreasing concentrations of alcohol: Absolute, 95%, 80% and 70%, for 2 minutes each. A quick rinse (1 minute in water) was performed and the slides were stained with Mayer's haematoxylin for 15-30 min. Slides were rinsed with water for 1 minute and placed in Scott's Tap Water Substitute (S.T.W.S.) for 3 minutes until the sections turned blue. Slides were washed for 5 minutes with water and were stained with eosin for 2 minutes. A quick dehydration was performed in 95% and absolute alcohol. The slides were then cleaned in xylene and sealed with a coverslip. This procedure stains nuclei in blue and tissue components in different shades of pink. Slides were used to determine neurological degeneration around the M2 region of the MCAs.

### *2.5.2. Quantification for Neural Damage:*

Neural and brain damage were analyzed by assessing cell vacuolation, neuron degeneration, areas of edema and area of cell infiltration. A semi-quantitative scoring scheme was used to determine the extent of neural damage by combining the scores obtained from all four assessments outlined in **Table 2.2** and adapted from Fedchenko et al. (176). Cell vacuolation and neuron degeneration are two important parameters that can be morphologically assessed using H and E stain for determining the degree of cell death. It is characterized by axonal swelling and associated cell death in the white matter occurring spontaneously or via a wide range of stimuli (177). The grading scheme for this cell death are ranked from 0 to 10, where cell count were graded on a point system. The vacuolation was graded 10 cells per point, with the maximum number of vacuolation quantifiable being 80. The degenerating neurons were graded 2 cells per point. Areas of edema and areas of cell infiltration (also indicators of brain injury and damage) were quantified separately, and graded 10% for each point, the total being the complete image area. The grading scheme for the area detection is a modified version adopted from the

“quickscore” system (178), that assigns values from 1 to 6 in proportion, and multiplication is recommended instead of addition for processing of final score range. A total final score was determined via summation of the four separate parameters to indicate total neuronal damage evident in the samples.

**Table 2.2.:** Scoring system for four semi-quantifiable parameters (Cell vacuolation, degenerating neurons, area of cell oedema and area of cell infiltration)

Score assigned	Number of Cells undergoing vacuolation (A)	Number of degenerating neurons (B)	Percentage of area of oedema (C)	Percentage of area of Cell infiltration (D)
0	0 (Lowest Value)	0 (Lowest Value)	0 (Lowest Value)	0 (Lowest Value)
1	1-10	1-2	1-10 %	1-10 %
2	11-20	3-4	11-20 %	11-20 %
3	21-30	5-6	21-30 %	21-30 %
4	31-40	7-8	31-40 %	31-40 %
5	41-50	9-10	41-50 %	41-50 %
6	51-60	11-12	51-60 %	51-60 %
7	61-70	13-14	61-70 %	61-70 %
8	71-80	15-16	71-80 %	71-80 %
9	81-90	17-18	81-90 %	81-90 %
10	91-100 (Highest Value)	19-20 (Highest Value)	91-100 % (Highest Value)	91-100 % (Highest Value)

Final Score for Neural Damage:  $A + B + C + D$

Final score is the total of the score assigned for cell vacuolation, neuron degeneration, area of oedema and area of cell infiltration. A High final score indicates higher brain damage. The data obtained from the images with objective magnification of 20x was used to determine the final score for each sample.

## 2.6. Western Blot

### 2.6.1. Sample Lysis and Aliquot preparation

MCA samples were lysed in radioimmunoprecipitation assay (RIPA) buffer (recipes for all solutions listed in **Table 2.3**) using precellys beater tubes (Bertin Corp, Maryland, USA). Two MCA's from each sample were homogenized in 150  $\mu$ l of RIPA Buffer. The protocol 2 (5000 RPM for 2 minutes and 20 seconds) was run in the precellys instrument (Bertin Corp, Maryland, USA) for sample homogenization. The samples were allowed to sit on ice for 15-20 minutes for the foam to settle down and the supernatant was collected from the beater tube and transferred to a new microcentrifuge tube which was then sonicated for 7 minutes. The beater tube was further centrifuged at 25000 RPM for 5 minutes at 5° C and the remaining lysate was transferred to the sonicated microcentrifuge tubes in order to maximise lysate yield per sample. The sample was then re-centrifuged at 25000 RPM for 5 minutes at 5° C and bicinchoninic acid (BCA) protein analysis was performed on the collected supernatant.

### 2.6.2. BCA Protein Assay

BCA Protein assay was performed to determine the amount of lysate sample present. One mL of BSA Stock was prepared in distilled water (1 mg/mL) for the protein assay and a standard curve was made in duplicate wells to make the following standard curve : 0, 2.5, 5, 10 and 20  $\mu$ g ( BSA Stock Solution) and 2.5  $\mu$ L RIPA Buffer was added to all wells Buffer (recipes for all solutions listed in **Table 2.3**). The lysate samples were then added to duplicate wells (2.5  $\mu$ L of sample lysate) and 300  $\mu$ L of BCA Reagent was added to all wells (Reagent A: Reagent B =1:20). The plate was covered and incubated for 30 minutes at 37°C and the absorbance was measured at 562 nm in a plate reader (Fluostar Optima, BMG Labtech, NC, USA). The absorbance values obtained for standard curve and samples were entered in an excel sheet. The amount of sample lysate required for 10  $\mu$ g protein was calculated on the basis of standard curve obtained by using Microsoft Excel 2010 (Microsoft Corporation, Redmond, WA, USA). Aliquots were prepared for 10  $\mu$ g protein for lysed sample in sample loading buffer (Laemmli Sample Buffer 5X +  $\beta$ -mercaptoethanol) and heated to 100°C for 3 minutes. Aliquots were allowed to cool down to room temperature for 5 minutes and stored at -20°C until use.

**Table 2.3.:** List of solutions used in western blot and immunofluorescence

1.1. Reagents for Western Blot:

1.1.1. RIPA Buffer

Stock Solutions	Volume made		
	2.5 mL	5 mL	10 mL
10x PBS	0.25	0.5	1
10% Triton-X	0.25	0.5	1
10% Deoxycholic Acid	0.125	0.25	0.5
1M Tris-HCL, pH 7.4	0.125	0.25	0.5
1M Beta-glycerophosphate	0.125	0.25	0.5
1M NaF	0.125	0.25	0.5
0.5M EDTA, pH 7.5	25 µL	50 µL	0.1
20% SDS	12.5 µL	25 µL	50 µL
10x protease inhibitors	0.25	0.5	1
10x phosphatase inhibitors	0.25	0.5	1
PMSF* (50 microgram/L)	7.5 µL	15 µL	30 µL
Sodium Orthovanidate (200mM)	25 µL	50 µL	0.1
Autoclaved dH <sub>2</sub> O	0.93	1.86	3.72

All units in mL, otherwise specified.

\*Water to be added first, PMSF just prior to use

1.1.2. BCA Reagent (Thermo Scientific) #23225

Reagents	Total Volume of BCA Reagent made	
	10 mL	20 mL
Pierce BCA Protein Assay Reagent A	9.8 mL	19.6 mL
Peirce BCA Protein Assay Reagent B	0.2 mL	0.4 mL

1.1.3. Albumin Standard (Thermo Scientific) #23209

Aliquots of 85 µL made out of 1 vial of 1 mL bovine Serum Albumin.

#### 1.1.4. Sample Buffer 5X

Solutions	Volume made	
	100 mL	200 mL
Glycerol	10 mL	20 mL
Stacking Buffer	2 mL	4 mL
20% SDS	25 mL	50 mL
Bromophenol Blue	0.125 g	0.250 g
dH <sub>2</sub> O	58 mL	116 mL

#### 1.1.5. Denaturing Solution

Solution used	Volume Made	
	500 µL	1000 µL
laemmli Buffer 5X	475 µL	950 µL
B-mercaptoethanol	25 µL	50 µL

#### 1.1.6. Recipe for Gel

##### 1.1.6.1. Separating/Running Gel

Solution used	Percentage of Gel for 2 mini gels				
	7.5%	8.5%	10%	12.5%	15%
Water (mL)	9.22	8.54	7.54	5.88	4.22
Acrylamide (mL)	5.00	5.67	6.67	8.33	10.0
Running Gel Buffer (mL)	5.00	5.00	5.00	5.00	5.00
20% SDS	100 µL	100 µL	100 µL	100 µL	100 µL
TEMED	20 µL	10 µL	10 µL	10 µL	10 µL
2.8% APS (mL)	0.66	0.66	0.66	0.66	0.66

#### 1.1.6.2. Stacking Gel

Solution used	Recipe for Gels	
	2 mini gels	1 mini gel
Water (mL)	9.50	4.75
Acrylamide (mL)	1.80	0.90
Running Gel Buffer (mL)	1.50	0.75
20% SDS	60 $\mu$ L	30 $\mu$ L
TEMED	35 $\mu$ L	17.5 $\mu$ L
2.8% APS (mL)	0.40	0.20

#### 1.1.6.3. Stacking Buffer (1 L)

1. Dissolve 59.8 g Tris in approximate 400 mL of dH<sub>2</sub>O
2. Adjust pH to 6.8 with 10N HCl (Do not go over)
3. Add dH<sub>2</sub>O up to 1 L
4. Filter Solution through 0.45  $\mu$ m filter

#### 1.1.6.4. Running Gel Buffer (1 L)

1. Add 181 g Tris to 600 mL of dH<sub>2</sub>O
2. Adjust pH to 8.9 with 10N HCl (Do not go over)
3. Add dH<sub>2</sub>O up to 1 L
4. Filter Solution through 0.45  $\mu$ m filter

#### 1.1.6.5. 2.8% APS (50 mL)

1. 0.28 g Ammonium Persulfate
2. 10 mL autoclaved dH<sub>2</sub>O

#### 1.1.6.6. 30% Acrylamide (37.5:1 Acrylamide:bisAcrylamide)

2. 37.5 g Acrylamide
3. 1g Bis-Acrylamide

4. Dissolve in 128 mL dH<sub>2</sub>O on heated stir-plate
5. Filter Solution through 0.45 µm filter
6. Measure pH to ensure pH is less than 7.0

#### 1.1.6.7. Electrophoresis Buffer (Protein Gel Running Buffer)

Chemicals used	Final Volume of 8 L
Tris Base	24.2 g
Glycine	115.4 g
SDS	8 g
dH <sub>2</sub> O	Make up to 8 L

#### 1.1.7. TBST

Chemicals used	Final Volume of 8 L
1 M Tris Base pH 8	80 mL
2.5 M NaCl	240 mL
Tween-20 50%	4 mL
dH <sub>2</sub> O	Make up to 4 L

#### 1.1.8. 1 M Tris Base pH 8

1. Dissolve 60.57 g of Tris Base in 500 mL of dH<sub>2</sub>O
2. Adjust the pH to 8 by 10N HCl
3. Filter Solution through 0.45 µm filter

#### 1.1.9. 2.5M NaCl

1. Dissolve 146.5g NaCl in 1 L dH<sub>2</sub>O in volumetric flask
2. Stir it for 1 hour. Make upto 1 L by adding dH<sub>2</sub>O

## 1.2. Reagents for Immunofluorescence:

### 1.2.1. TBS

Chemicals used	Final Volume of 8 L
1 M Tris Base pH 8	80 mL
2.5 M NaCl	240 mL
dH <sub>2</sub> O	Make up to 4 L

### 1.2.2. Rest of the solutions:

Solution	Stock Solution Used	Diluted in
1X PBS (1 L)	10X PBX (100 mL)	dH <sub>2</sub> O (900 mL)
10% NGS (10 mL)	100% NGS (1 mL)	1X PBX (9 mL)
1% SDS (10 mL)	10% SDS (1 mL)	1X PBS (9 mL)
50/50 Glycerol (10 mL)	Glycerol (5 mL)	dH <sub>2</sub> O (5 mL)

### 2.6.3. SDS-PAGE and immunoblotting

Each sample aliquot containing 10 µg of protein was loaded in to separate lanes for electrophoreses on 10% SDS-PAGE gels. The gels were run at 15 mA/gel while samples were in stacking gel and at 22 mA/gel after samples entered the running gel Buffer (recipes for all solutions listed in **Table 2.3**). The proteins on the gel were then transferred to polyvinylidene fluoride (PVDF) membrane (EMD, Millipore, MA, USA) at 100V for one hour, blocked for 60 minutes by 5% non-fat dry milk (NFDM) in Tris-buffered Saline and Tween 20 (TBST), and incubated overnight at 4°C with primary antibodies of interest (as listed in the **Table 2.4**). Primary antibody dilutions ranged from 1:1,000 to 1:3,000 based on the antibody. The membrane was washed 5 times at 5 minutes interval with TBST, followed by incubating the membrane in species-specific antibody conjugated with horseradish peroxidase (HRP) for 60 minutes at room temperature. The membrane was again washed 5 times at 5 min intervals before imaging. The bands were detected and visualized with chemiluminescent substrate (SuperSignal West Pico, Pierce, Rockford, IL, USA) using the enhanced chemiluminescence imager: LAS400 (GE Healthcare, Chicago, IL, USA). Densitometry analysis of imaged blots was performed on the same system by Imagequant TL (GE Healthcare, Chicago, IL, USA). After imaging the same membrane was stripped with stripping buffer for 10 minutes at 50°C. The membrane was washed once with TBST for 5 minutes and then re-blocked with 5% milk in TBST for an hour and incubated overnight with primary antibody (Phosphorylated or Total protein or GAPDH). The same process of the washes, incubation and detection was repeated for the detection of total protein and/or control protein. The loaded total protein was normalized to the Glyceraldehyde 3-phosphate dehydrogenase (GAPDH) protein band density. Loading proteins like beta-actin and alpha-tubulin were initially attempted, but gave inconsistent detection between samples.

**Table 2.4.:** Specific details for the blocking solution, antibodies and reagents used in protocols for western blot.

<b>Protein of interest</b>	<b>Blocking Solution:</b> (Day 1: 1 hour)	<b>Primary Antibody</b> (Day 1: Overnight) <i>[company of purchase]</i>	<b>Secondary Antibody</b> (Day 2: Afternoon) <i>[Santacruz unless otherwise specified]</i>	<b>Primary Antibody</b> (Day 2: Overnight) <i>[company of purchase]</i>	<b>Secondary Antibody</b> (Day 3: Afternoon) <i>[Santacruz unless otherwise specified]</i>
ERK1/2	5% Milk in TBST	P-ERK 1/2 (1:1000) in 5% Milk (10 mL). Rabbit mAb. <i>[Cell Signalling (4370S)]</i>	Anti-Rabbit HRP Labelled (1:3000) in 5% Milk (15 mL).	T-ERK1/2 (1:1000) In 5% Milk (10 mL).Rabbit mAb. <i>[Cell Signalling (4695S)]</i>	Anti-Rabbit HRP Labelled (1:3000) in 5% Milk (15 mL).
p38MAPK	5% Milk in TBST	P-p38MAPK (1:1000) in 5% Milk (10 mL). Rabbit mAb. <i>[Cell Signalling (4511S)]</i>	Anti-Rabbit HRP Labelled (1:3000) in 5% Milk (15 mL).	T-p38MAPK (1:1000) in 5% Milk (10 mL). Rabbit mAb. <i>[Cell Signalling (9212S)]</i>	Anti-Rabbit HRP Labelled (1:3000) in 5% Milk (15 mL).
PKC	5% Milk in TBST	P-PKC (1:750) in 5% Milk (10 mL) Rabbit mAb. <i>[Cell Signalling (9371S)]</i>	Anti-Rabbit HRP Labelled (1:3000) in 5% Milk (15 mL).	T-PKC (1:50) in 5% Milk (10 mL) Mouse mAb. <i>[Santa Cruz (SC-17804)]</i>	Anti-Mouse HRP Labelled (1:2000) in 5% Milk (15 mL).
GAPDH	5% Milk in TBST	GAPDH (1:1000) in 5% Milk (10mL) Rabbit mAb. <i>[Cell Signalling (14C10)]</i>	Anti-Rabbit HRP Labelled (1:3000) in 5% Milk (15 mL).	As applicable	As applicable

#### *2.6.4. Quantification of bands*

The imaged blots were quantified by Imagequant TL Software. The sample lanes were first detected, followed by detection of the protein of interest. The band area was adjusted individually to accommodate entire band for each sample. The bands were then calibrated for background with rolling ball (50) option. The peaks of bands were determined manually and the densitometry intensity of bands were measured. A similar process was followed to obtain the densitometry for total protein or loading Control (GAPDH). For obtaining relative densitometry, the ratio of phosphorylated over total protein and total protein over GAPDH was determined by Microsoft Excel 2010 (Microsoft Corporation, Redmond, WA, USA).

#### *2.7. Statistical analysis*

Statistical analysis was performed using Excel 2010 (Microsoft Corporation, Redmond, WA, USA) and SigmaPlot 12.5 (Systat Software Inc., San Jose, CA, USA). Data were analyzed using unpaired 2 tailed Student's T-test. Values of  $p < 0.05$  were considered statistically significant.

### **3. Results:**

#### ***3.1. Detection of phosphorylated and total MLC in MCA by immunofluorescence***

MCA Vessels from pre-stroke and post-stroke SHRsp rats were stained for detection of phosphorylated and total MLC. **Figure 3.1A** shows representative images of vessels from each group stained for phosphorylated MLC. The intensity of fluorescent signals from phosphorylated MLC stain was relatively low in both experimental groups resulting in a low mean gray value. MLC was detected primarily in the smooth muscle cells of the MCA. Semi-quantitative analysis showed significantly increased localization of phosphorylated MLC in post-stroke MCA's compared to pre-stroke (**Figure 3.1B**;  $P < 0.05$ ). The expression of total MLC is shown by representative images in **Figure 3.2A**. **Figure 3.2B** shows the semi-quantitative analysis of the fluorescence signal from the total MLC staining for both experimental groups. There was no statistically significant difference between the mean gray value of total MLC in MCA of pre-stroke and post-stroke SHRsp rats ( $P > 0.05$ ).

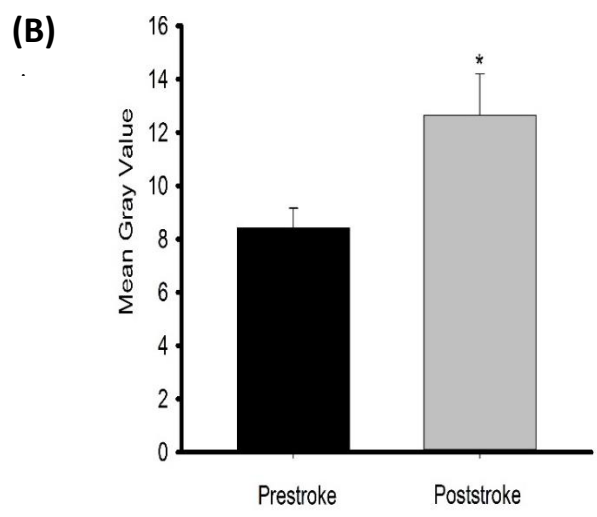
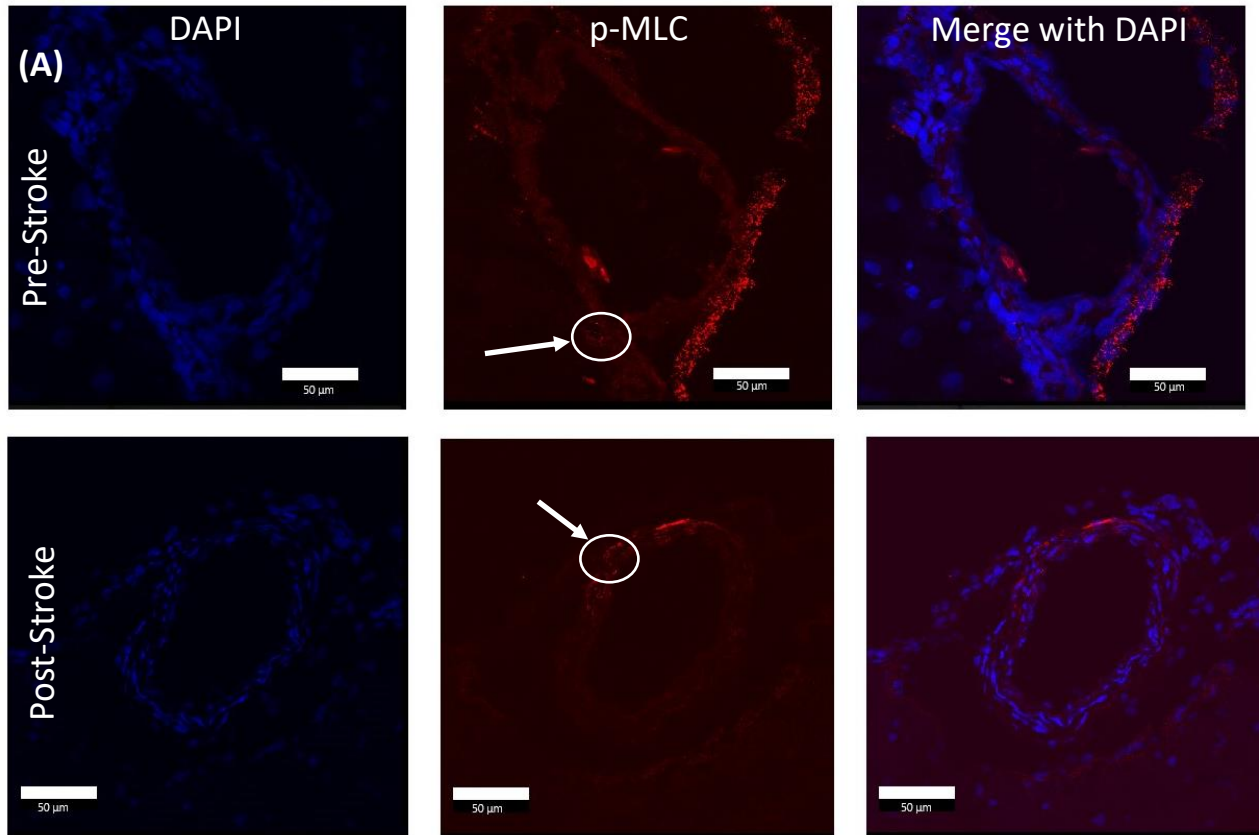


**Figure 3.1:** (A) Representative images for phosphorylated MLC Staining (P-MLC2 (1:75), Cy5 (1:400) and DAPI (1:1000)). 8μm slices of MCA were imaged as a Z-stack at 40x objective using confocal microscopy and fluoview software. Semi-Quantification of images performed by Image J software. (B) IF Analysis: Mean Gray Value for phosphorylated MLC in MCAs of pre-stroke and post-stroke animals (n=6 per group). \* indicates  $p < 0.05$  analyzed using unpaired Student's t-test. White arrows indicate phosphorylated MLC staining in the smooth muscle cells of MCA.

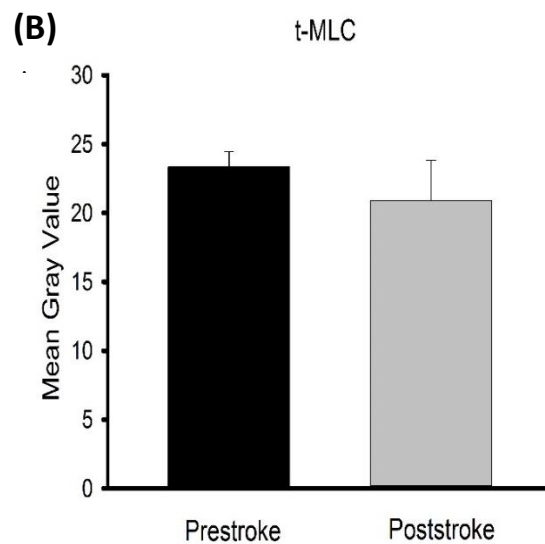
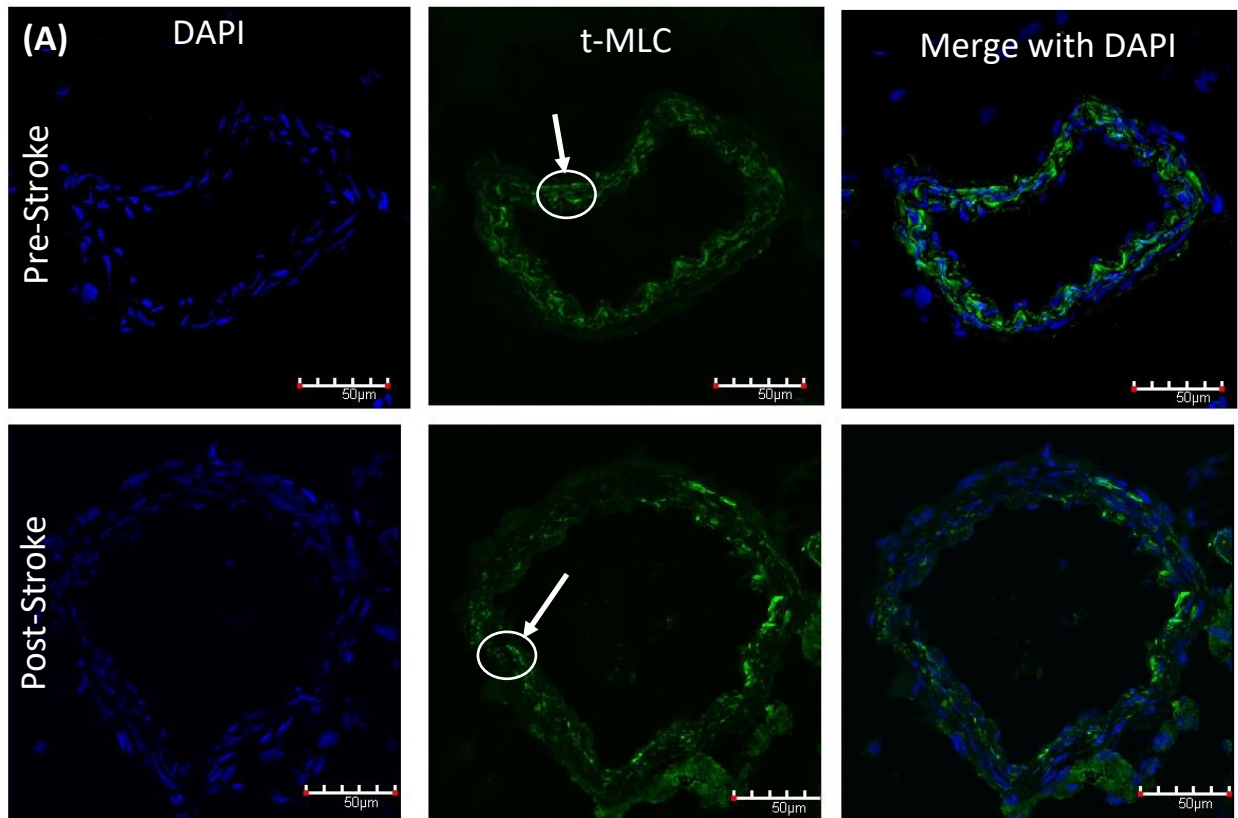


**Figure 3.2:** (A) Representative images for Total MLC Staining (T-MLC2 (1:250), Cy5 (1:400) and DAPI (1:1000)). 8µm slices of MCA were imaged as a Z-stack at 40x objective using confocal microscopy and fluoview software. Semi-Quantification of images performed by Image J software. (B) IF Analysis: Mean Gray Value for total MLC in MCAs of pre-stroke and post-stroke animals (n=5 per group). White arrows indicate total MLC staining in the smooth muscle cells of MCA.

### ***3.2. Detection of phosphorylated and total MLC in MCA by western blot***

Western blot analysis to obtain a ratio of phosphorylated MLC over total MLC in the MCA samples did not yield any results despite making major and minor modifications such as: increasing sample loading, increasing concentration of primary and/or secondary antibody, consulting with technicians from the antibody company, trying antibodies from another companies and such. Although weak bands could be seen for total MLC after modifications in the procedure, the blots failed to show up any signal for phosphorylated MLC and hence the ratio of phosphorylated over total MLC could not be obtained. The bands of total MLC were normalised to loading control (GAPDH), but the signal for total MLC was very weak and hence it skewed the ratio of total MLC over GAPDH.

### ***3.3. Detection of phosphorylated and total PKC in MCA by immunofluorescence***

Expression of phosphorylated and total PKC in MCA vessels of pre-stroke and post-stroke SHRsp rats was determined by immunofluorescent staining. Both phosphorylated, as well as total PKC, were highly expressed in the smooth muscle cells relative to the endothelium. **Figure 3.3A** shows representative images for staining of phosphorylated PKC from both groups. Semi-quantitative analysis of phosphorylated PKC staining, in the form of mean gray value showed significantly greater expression in pre-stroke compared to post-stroke (**Figure 3.3B**;  $P < 0.001$ ). Detection of total PKC was performed by staining MCA's from both groups (**Figure 3.4A**). There was no difference in expression of total PKC between the groups. (**Figure 3.4B**);  $P > 0.05$ ).

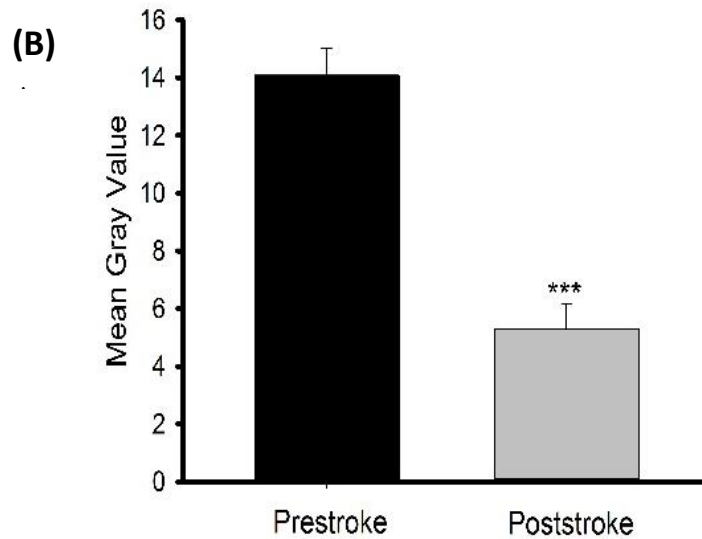
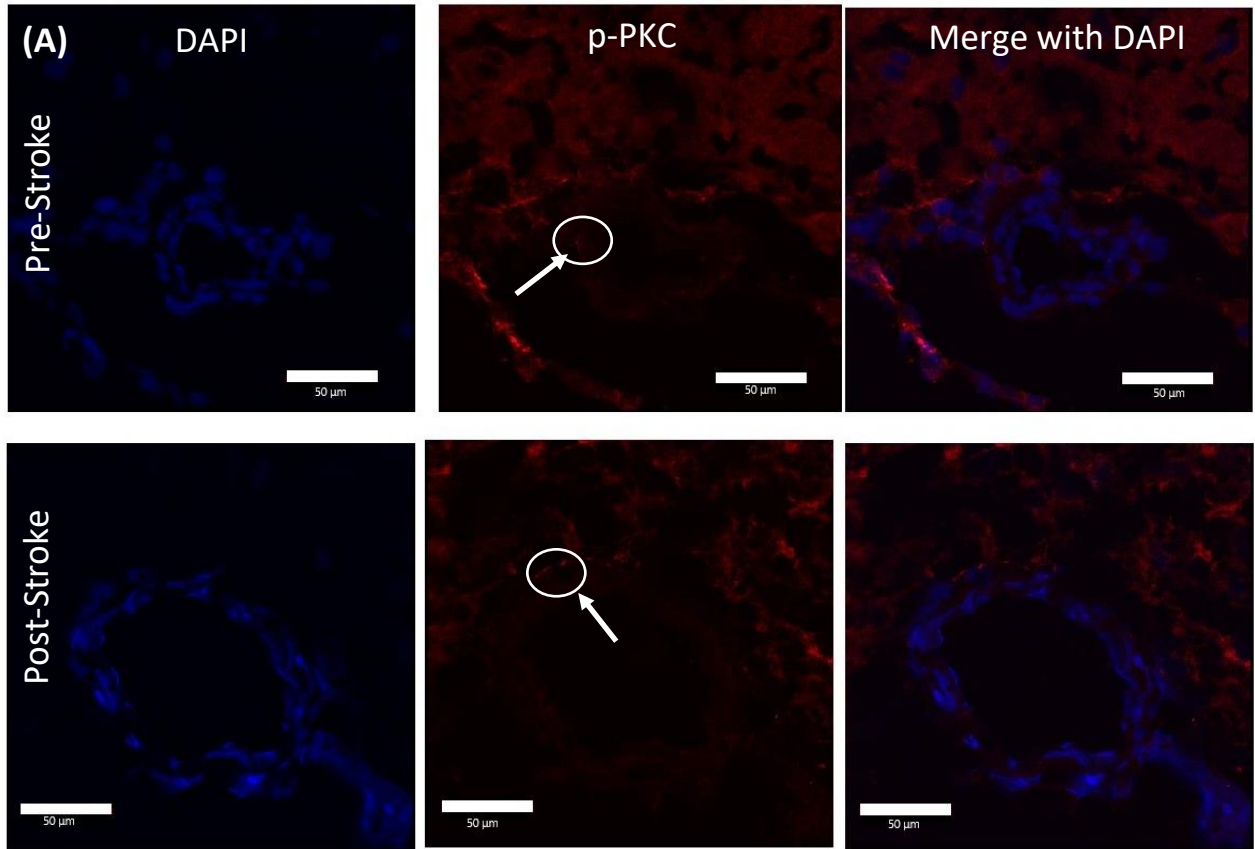


**Figure 3.3:** (A) Representative images for Phosphorylated PKC Staining (P-PKC (1:75), Cy5 (1:400) and DAPI (1:1000)). 8 $\mu$ m slices of MCA were imaged as a Z-stack at 40x objective using confocal microscopy and fluoview software. Semi-Quantification of images performed by Image J software. (B) IF Analysis: Mean Gray Value for phosphorylated PKC in MCAs of pre-stroke and post-stroke animals (n=6 per group). \*\*\* indicates p<0.001 analyzed using unpaired Student's t-test. White arrows indicate phosphorylated PKC staining in the smooth muscle cells of MCA.

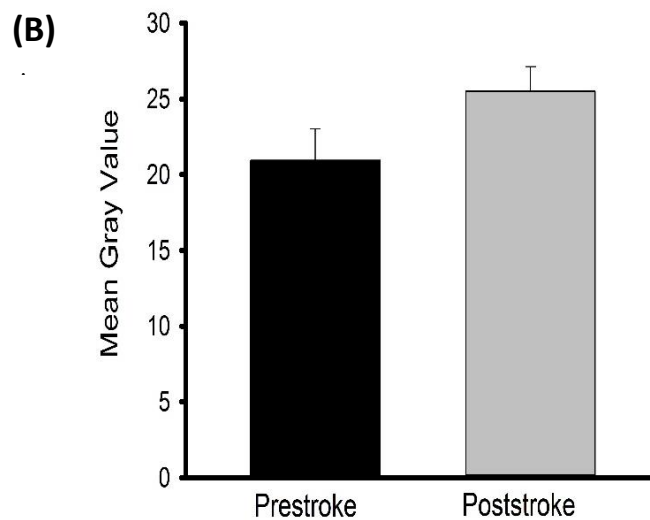
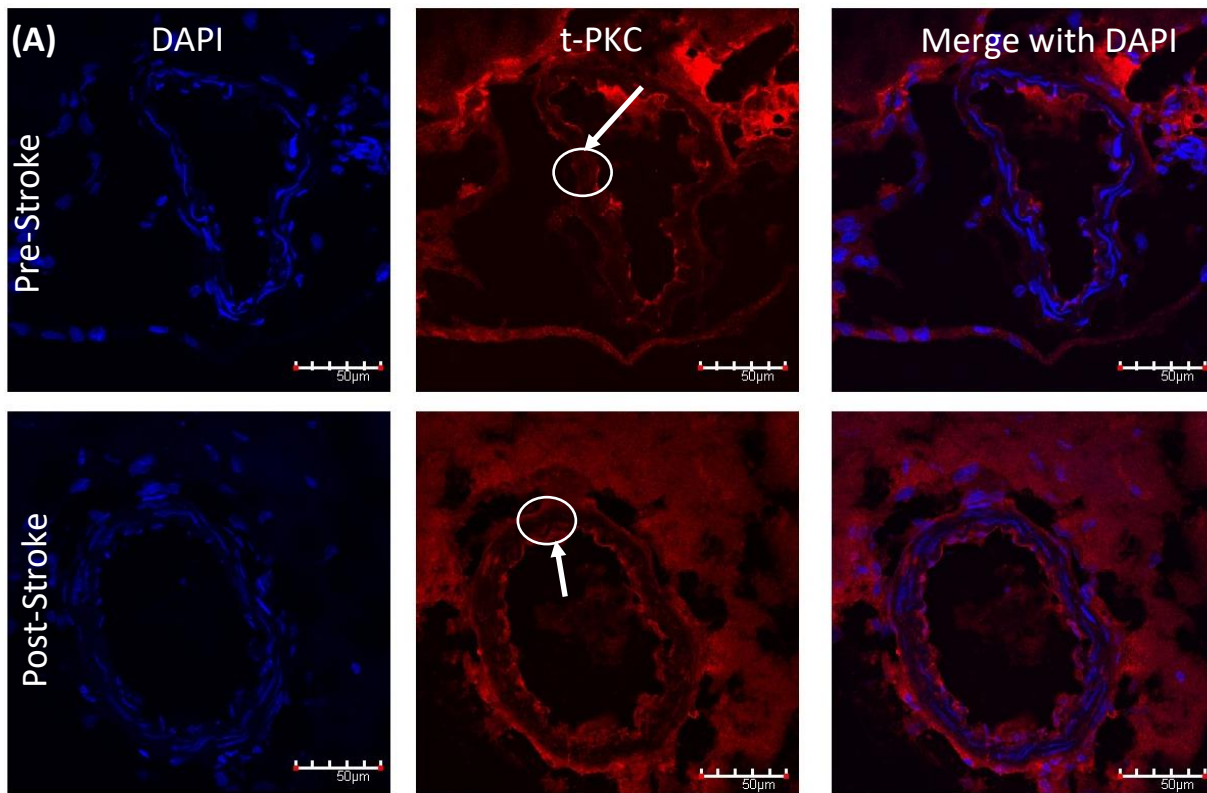


**Figure 3.4:** (A) Representative images for Total PKC Staining (T-PKC (1:50), Cy5 (1:400) and DAPI (1:1000)). 8µm slices of MCA were imaged as a Z-stack at 40x objective using confocal microscopy and fluoview software. Semi-Quantification of images performed by Image J software. (B) IF Analysis: Mean Gray Value for total PKC in MCAs of pre-stroke and post-stroke animals (n=6 per group). White arrows indicate total PKC staining in the smooth muscle cells of MCA.

### ***3.4. Detection of phosphorylated and total PKC in MCA by western blot***

The ratio of phosphorylated PKC over total PKC was obtained using western blot.

Representative images of blots and statistical analysis for phosphorylated PKC and total PKC are shown in **figure 3.5A**. The ratio of phosphorylated over total PKC was significantly lower in the post-stroke samples compared to pre-stroke samples ( $P < 0.05$ ), and was consistent with IF data (Figure 3.3A), showing decreased levels of P-PKC. The representative images for the blots for total PKC and GAPDH (Loading Control) are shown in **figure 3.5B**. No statistical difference was observed in the ratio of total PKC over GAPDH between the sample groups ( $P > 0.05$ )

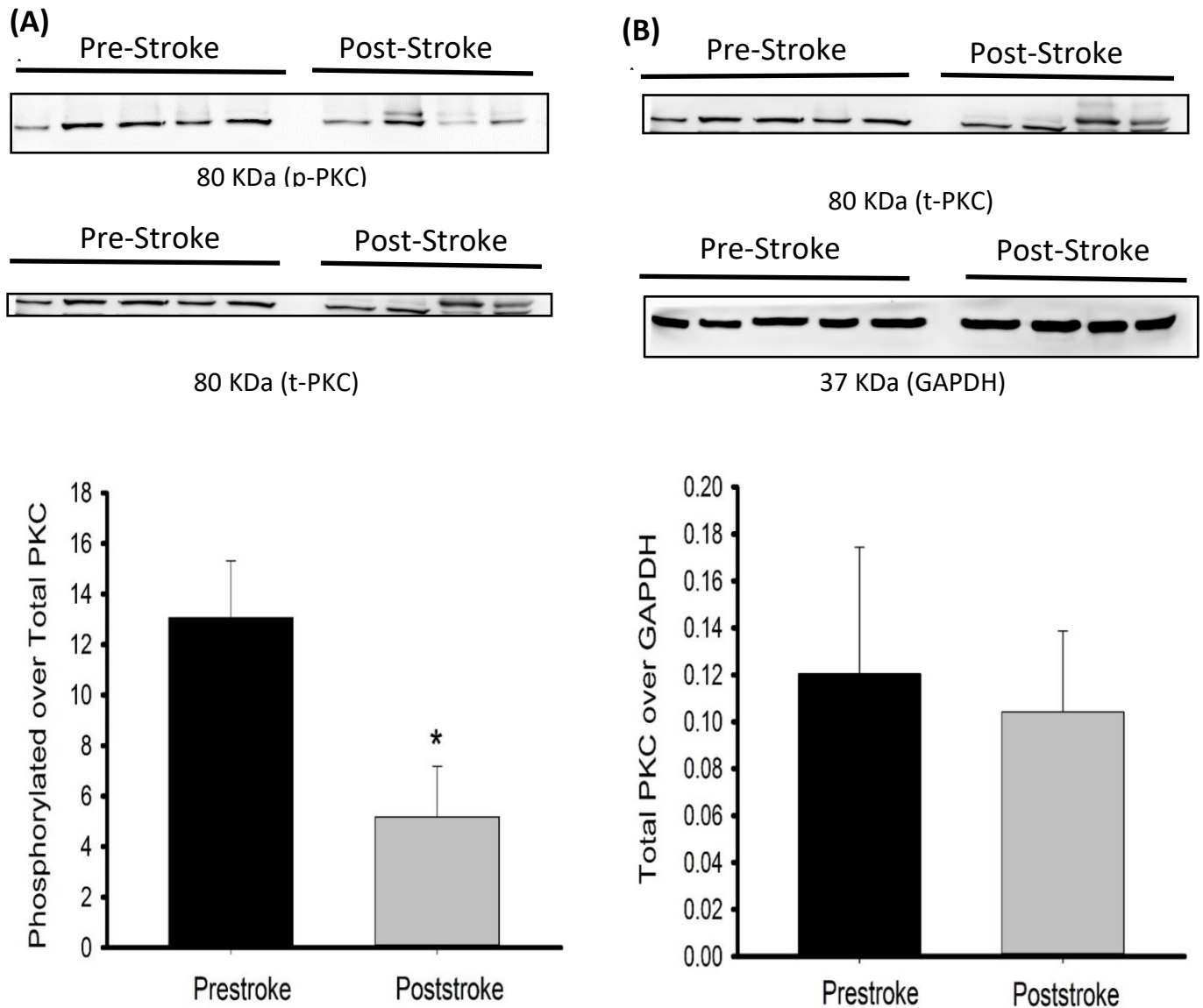


**Figure 3.5:** (A) Representative image for Phosphorylated and Total PKC bands (P-PKC (1:750) and T-PKC (1:50)); WB Analysis: Relative densitometry for Phosphorylated/Total PKC. (B) Representative image for Total PKC and GAPDH bands; WB Analysis: Relative densitometry for Total PKC/GAPDH. \* indicates  $p < 0.05$  analyzed using unpaired Student's t test.

### ***3.5. TRPV4 Expression in MCA by immunofluorescence***

MCA vessels from the pre-stroke and post-stroke SHRsp rats was stained to detect the expression of TRPV4. Upon staining, TRPV4 was found to be expressed to a greater extent in the endothelial layer compared to the smooth muscle cell layer of the MCA. **Figure 3.6A** shows representative images for TRPV4 staining from both pre and post-stroke groups. The semi-quantitative analysis of the mean gray value of TRPV4 staining showed significantly higher expression of TRPV4 in pre-stroke samples compared to post-stroke samples (**Figure 3.6B**;  $P < 0.05$ ).

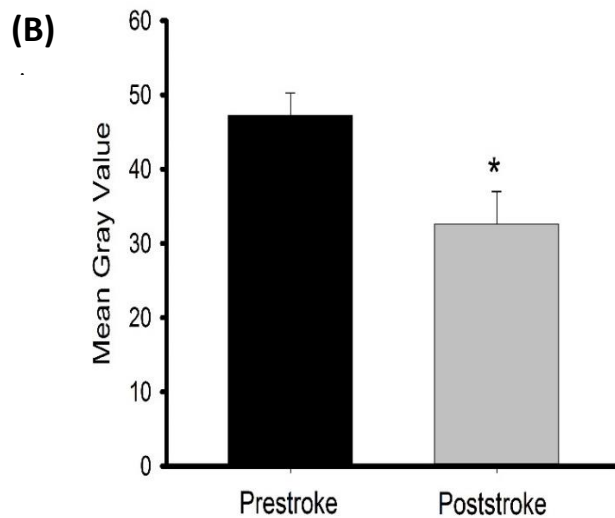
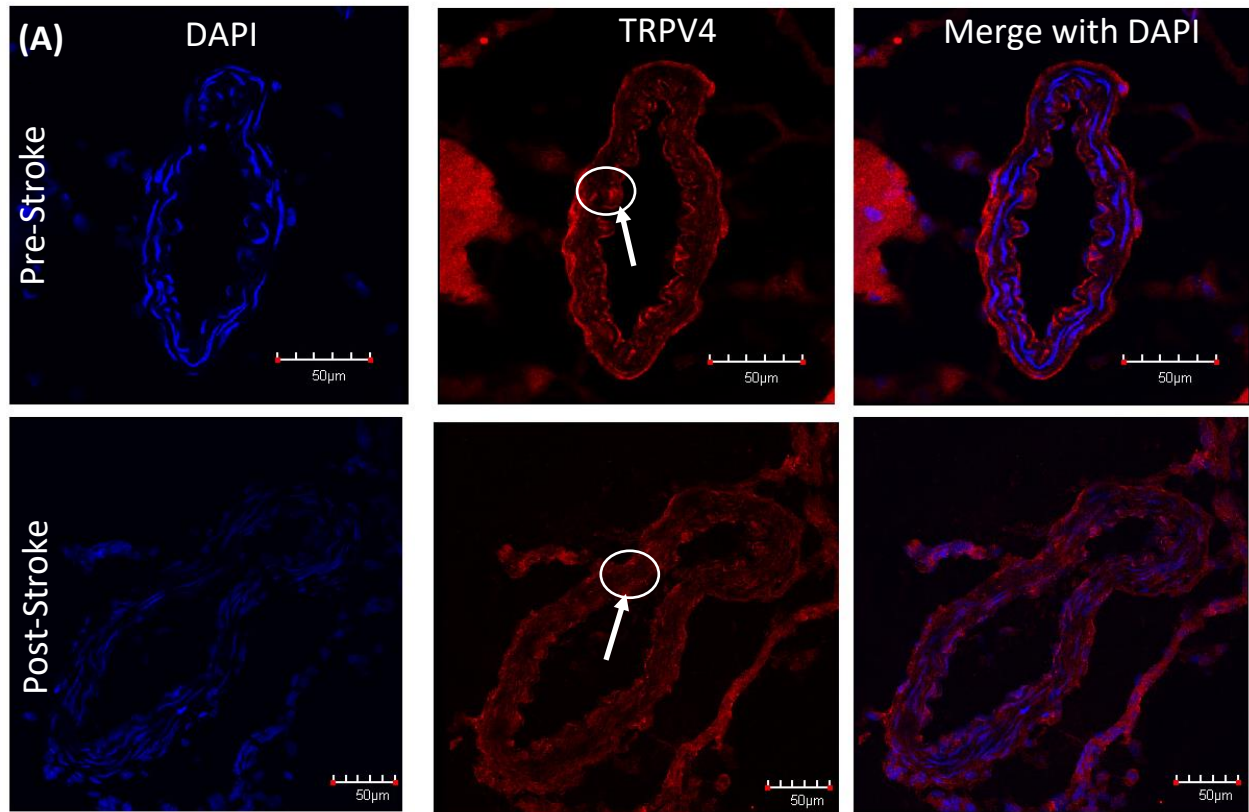


**Figure 3.6:** (A) Representative images for TRPV4 Staining (TRPV4 (1:100), Cy5 (1:300) and DAPI (1:1000)). 8µm slices of MCA were imaged as a Z-stack at 40x objective using confocal microscopy and fluoview software. Semi-Quantification of images performed by Image J software. (B) IF Analysis: Mean Gray Value for TRPV4 in MCAs of pre-stroke and post-stroke animals (n=6 per group). \* indicates p<0.05 analyzed using unpaired Student's t-test. White arrows indicate TRPV4 staining in the endothelium of MCA.

### ***3.6. Analysis of phosphorylated and total p38MAPK by immunofluorescence***

MCA vessels from pre-stroke and post-stroke SHRsp rats were stained for phosphorylated and total p38MAPK, and both were found to be expressed in greater quantity in the smooth muscle cells compared to the endothelium. **Figure 3.7A** shows representative images of vessels from each group for phosphorylated p38MAPK staining. The qualitative analysis of the cross section of a stacked image of the vessel showed phosphorylated p38MAPK was expressed mainly in the vascular smooth muscle cell layer of the MCA. **Figure 3.7B** shows the semi-quantitative analysis of the phosphorylated p38MAPK staining on the MCA in the form of mean gray value. There was no statistically significant difference in expression of phosphorylated p38MAPK compared to post-stroke MCAs. The expression of total P38MAPK can be seen by representative images in **Figure 3.8A**. **Figure 3.8B** shows mean gray value (semi-quantitative) analysis of total p38MAPK in MCA of pre-stroke and post-stroke animals. The expression of total p38MAPK was significantly increased in pre-stroke samples in comparison to post-stroke samples ( $P < 0.001$ ).

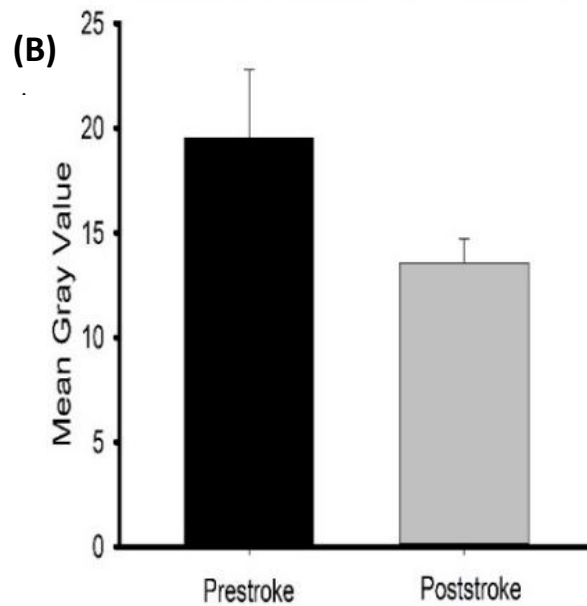
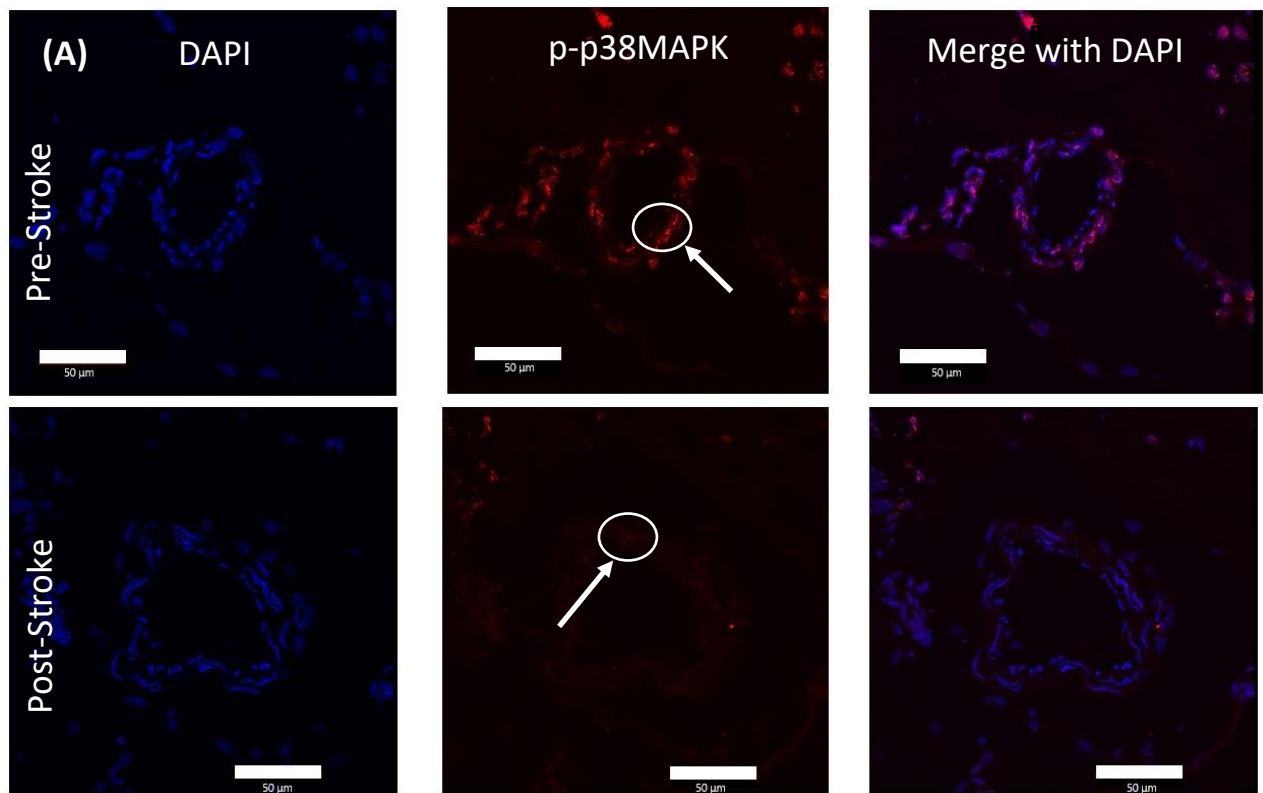


**Figure 3.7:** (A) Representative images for Phosphorylated p38 MAPK Staining (p-p38MAPK (1:100), Cy5 (1:400) and DAPI (1:1000)). 8 $\mu$ m slices of MCA were imaged as a Z-stack at 40x objective using confocal microscopy and fluoview software. Semi-quantification of images performed by Image J software. (B) IF Analysis: Mean Gray Value for Phosphorylated p38 MAPK in MCAs of pre-stroke and post-stroke animals (n=6 per group). White arrows indicate phosphorylated p38MAPK staining in the smooth muscle cells of MCA.

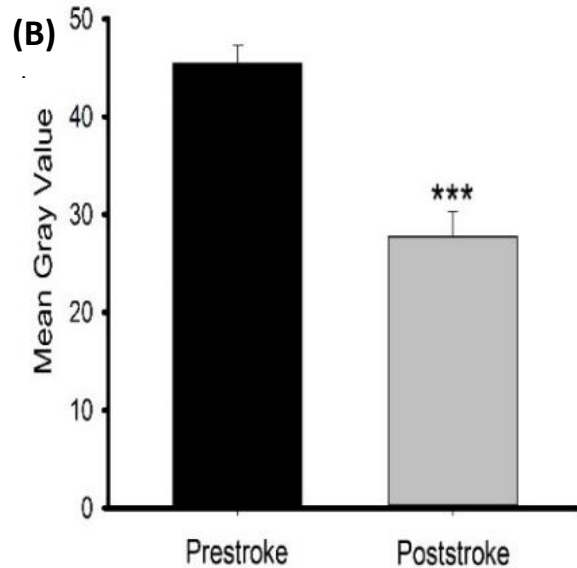
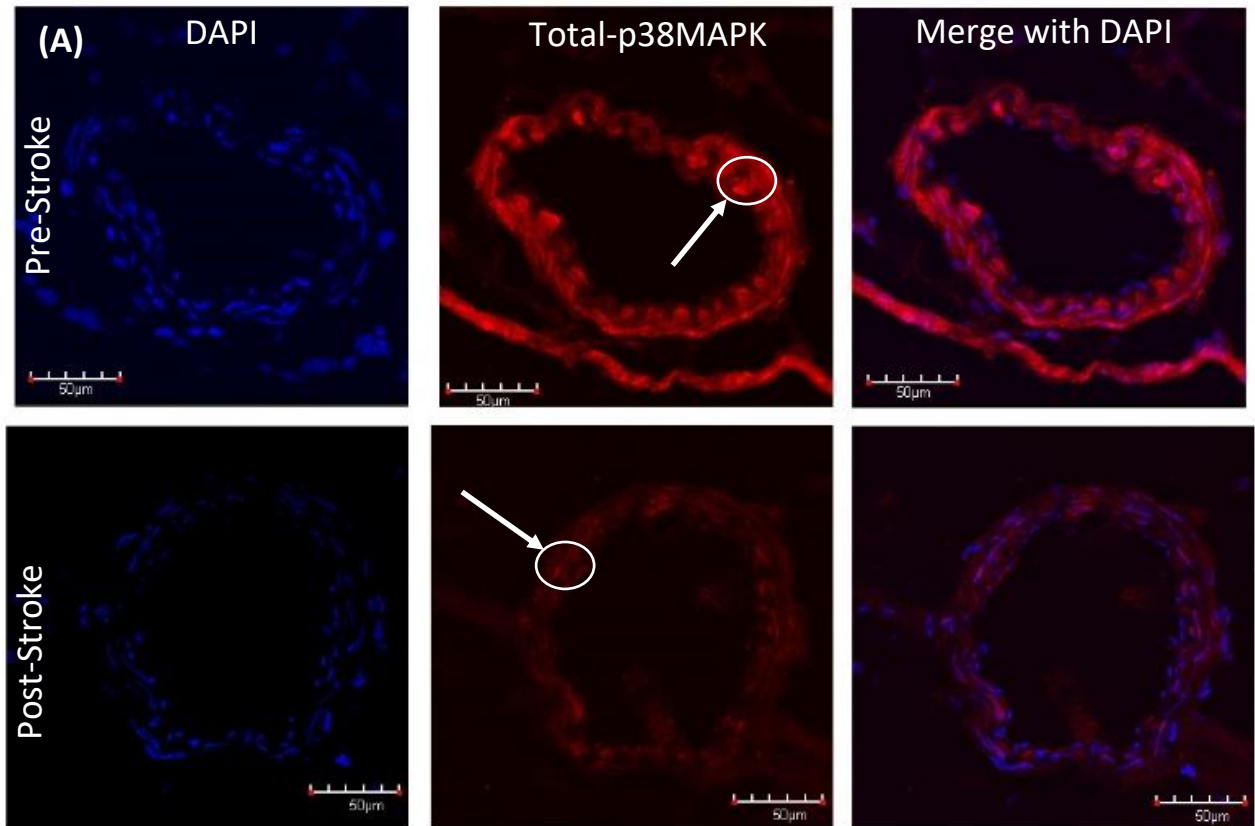


**Figure 3.8:** (A) Representative images for Total p38 MAPK Staining (T-p38MAPK (1:100), Cy5 (1:150) and DAPI (1:1000)). 8μm slices of MCA were imaged as a Z-stack at 40x objective using confocal microscopy and fluoview software. Semi-Quantification of images performed by Image J software. (B) IF Analysis: Mean Gray Value for total p38 MAPK in MCAs of pre-stroke and post-stroke animals (n=6 per group). \*\*\* indicates  $p < 0.001$  analyzed using unpaired Student's t-test. White arrows indicate total p38MAPK staining in the smooth muscle cells of MCA.

### ***3.7. Analysis of phosphorylated and total p38MAPK by western blot***

Western blot analysis was performed to obtain a ratio of phosphorylated (active) over total p38MAPK. **Figure 3.9A** shows representative images and quantification of the results for western blot bands for phosphorylated p38MAPK and total p38MAPK. The semi-quantitative analysis of the blots showed higher relative amounts of phosphorylated p38MAPK over total p38MAPK in post-stroke samples compared to pre-stroke samples; however, there was no statistical difference of phosphorylated p38MAPK over total p38MAPK between groups. The pre-stroke and post-stroke MCA samples were normalised for loading control by GAPDH. **Figure 3.9B** shows representative images of blots for total p38MAPK and GAPDH and it also shows semi-quantitative analysis of total p38MAPK and GAPDH which shows the ratio of total p38MAPK over GAPDH to be higher in pre-stroke compared to post-stroke.

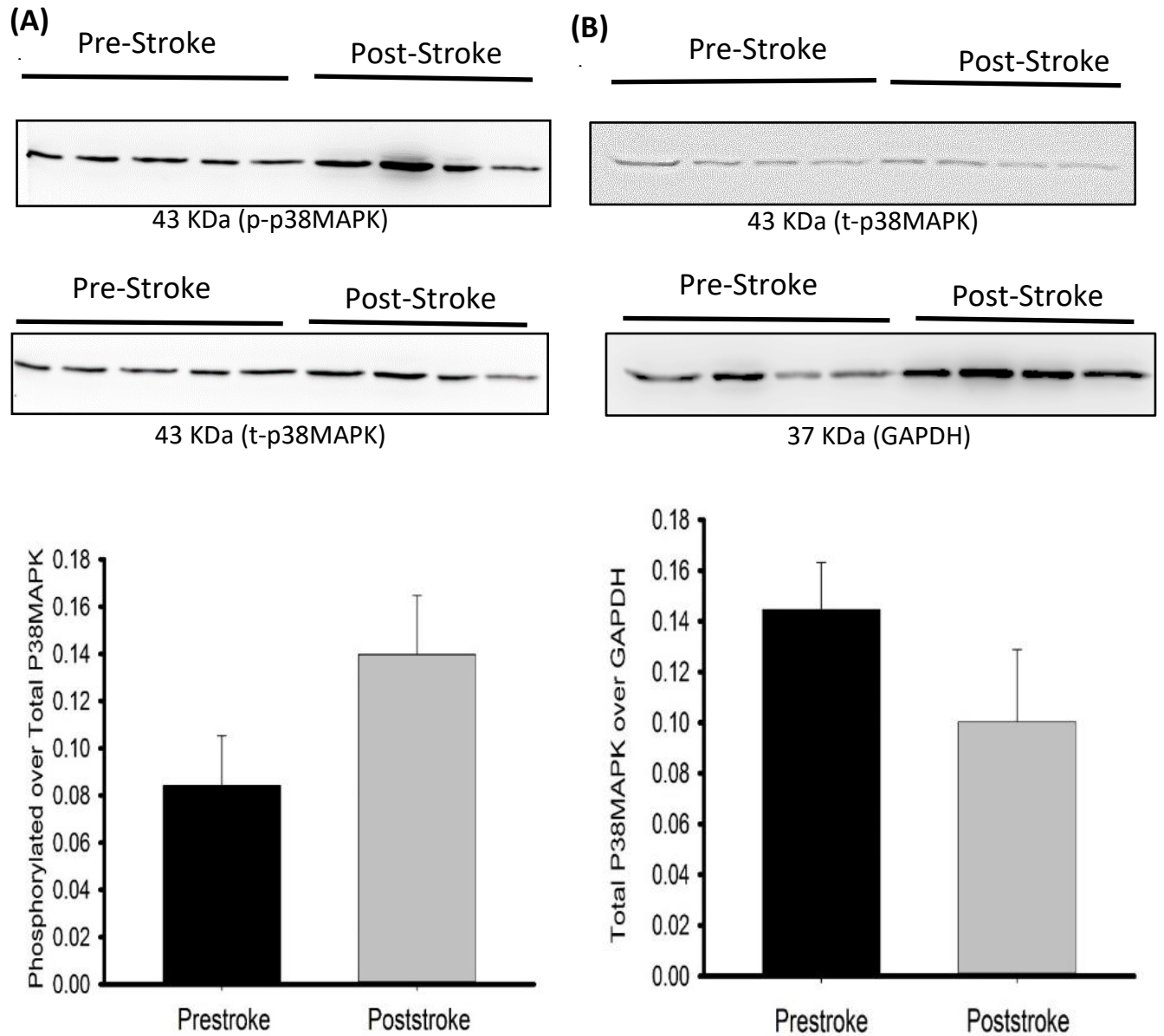
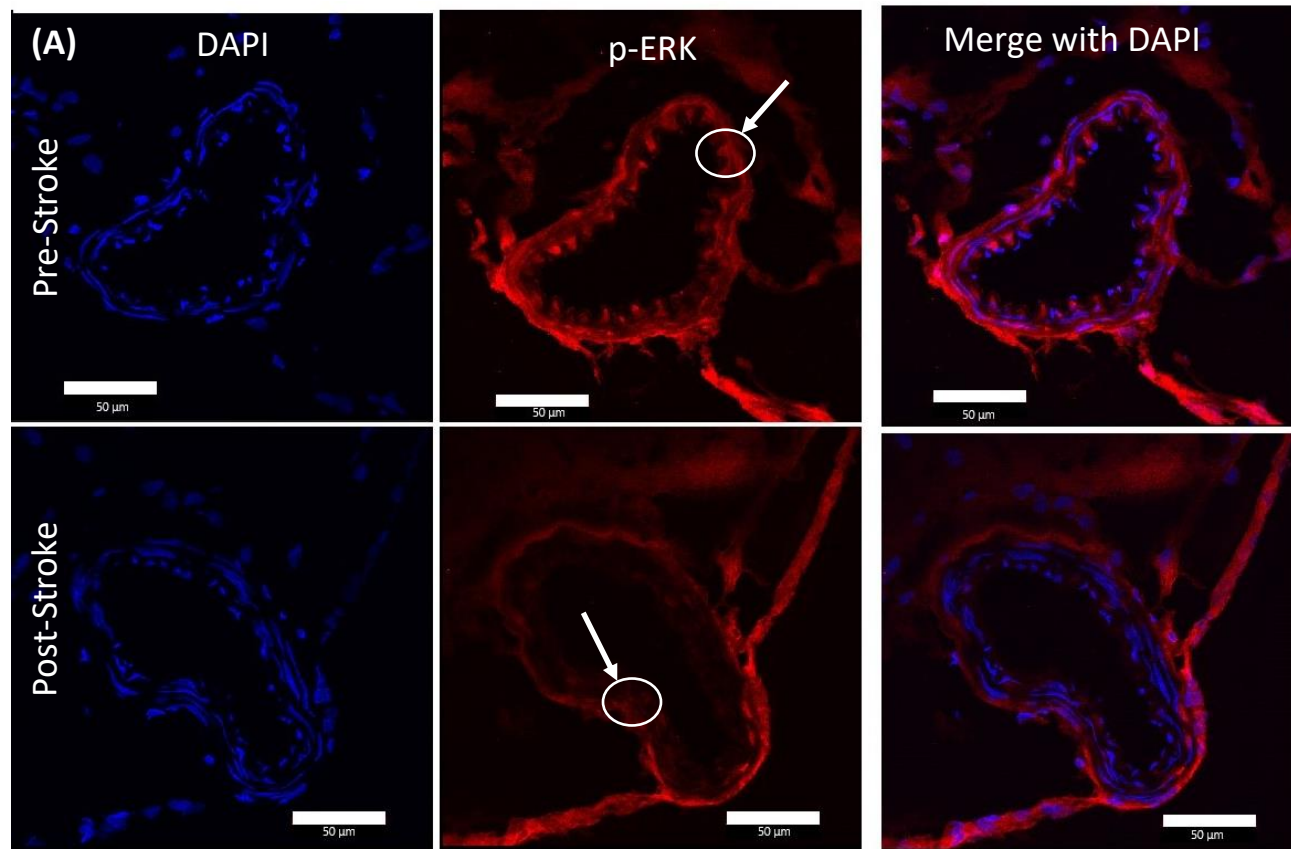


**Figure 3.9:** (A) Representative image for Phosphorylated and Total p38MAPK bands (P-p38MAPK (1:1000) and T-p38MAPK (1:1000)); WB Analysis: Relative densitometry for Phosphorylated/Total p38MAPK. (B) Representative image for Total p38MAPK and GAPDH bands; WB Analysis: Relative densitometry for Total p38MAPK/GAPDH.

### ***3.8. Analysis of phosphorylated and total ERK1/2 by immunofluorescence***

Phosphorylated and total ERK1/2 levels were determined by immunofluorescent staining of MCA vessels in pre-stroke and post-stroke SHRsp rats. Upon staining, phosphorylated and total ERK1/2 were found in both smooth muscle, as well as the endothelial layer of the MCA in both groups. **Figure 3.10A** shows representative images for staining of phosphorylated ERK1/2 from each group. Semi-quantitative analysis of phosphorylated ERK1/2 staining, via mean gray value, showed higher levels in pre-stroke compared to post-stroke animals, however no statistical significant difference was found (**Figure 3.10B**;  $P>0.05$ ). MCA vessels from both groups were stained for detection of total ERK1/2 (**Figure 3.11A**). Pre-stroke samples showed statistically significantly greater expression of total ERK1/2 compared to post-stroke samples (**Figure 3.11B**;  $P<0.05$ ).



(B)

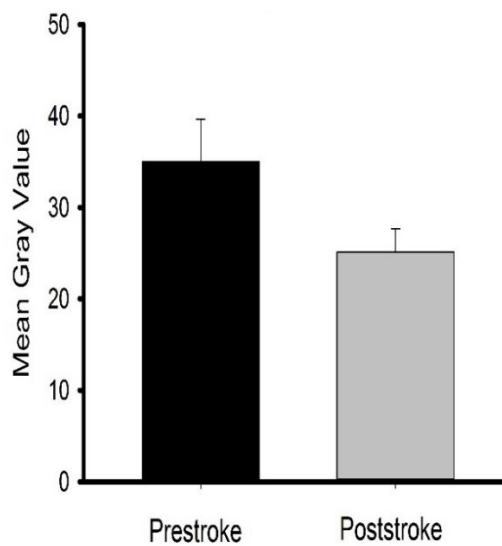


**Figure 3.10:** (A) Representative images for Phosphorylated ERK1/2 Staining (P-ERK1/2 (1:100), Cy5 (1:200) and DAPI (1:1000)). 8 $\mu$ m slices of MCA were imaged as a Z-stack at 40x objective using confocal microscopy and fluoview software. Semi-Quantification of images performed by Image J software. (B) IF Analysis: Mean Gray Value for phosphorylated ERK1/2 in MCAs of pre-stroke and post-stroke animals (n=6 per group). White arrows indicate phosphorylated ERK1/2 staining in the smooth muscle cells of MCA.

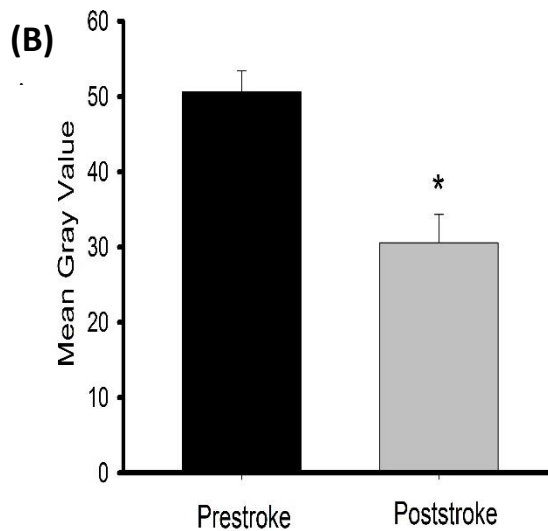
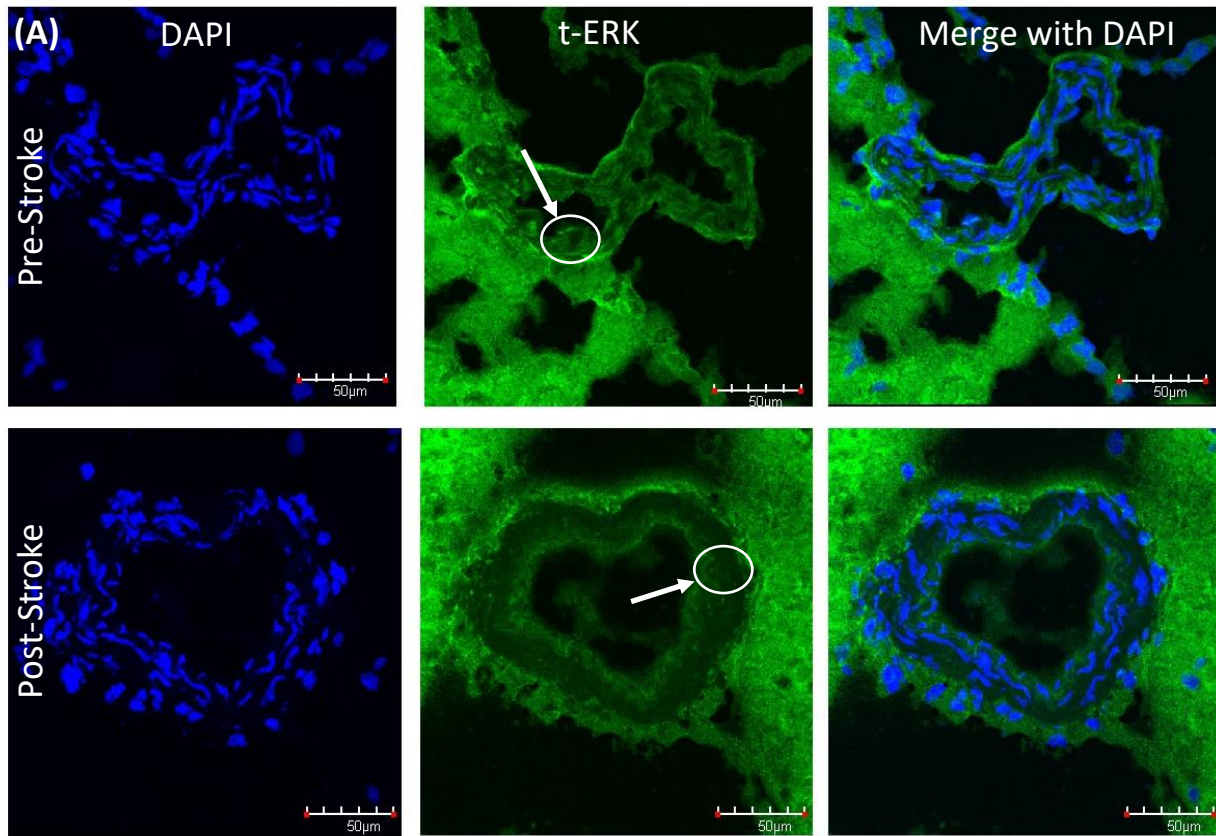


**Figure 3.11:** (A) Representative images for Total ERK1/2 Staining (T-ERK1/2 (1:75), Cy2 (1:300) and DAPI (1:1000)). 8 $\mu$ m slices of MCA were imaged as a Z-stack at 40x objective using confocal microscopy and fluoview software. Semi-Quantification of images performed by Image J software. (B) IF Analysis: Mean Gray Value for total ERK1/2 in MCAs of pre-stroke and post-stroke animals (n=6 per group). \* indicates  $p < 0.05$  analyzed using unpaired Student's t-test. White arrows indicate total ERK1/2 staining in the smooth muscle cells of MCA.

### ***3.9. Analysis of phosphorylated and total ERK 1/2 by western blot***

To determine the ratio of phosphorylated ERK1/2 over total ERK1/2, western blot analysis was performed on the MCA samples from both groups. **Figure 3.12A** shows representative images of blots and quantitative analysis for phosphorylated ERK1/2 and total ERK1/2. Post-stroke samples showed significantly greater relative levels of phosphorylated ERK1and2 over total ERK1and2 compared to pre-stroke samples ( $P < 0.05$ ). Samples from both groups were normalised by using GAPDH as the loading control (**Figure 3.12B**). No significant difference was seen between the two groups, as the ratio of total ERK1and2 over GAPDH was consistent in pre-stroke as well as post-stroke groups ( $P > 0.05$ ).

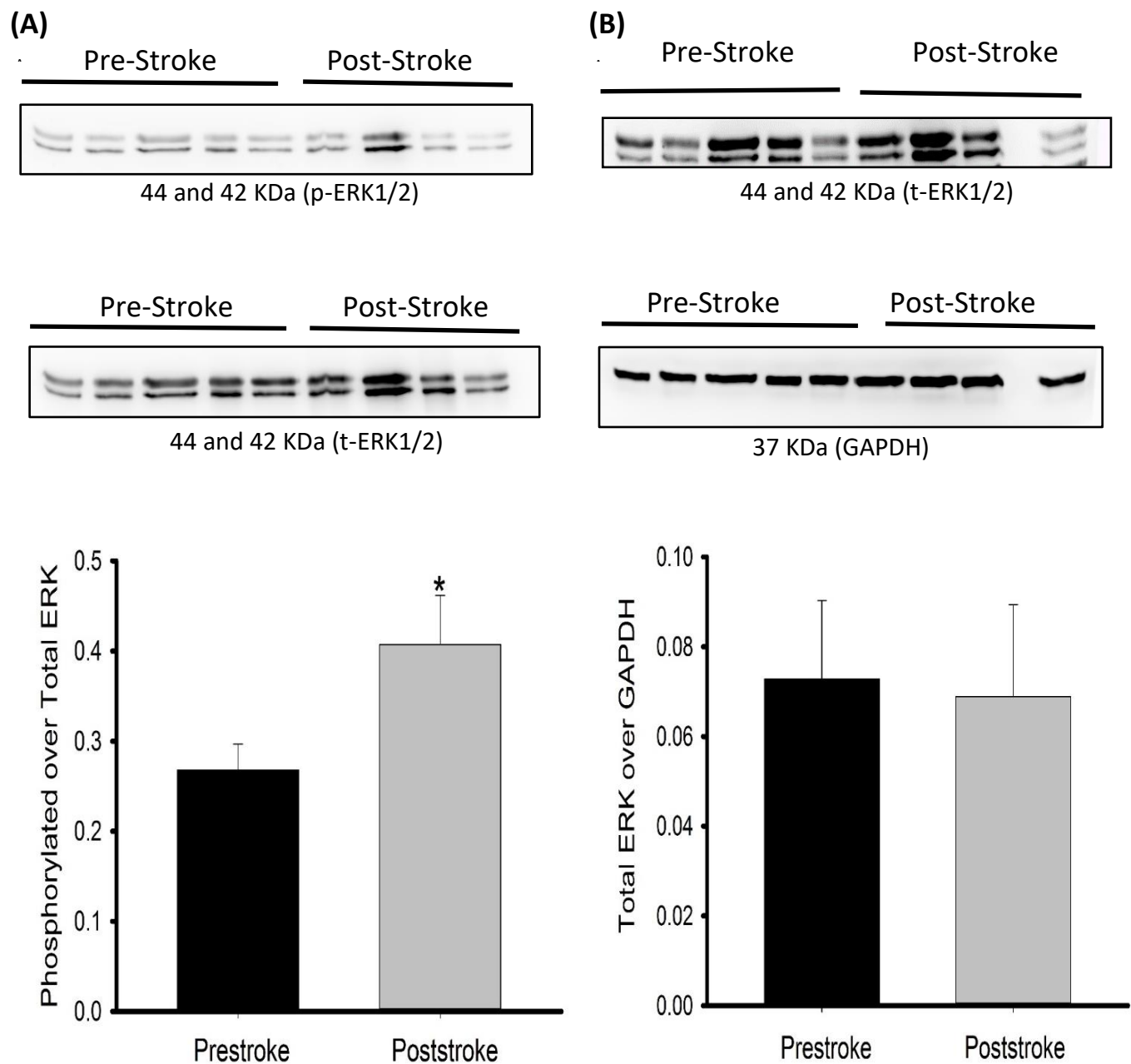


**Figure 3.12:** (A) Representative image for Phosphorylated and Total ERK1/2 bands (P-ERK1/2(1:1000) and T-ERK1/2 (1:1000)); WB Analysis: Relative densitometry for Phosphorylated/Total ERK1/2. (B) Representative image for Total ERK1/2 and GAPDH bands; WB Analysis: Relative densitometry for Total ERK1/2/GAPDH. \* indicates  $p < 0.05$  analyzed using unpaired Student's t test.

### **3.10 Neuro-inflammation: Astrocyte and Microglia Analysis by immunofluorescence**

The brain sections located near the MCA vessels of pre-stroke and post-stroke SHRsp rats were stained for microglia and astrocytes with anti-iba1, anti-GFAP (respectively), and DAPI. **Figure 3.13A** shows representative images for immunofluorescent detection of DAPI, astrocytes, microglia and merge images for both groups. Post-stroke brain sections showed significantly higher immunofluorescent staining for astrocytes spread compared to pre-stroke samples (**Figure 3.13B**). There was a significant increase in staining of activated microglial cells in post-stroke samples, particularly in the total cell count, which includes both cell types (slightly activated and completely activated) phenotypes of activated microglia (**Figure 3.13C**;  $P < 0.05$ ).

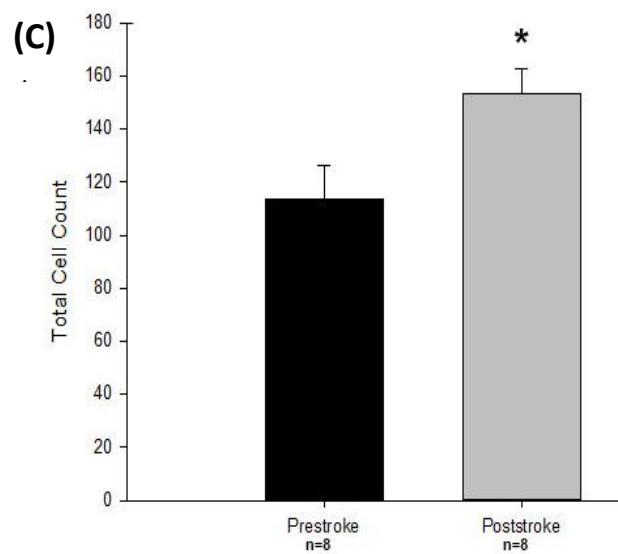
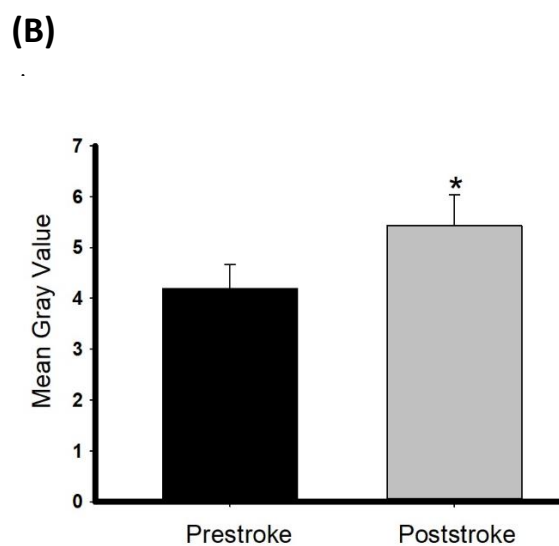
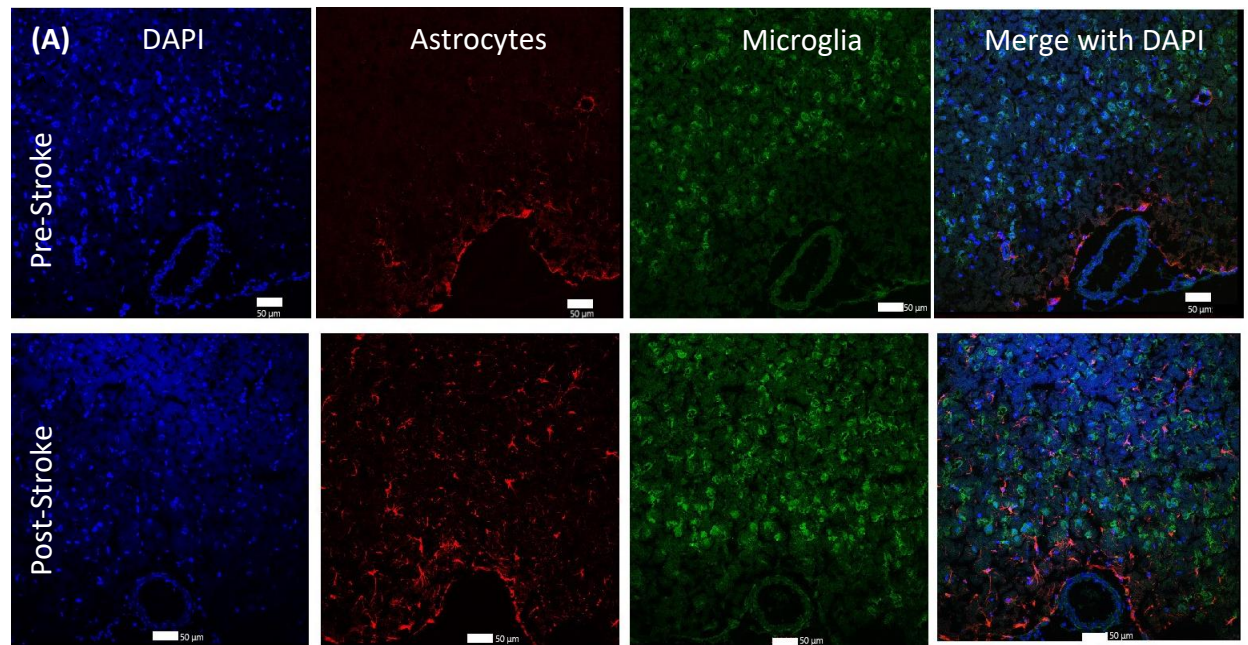
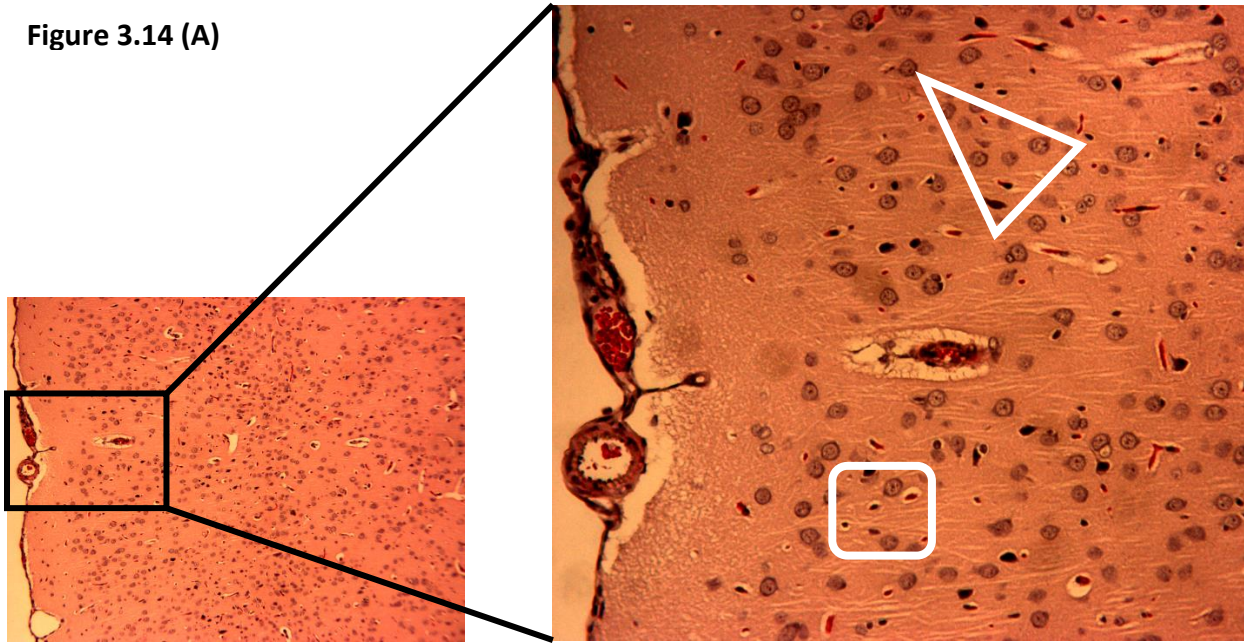


**Figure 3.13:** (A) Representative images for Astrocytes and Microglia (GFAP-Cy3 (1:1000), Iba 1 (1:1000), Cy5 (1:150) and DAPI (1:1000)). MCA and brain tissue sliced at 8 $\mu$ m and imaged at 20x objective using confocal microscopy and fluoview software. Semi-Quantification of imaged performed by Image J software. IF Analysis : (B) Mean Gray Value for Astrocytes and (C) Total Cell count of activated microglia near middle cerebral arteries of pre-stroke and post-stroke animals (n=8 per group). \* indicates  $p < 0.05$  analyzed using unpaired Student's t test.

### **3.11 Neural damage: H and E Stain**

Brains from the pre-stroke and post-stroke groups were stained with H and E (**Figure 3.14A-D**) and imaged to determine the extent of neural and intracerebral damage, near the MCA, located in the area of the M2 section [anterior region extending from insula with the opercular segments (parietal and temporal) included]. Post-stroke samples showed a significant increase in total brain damage scoring represented by total of cell vacuolation, neuron degeneration, areas of edema, and cell infiltration, compared to pre-stroke samples (**Figure 3.15**). Out of all four parameters, the most characteristic sign of neural damage in the post-stroke group appeared to be the presence of cell vacuolation whereas the least occurring sign of neural damage in both experimental groups was edema.

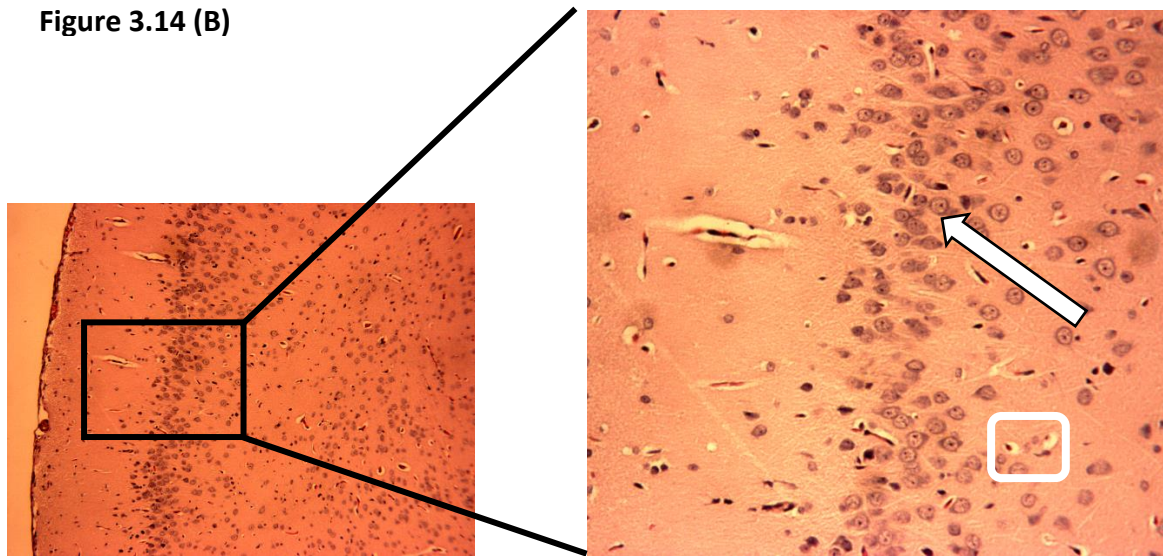
Figure 3.14 (A)



(Pre-stroke) 10X

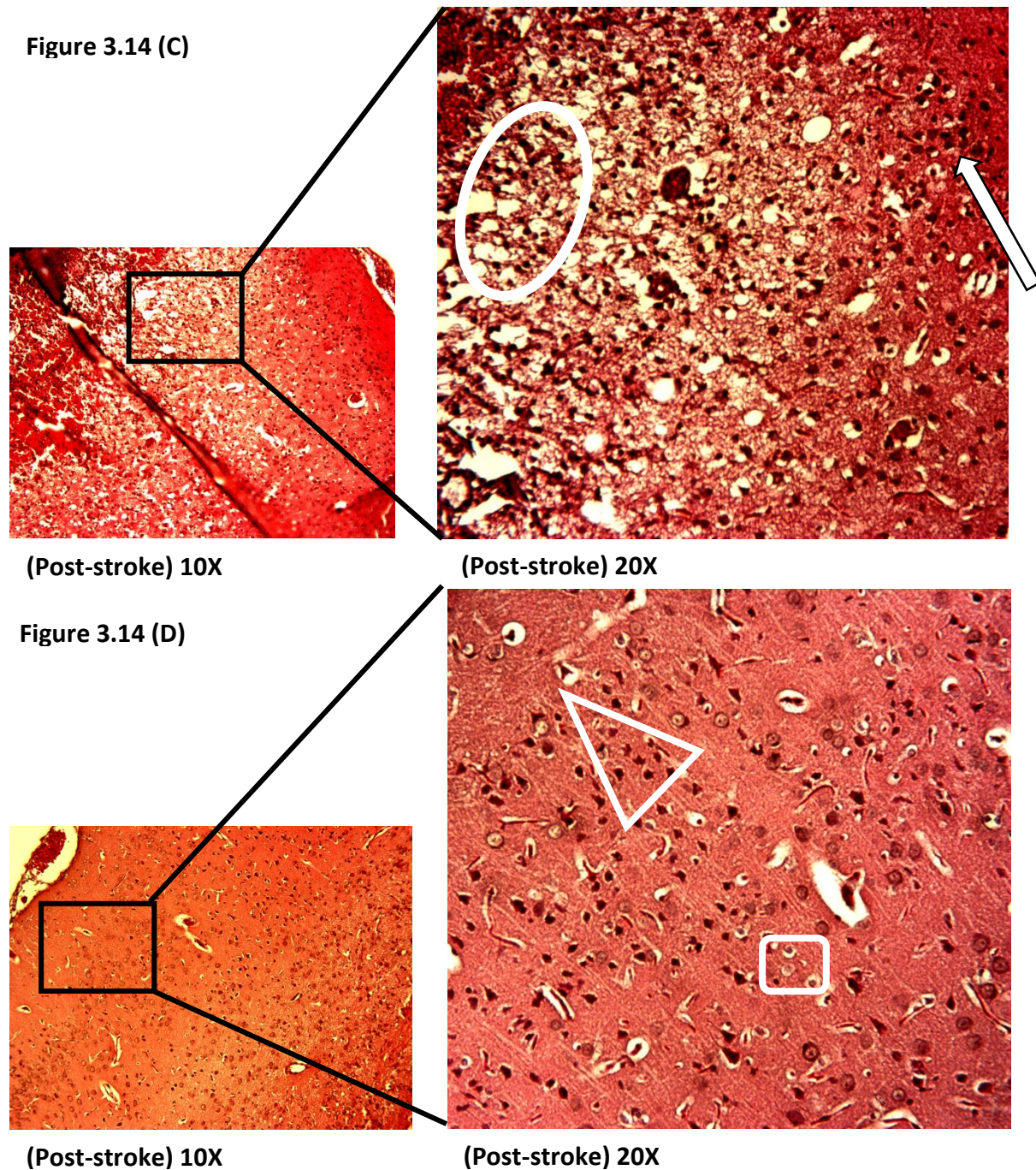
(Pre-stroke) 20X

Figure 3.14 (B)



(Pre-stroke) 10X

(Pre-stroke) 20X



**Figure 3.14:** Representative images of H and E stains of brain slices (6  $\mu\text{m}$ ) imaged at 10x (total magnification 100x) and 20x objectives (total magnification 200x) for pre-stroke (**A and B**) and post-stroke (**C and D**). Areas of neural cell vacuolation (white rhombus), neural degeneration (white triangle), area of oedema (white circle), and cell infiltration of inflammatory origin (long white arrow) are indicated between the images (**A–D**).

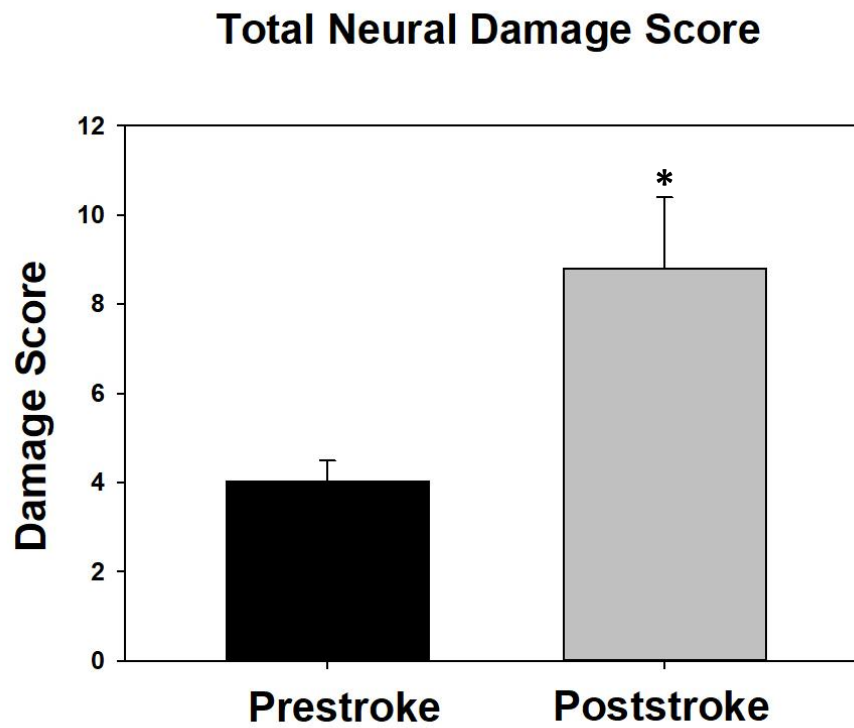


**Figure 3.15:** Total Neural Damage Scoring by H and E staining of brains, for pre-stroke (n=6) and post-stroke (n=4) groups. \* indicates  $p < 0.05$  analyzed using unpaired Student's t-test.

#### **4. Discussion:**

Previous research by our group found significant pathophysiological changes in the vascular function of the MCA in pre-stroke and post-stroke SHRsp, with a loss of autoregulation in the post-stroke MCAs (179). We wished to investigate the potential role of various cellular signalling mechanisms associated with the contractile properties of the vessel and inflammatory factors effected by stroke. The focus of the work was to investigate possible differences in the expression of cellular signalling components involved in contraction of the MCA, focusing on MLC and PKC, where the activation of PKC was significantly lower in the post-stroke MCA compared to pre-stroke MCA samples. We also analysed inflammatory mediators affecting the vascular integrity as represented by MAPK and ERK. Our work indicates the post-stroke MCAs expresses increased activation of MAPK & ERK compared to pre-stroke MCA.

We also determined the degree of neural inflammation accompanied in the brain region surrounding the MCA (by investigating astrocytes spread and microglial activation) and identifying neuronal damage in the brains of pre-stroke and post-stroke SHRsp. Our experiments clearly display the increase in expression of inflammatory proteins in MCA is accompanied by significant neurological damage as well as inflammatory upregulation (activated astrocytes & microglia) in the brain region surrounding the MCAs in post-stroke compared to pre-stroke animals..

We used both qualitative and semi-quantitative approaches with immunofluorescence and immunohistochemistry to determine the expression and localization of proteins, and analyze cell morphology in cross-sections of MCA vessels and brain tissues. As well, expression of specific proteins in the entire MCA were quantified using western blot. In all we analysed the changes in

expression of cellular signalling involved in MCAs of pre-stroke (before stroke) and post-stroke (after-stroke) SHRsp rats..

The MCA undergoes both vasodilation and vasoconstriction to maintain the consistent blood flow, with the vascular smooth muscle cells and endothelium being the contributors in both of the processes. The contraction of vascular smooth muscle is activated primarily by phosphorylation at S19 of the 20-KDa regulatory light chain subunits of myosin II. This phosphorylation is catalyzed by Calcium/calmodulin-dependent myosin light chain kinase, in a healthy vessel (67). Numerous contractile stimuli, such as an increase in intraluminal pressure (180), membrane depolarization influenced by neurotransmitter release, blood-borne hormones and cytokines, or locally released factors from endothelial and surrounding cells trigger an increase in  $Ca^{[2+]}$  (181) leading to smooth muscle cell contraction (67). The released calcium binds to calmodulin, which in turn acts on an enzyme activating Myosin Light Chain Kinase (MLCK). The phosphorylation of MLCK further phosphorylates and activates MLC, causing cross-bridge cycling of myosin heads along the actin filaments and shortening or contraction of the smooth muscle cell causing vessels to contract (181). Any changes in the levels of MLC and/or MLCK might affect the normal functioning of the vessel.

The loss of autoregulation in cerebral arteries that may occur at the onset of stroke is due to the loss of normal functioning of the vessels to respond to pressure and absence of the normal contractile cycle, therefore it is possible that changes in phosphorylation of MLC might be affecting the contractility of the vessel. Interestingly, the post-stroke MCA vessels showed significantly higher expression of phosphorylated MLC compared to pre-stroke MCA vessels which was not originally expected. However, the result may be due to changes in the availability of F-actin for binding.

Previous research in our lab comparing specific actin expression before and after stroke indicated a decrease in the ratio of filamentous actin (F-Actin) compared to globular actin (G-Actin) available after stroke. Studies in isolated smooth muscle cells, as well as the tracheal smooth muscle layer, have indicated the importance of F-actin, as an increase in F-actin and decrease in G-Actin was observed during exposure to a contractile stimuli (65). Tropomyosin strands seen to be responsible for myosin-actin interaction, are present on the F-actin filaments in smooth muscles, which link together to form end to end polymeric strands on F-actin filaments to increase mechanical strength of the muscle contraction (182). The decrease in concentration of F-Actin directly affects the activity of tropomyosin leading to decreased contractility. Therefore, the decrease in F-Actin after stroke may result in less tropomyosin available for the P-MLC to bind to, keeping the level of the P-MLC higher as it stays unused during the event of stroke. As the development of contractile force in smooth muscle requires actin polymerization and the MLC phosphorylation to work in parallel signalling pathways, absence of either pathway hinders the normal functioning of the smooth muscle.

Another possible reason for MCA dysfunction maybe that as the MCA loses its auto-regulatory mechanism due to chronic high blood pressure, during which a compensatory mechanism may over activate and lead to hyper-activation of MLC. The vessels undergo remodelling during chronic hypertension leading to stiffened cerebral arteries (183). This may lead to the vessel having a lesser capacity to contract and the need of P-MLC is not same as it was before vascular remodelling, as vascular remodelling in hypertension has shown to modify contractile state of the vessel (184). The lack of difference in expression in the total MLC within the samples suggests that the phosphorylation of MLC is the primary issue that is likely

associated with the decrease in the contractile function of the smooth muscle cells, rather than the quantifiable amount of total MLC.

Contraction of VSMC involves activation of multiple interlinked pathways that include phosphorylation of MLC, linked to activation of PKC. We have noted that PKC activity is significantly decreased in post-stroke vessels when stimulated with phorbol ester in pressure dependent constriction experiments (185). Therefore we investigated the importance of PKC in the contractile pathway following stroke. Activation of PKC has shown to increase the myofilament force sensitivity to  $[Ca^{2+}]$ , MLC phosphorylation and eventually maintenance of VSM contraction (81). Studies in ovine MCAs have shown that PKC increases vascular tone by decreasing myosin light chain phosphatase (MLCP) activity, thus increasing MLC phosphorylation (186). Any changes in the PKC activity will therefore affect the activity associated with MLC contractile activity.

Our analysis of MCA's was for phospho-PKC, which included both conventional and novel isoforms of PKC at the serine 660 site, one of the main phosphorylation sites regulating PKC subcellular localization (187). In our samples, phosphorylated PKC was significantly lower in post-stroke MCA, when compared to pre-stroke MCA. Lower levels of activated PKC in post-stroke MCA may be due to decreased calcium influx after stroke, as studies have shown that calcium released from intracellular stores most often regulates activation of PKC (73). Similar to calcium, diacylglycerol (DAG) also independently regulates activation of different isoforms of PKC (73). The intracellular concentration of calcium triggers association of PKC isozymes with the membrane where DAG interacts with PKC to stimulate activity. The stimulation of PKC is therefore dependent on the duration as well as the magnitude of the DAG signal (188). Studies in diabetic vasculature have shown DAG and its analogues activate specific isoforms of PKC

(74,189). The down regulation of either DAG or calcium may directly lower the activation of different isoforms of PKC occurring in the post-stroke samples. The MCA's in post-stroke SHRsp have shown decreased vascular functioning and loss of the auto-regulatory mechanism. This loss of functionality could be attributed to the underlying structural changes occurring in the MCA during the transition from pre-stroke to post-stroke, especially when exposed to chronic high blood pressure (183). Activation of PKC has been shown to mediate long term cell functions such as cell differentiation, that can contribute to vascular remodelling (78). Enhanced activation of PKC has also been linked to processes that contribute to acceleration of vascular inflammation and atherosclerosis, in diabetes, via a mechanism that includes modulation of gene transcription and signal transduction in the vascular wall (190). Significantly higher levels of phosphorylated PKC, over total PKC, at the pre-stroke stage may signal an over activated PKC pathway leading towards the vascular remodelling during the initial stage of high blood pressure development progressing over time towards loss in vascular integrity and eventually loss in vascular functioning post-stroke. The changes associated with over activation of PKC during the pre-stroke transitional stage may have therefore led to vascular remodelling and loss of PKC function post-stroke.

A few PKC isoforms are calcium dependent and can further activate calcium channels. Interestingly, studies have shown upregulation of PKC signalling via light-sensitive Gq-coupled receptor results in TRPV4-mediated Ca<sup>[2+]</sup> influx in endothelial cells (82,191). The link between PKC activation and TRPV4 activity is further supported by a study in hypertensive mice showing TRPV4 activity being inhibited in aorta in the presence of a PKC inhibitor (192). The changes observed in PKC activity in the MCA likely affect TRPV4. As TRPV4 is essential in the

regulation of vascular function during mechanical stress, its role in MCA during stroke development was investigated.

We expected TRPV4 expression to be increased in post stroke MCAs as the TRPV4 channels, when activated, vasodilate vessels. This would likely contribute to the inability of MCAs to contract in response to pressure dependent constriction (PDC) during stroke. However the expression of TRPV4 was significantly lower in post-stroke compared to pre-stroke animals. One of the possible reasons may be that the decrease in PKC activation during stroke may have influenced the decrease in TRPV4 expression in post-stroke samples. A study in cell culture showed that PKC phosphorylates TRPV4 at Ser824 leading to enhancement of TRPV4 channel function in the presence of PKC (193). Several other studies have shown PKC to be an important mediator in regulating activation of TRPV4 channels in the endothelial cells and in the nephrons (82,194), which possibly reflect the reason for lower TRPV4 channel expression accompanied with lower activation of PKC in post-stroke MCA.

The decrease in TRPV4 expression post-stroke may also be associated with the vascular remodelling and stiffening present in the post-stroke MCAs. Vascular remodelling is accompanied by deposition of calcium and thinning of the endothelial layer (195), making the vessel less responsive to various stimuli. As TRPV4 channels are highly osmo-sensitive and mechano-sensitive (196), the absence or diminished detection of either stimuli due to thinning of the endothelial layer during vascular stiffening may impact the expression of TRPV4, as seen in the post-stroke samples.

Conversely, the increase in TRPV4 channels in pre-stroke MCA may be due to increased phosphorylation of PKC in the pre-stroke stage. TRPV4 channels are primarily responsible for calcium influx, but are also known to play a role in cell proliferation in the vasculature. A study

by Hatano *et.al.* evaluating TRPV4 expression in human brain capillary endothelial cells (HBCEs) showed TRPV4 activation could partially regulate cell proliferation of HBCEs (94), leading to the possible remodelling of the cerebral vessels during the pre-stroke transition stage and the changes in intima-media thickness and stiffening observed in post-stroke MCA.

The post-stroke MCA samples showing decreased expression of TRPV4 accompanied with significantly lower ratio of activated PKC over total PKC suggest dysfunctional contractile mechanism during stroke. These changes are likely partly responsible for the loss of pressure dependent constriction seen in the post-stroke samples, associated with changes in inflammatory signalling in the post-stroke MCA. MAPK cascade which includes P38 MAPK and ERK1/2 are the main inflammatory signalling pathways involved, controlling a broad spectrum of cellular processes, stress responses and inflammation (115).

p38 MAPK and ERK are two MAPK signalling pathways we investigated, as p38 MAPK has been implicated in endothelial injury and inflammation (113) and ERK has been associated with signalling that governs cell proliferation, differentiation and cell survival through apoptosis (121). Activation of both p38 MAPK and ERK 1/2 activates transcription factors leading to generation of more inflammatory mediators and likely involved in remodelling and influencing contractile mechanisms. Our results indicate that the total pool of p38 MAPK and ERK1/2 is significantly higher in pre-stroke compared to post-stroke, leading to more total protein available for activation in the pre-stroke phase. However, the ratio of activated over total p38 MAPK and ratio of activated over total ERK1/2 was significantly higher in post stroke, suggesting the presence of inflammatory process after stroke.

The ratio of activated 38 MAPK/total p38 MAPK, as well as activated ERK/total ERK, in post-stroke MCA may be due to the presence of stress related signals in the cerebral vasculature.

MAPKs are known to transduce stress related signals through a chain of interlinked pathways that lead to induction of inflammation (114). They serve as a link between extracellular signals and fundamental cellular processes (such as growth, proliferation, migration, apoptosis and metabolism) (117). p38 MAPK is also known to be activated downstream from TLR activation to promote production of various pro-inflammatory cytokines, such as TNF- $\alpha$ , IL-1 $\beta$ , IL-6 and IFN- $\gamma$  (113,197), suggesting an increase in stress related signal causing more inflammation in the vessel and further increasing inflammatory signalling in the post-stroke MCA. An increase in MAPK signalling has been linked with increases in inducible nitric oxide synthase (iNOS) and cyclooxygenase-2 (COX-2) (113), serving as an intermediate responsible for recruiting mediators that are more inflammatory during the post-stroke stage.

Similar to p38 MAPK, a significantly higher ratio of activated ERK over total ERK in the post-stroke samples could be because of an increase in pro-inflammatory stimuli (such as IL-1 $\beta$ ) in the vessels itself (122). Different molecular patterns associated with sensing functional or structural changes in the vasculature, like pathogen associated molecular patterns (PAMPS) and danger associated molecular patterns (DAMPS) (197), activate and increase ERK phosphorylation in the post-stroke MCA. Other reasons for a higher ratio of activated over total ERK in post-stroke MCA may be due to accumulation of blood and its components, which causes generation of pro-inflammatory environment (152). The SHRsp rats may have suffered multiple micro-hemorrhages causing leaky blood vessels before suffering a major stroke which potentiates further damage to the MCA due to the local inflammation. It is also possible that the increase in activated over total ERK post-stroke is a compensatory mechanism for the loss of contractile function, as increase in ERK pathway has shown to activate actin through its downstream pathway causing vessels to contract (124).

The role of ERK in potentiating vascular dysfunction likely starts at the pre-stroke stage. Exposure to chronic high blood pressure prior to stroke can cause an increase in inflammatory signalling, as a study of cerebral and coronary arteries in SHR showed significantly higher levels of phosphorylated ERK1/2 (198), implicating its role in the response to sustained high blood pressure. During exposure to chronic high blood pressure, the vessels suffer extreme shear stress and circumferential stretch, causing extensive endothelial damage, and extracellular matrix imbalances (199). There is likely a resulting generation of a strong inflammatory response (200). The sustained high blood pressure throughout the transition phase from pre-stroke to post-stroke can activate inflammatory signalling due to the presence of numerous stimuli and pro-inflammatory mediators leading to increase in the ratio of activated over total MAPK and ERK in post-stroke MCA.

Studies have shown ERK to mediate vasoconstriction by activation of MLCK, leading to increased phosphorylation of MLC and causing contraction of the vessel (125). An interesting study in porcine palmar lateral vein showed inhibition of ERK caused reduction in MLC phosphorylation, inhibiting contraction of the vessel (201). Our data indicates an increase in activation of MLC alongside an increase in ratio of activated ERK, in post-stroke MCA's, may be an indication of an inter-connected signalling pathway to help MCA compensate to chronic high blood pressure and contract in order to rescue normal functioning during the post-stroke stage.

MAPK activity in the brain region has been linked with microglial activation associated with increased inflammatory activity. Phosphorylated p38 MAPK has been detected in neurons and microglia of ischemic brain tissue in the hippocampus of gerbils, demonstrating its role in the acute inflammatory response (120). In striatal slices of Wistar rats, that had ICH artificially

induced, it was shown that inhibition of MAPK pathways in ICH, decreased survival of activated microglia (202). Therefore, we suspect higher inflammatory activity in the MCA is often accompanied by increased inflammation in the brain region near MCA, contributing to more damage in the brain during stroke. To determine the presence of neural inflammation, we analyzed the expression of microglia and astrocytes, as these two cell types have been implicated in numerous cerebral diseases (129).

The brain regions surrounding the post-stroke MCAs, the anterior region extending from insula with the opercular segments (parietal and temporal), showed significantly higher levels of activated microglia compared to the brain regions around the pre-stroke MCA. This reflects an increase in neural inflammation in tandem with increased vascular inflammation. Microglial cells that are activated and/or displayed an inflammatory phenotype (an amoeboid shape and very short dendrites) generally reduce cell proliferation, survival and function of new neurons (129), in addition to inducing further inflammatory feedback to the MCA during stroke from the external surface of the vessel. Also, higher levels of activated microglia in post-stroke samples may be due to an innate tendency of the activated microglia to undergo apoptosis, seen in murine models of neurodegenerative diseases (203,204) and release more pro-inflammatory mediators, in turn recruiting and activating more microglia (203). Activated microglial cells also undergo phagocytosis during a strong inflammatory response and destroy themselves, releasing neurotoxic agents such as reactive oxygen species and pro-inflammatory cytokines (205), causing a further increase in the recruitment and activation of microglia.

Microglial activation has been shown to involve activation of inflammatory pathways such as p38MAPK (206), and generate TNF- $\alpha$  and IL-1 $\beta$ , inducing a detrimental effect in the brain (207). The presence of high levels of pro-inflammatory mediators in the brain region

surrounding the MCA, due to activation of microglia, likely serves as a stimulus to further activate mediators such as MAPK (206), in the MCA during stroke. Microglial cell production of pro-inflammatory cytokines such as TNF- $\alpha$ , IL-1 $\beta$ , IL-6 (208), as well as chemokine CXCL2, promotes neuro-inflammation and recruitment of blood-derived leukocytes to the brain (209), as well as activates key factors affecting vascular integrity. A study by Del Zoppo *et al.* showed that the microglial cell activation led to metalloproteinase-9 (MMP-9) generation, a key factor in blood brain barrier damage (210). In conditions that activate microglial cells, the MCAs are likely exposed to undue stress and vascular remodelling, as MMP-9 is directly responsible for degrading extracellular matrix (ECM) proteins and activating cytokines and chemokines in the brain and cerebro-vasculature (210).

The activation of microglia in the post-stroke samples was accompanied with significantly higher astrocytes spread in the post-stroke brain regions around the MCA. Both microglia and astrocytes are well known to show an immune response during brain damage (210-212). Astrocytes are found throughout the brain and increase in astrocyte accumulation is seen near the site of damage as they contribute to local inflammatory responses by producing pro-inflammatory cytokines (213). Astrocyte scar formation (astrogliosis) develops by new proliferative astrocytes that form an interface between viable CNS neural parenchyma and non-neural cells at the site of damage (214) and contribute to neuro-inflammation on the neighbouring neurons. An interesting study showed astrogliosis induced detrimental effects on the CNS in the event of prenatal asphyxia, and it was accompanied by degeneration in the synapses and loss of axonal neuro-filaments (215) and thus the potential to cause harmful effects such as exacerbating inflammation (216), occurring during stroke and causing loss of neuronal conduction in the post-stroke samples. The trend toward astrogliosis and astrocyte spread near

the MCA region in post-stroke samples indicate the magnitude of damage after stroke is likely due to increase in inflammatory response.

Astrocytes are also known to regulate vascular smooth muscle cells and affect structural integrity in small cerebral vessels in deep brain regions (217). A study in adult mice showed absence of astrocytic laminin led to impaired function of VSMC, and exhibited VSMC fragmentation, and vascular wall disassembly, making it an important mediator in structural integrity of cerebral vessels during stroke. An increase in astrocyte spread leads to scar formation and expression of proteoglycans that impede neuronal growth and inhibit structural and functional recovery (218) of the MCA and neighbouring blood vessels following stroke.

The full involvement of astrocytes and microglia in the development and progression of stroke is a complex issue as they have been shown to be both neuro-toxic and neuro-protective based on the stage of growth and activation. Activated microglia are classified as M1 (pro-inflammatory) and M2 (neuro-protective). Transient M2 phenotype shifts to M1 phenotype during an injury as a higher ratio of M1 to M2 has been witnessed in ischemic brain injury (219). M2 phenotype during the recovery stage phagocytise dead neurons in order to prevent secondary inflammatory response and promote tissue regeneration. Although we identified activated microglia by two cell types (slightly activated and completely activated) based on established morphology (short dendrites, large nucleus and an amoeboid shape) upon Iba-1 staining, we did not specifically check for M1 or M2 phenotype, therefore we cannot accurately establish the timeline of the injury process within our system without further research.

Astrocytes can also serve dual roles depending on the type of receptor it activates and extent of damage. An astrocyte activation can act through tumour necrosis factor receptor-1 (TNFR1) to increase neurotoxicity and induce apoptosis, while TNFR2 activation would be

neuro-protective in neurons and glia (215). The primary factor that plays an important role in determination of differential action of astrocytes is the extent of damage. In initial stages of damage, the astrocytes traffic the immune and inflammatory cells throughout the damaged area of the brain, and hence limit the spread of potentially neurotoxic inflammation. Once past a threshold, astrocytes reverse its role and becomes neuro-toxic by releasing reactive oxygen species and pro-inflammatory cytokines (216). Activation of astrocytes have also shown to induce accumulation of excessive glutamate during brain damage (220) causing more brain damage in neighbouring brain tissue. Analysis of the downstream signalling of astrocyte-activated proteins would further illuminate the specific stage of the inflammatory process in our model.

In order to clarify the effect of stroke on the neighbouring cells and tissue we decided to further analyze neural changes by measuring changes in neural cell vacuolation, neural degeneration, area of edema and cell infiltration of inflammatory origin, originating from the brain regions near MCA. Neuron degeneration and cell vacuolation have been associated with cell death, that is seen to occur spontaneously with a broad range of inductive stimuli (153) such as the presence of pro-inflammatory cytokines and blood derived factors. We used a modified scoring system to analyze and determine neuronal damage in other disease models (221-223).

Brain regions near the post-stroke MCA showed elevated levels of neural damage compared to pre-stroke brain regions. Degenerating neurons and cell vacuolation were the two most prominent changes observed in the post-stroke samples that indicate higher neural damage in the brain regions near the MCA following stroke. Axon degeneration has been widely seen in neurodegenerative diseases including stroke and motor neuropathies (224). It is also believed to result in impaired delivery of impulses across the neural network and further leading to

cytoskeletal breakdown (224). This would cause a significant decrease in the neural network, leading to decrease in detection of the brain damage, and conduction of signals at the site of damage. I believe a similar prognosis occurs in the post-stroke samples, resulting in a prolonged delay in the repair processes to come into effect, making the brain regions during stroke less responsive and functional to the brain damage.

Edema, one of the signs of brain damage, was also seen to be increased in the post-stroke samples compared to the pre-stroke samples. Edema is generally seen after brain injuries such as stroke and head trauma, and can be either vasogenic or cytotoxic depending on the disease state (154). The greater edema in the post-stroke samples can result from accumulation of fluid resulting from disruption of BBB or cell swelling (154), leading to neuro-inflammation and neuro-degeneration (225), effecting the brain and vascular functioning in stroke. This disruption of the BBB directly affects the brain homeostasis, regulation of influx and efflux (225) of toxins in the brain and MCA, suggesting clear signs of damage after stroke due to increased inflammatory stimuli directly affecting neural and vascular function.

#### ***4.1. Limitations and future directions***

Although we see clear changes in the inflammatory and contractile signalling pathways before and after stroke in the samples obtained from the SHRsp rats, there are several limitations to our data. Our data shows the catastrophic damage which is evident in the post-stroke samples, but the *exact time frame* of damage is unknown. The changes seen in post-stroke samples likely occur during the transition period from pre-stroke to post-stroke, particularly after exposure to chronic high blood pressure during this transition. To identify the stages at which the exact changes occur, it is necessary to obtain samples at regular intervals, such as every 7 days from

the pre-stroke stage to post-stroke stage. For future work, sampling at regular intervals will not only allow detection of the exact time frame for the underlying signalling changes but it will also allow for understanding the structural and functional changes associated with changes in signalling.

For our experiments SHRsp rats were fed Japanese style high salt diet (4% NaCl), as it accelerates the stroke progression and reduces the experimental timeline, making it favourable to obtain specimens in a focused and predictable time frame. The focus of our experiments was to establish the changes occurring in the MCA before and after stroke rather than the effect of change in diet on stroke progression. An important control for disease progression would be obtaining samples from SHRsp fed normal salt diet (0.59% NaCl) and comparing the results with high salt diet SHRsp samples (age-matched). The data would serve as an appropriate comparison for the disease model and determine the role of salt in stroke.

The samples from both pre-stroke and post-stroke animals were analyzed for the expression of contractile proteins, calcium channels and inflammatory mediators by immunofluorescence, a semi-quantitative method. The method involves determining only one cross-section of the vessel and may not be a correct representation of the changes happening in the entire vessel. The sliced section of MCA used for detection may not be from the site of damage. Conversely, there are chances that the sliced MCA used for analysis may be a part of a vessel that is perfectly healthy, so the results from immunofluorescence cannot be considered to be a clear depiction of the changes occurring in the entire vessel. For future investigation, it would be recommended to analyze multiple sections at regular intervals from the same vessel to ensure the changes seen in the immunofluorescence studies resemble the actual changes in the entire vessel. Although the TRPV4 expression was significantly lower in the post-stroke samples

compared to pre-stroke samples, we did not measure the channel activity (conductance), which may have given us a better understanding of calcium channel activity in the MCA.

Further investigation is also warranted into determination of microglial phenotype and expression of activated astrocytes as their determination will help understand the role of astrocytes and microglia in stroke. Investigating specific markers such as MMP-9, CD-36, IL-1, IL-8 and TNF-alpha would help clarify the extent of inflammation in the MCA as well as in the brain during stroke.

#### ***4.2. Conclusion***

Our results demonstrate that the combination of increased inflammatory expression and decreased contractile signalling is responsible for the loss of auto-regulatory mechanisms in the MCA after stroke. These changes during stroke are accompanied with an increase in neural damage as well as neuro-inflammation, affecting the brain region surrounding the MCA during stroke. The presence of inflammation in the MCA and surrounding brain region induce the structural and functional changes seen in MCA after stroke.

## **References**

- (1) About Stroke. 2016; Available at: [http://www.strokeassociation.org/STROKEORG/AboutStroke/About-Stroke\\_UCM\\_308529\\_SubHomePage.jsp#](http://www.strokeassociation.org/STROKEORG/AboutStroke/About-Stroke_UCM_308529_SubHomePage.jsp#). Accessed Oct/19, 2017.
- (2) Benjamin EJ, Blaha MJ, Chiuve SE, Cushman M, Das SR, Deo R, et al. Heart Disease and Stroke Statistics-2017 Update: A Report From the American Heart Association. *Circulation* 2017 Mar 7;135(10):e146-e603.
- (3) Meschia JF, Bushnell C, Boden-Albala B, Braun LT, Bravata DM, Chaturvedi S, et al. Guidelines for the Primary Prevention of Stroke: A Statement for Healthcare Professionals From the American Heart Association/American Stroke Association. *Stroke* 2014 10/28;45(12):3754-3832.
- (4) Sacco RL, Kasner SE, Broderick JP, Caplan LR, Connors JJ, Culebras A, et al. An Updated Definition of Stroke for the 21st Century. *Stroke* 2013 07/01;44(7):2064.
- (5) del Zoppo GJ, Hallenbeck JM. Advances in the vascular pathophysiology of ischemic stroke. *Thromb Res* 2000 May 1;98(3):73-81.
- (6) Frizzell JP. Acute stroke: pathophysiology, diagnosis, and treatment. *AACN Clin Issues* 2005 Oct-Dec;16(4):421-40; quiz 597-8.
- (7) Duan X, Wen Z, Shen H, Shen M, Chen G. Intracerebral Hemorrhage, Oxidative Stress, and Antioxidant Therapy. *Oxidative Medicine and Cellular Longevity* 2016 03/28;2016:1203285.
- (8) Meschia JF, Bushnell C, Boden-Albala B, Braun LT, Bravata DM, Chaturvedi S, et al. Guidelines for the primary prevention of stroke: a statement for healthcare professionals from the American Heart Association/American Stroke Association. *Stroke* 2014 Dec;45(12):3754-3832.
- (9) Caplan LR. Intracerebral haemorrhage. *Lancet* 1992 Mar 14;339(8794):656-658.
- (10) Qureshi AI, Mendelow AD, Hanley DF. Intracerebral haemorrhage. *Lancet* 2009 May 9;373(9675):1632-1644.
- (11) Gustavsson A, Svensson M, Jacobi F, Allgulander C, Alonso J, Beghi E, et al. Cost of disorders of the brain in Europe 2010. *Eur Neuropsychopharmacol* 2011 Oct;21(10):718-779.
- (12) Howard G, Cushman M, Howard VJ, Kissela BM, Kleindorfer DO, Moy CS, et al. Risk factors for intracerebral hemorrhage: the REasons for geographic and racial differences in stroke (REGARDS) study. *Stroke* 2013 May;44(5):1282-1287.

- (13) O'Donnell MJ, Xavier D, Liu L, Zhang H, Chin SL, Rao-Melacini P, et al. Risk factors for ischaemic and intracerebral haemorrhagic stroke in 22 countries (the INTERSTROKE study): a case-control study. *The Lancet* 2010 10–16 July 2010;376(9735):112-123.
- (14) Broderick JP, Brott T, Tomsick T, Huster G, Miller R. The risk of subarachnoid and intracerebral hemorrhages in blacks as compared with whites. *N Engl J Med* 1992 Mar 12;326(11):733-736.
- (15) Rubio-Ruiz ME, Perez-Torres I, Soto ME, Pastelin G, Guarner-Lans V. Aging in blood vessels. Medicinal agents FOR systemic arterial hypertension in the elderly. *Ageing Res Rev* 2014 Nov;18:132-147.
- (16) Camacho EJ, LoPresti MA, Bruce S, Lin D, Abraham ME, et al. The Role of Age in Intracerebral Hemorrhage: An Intricate Relationship. *Austin J Cerebrovasc Dis & Stroke* 2014;1(5):1022.
- (17) Haast RAM, Gustafson DR, Kiliaan AJ. Sex differences in stroke. *Journal of Cerebral Blood Flow & Metabolism* 2012 09/02;32(12):2100-2107.
- (18) Forte P, Kneale BJ, Milne E, Chowienczyk PJ, Johnston A, Benjamin N, et al. Evidence for a difference in nitric oxide biosynthesis between healthy women and men. *Hypertension* 1998 Oct;32(4):730-734.
- (19) Hillbom M. Alcohol consumption and stroke: benefits and risks. *Alcohol Clin Exp Res* 1998 Oct;22(7 Suppl):352S-358S.
- (20) Ariesen MJ, Claus SP, Rinkel GJE, Algra A. Risk Factors for Intracerebral Hemorrhage in the General Population. *Stroke* 2003 08/01;34(8):2060.
- (21) Woo D, Sauerbeck LR, Kissela BM, Khoury JC, Szaflarski JP, Gebel J, et al. Genetic and Environmental Risk Factors for Intracerebral Hemorrhage. *Stroke* 2002 05/01;33(5):1190.
- (22) Tsai CF, Jeng JS, Anderson N, Sudlow CLM. Comparisons of Risk Factors for Intracerebral Hemorrhage versus Ischemic Stroke in Chinese Patients. *Neuroepidemiology* 2017;48(1-2):72-78.
- (23) Poulter NR, Prabhakaran D, Caulfield M. Hypertension. *The Lancet* 2015 22–28 August 2015;386(9995):801-812.
- (24) Garfinkle MA. Salt and essential hypertension: pathophysiology and implications for treatment. *Journal of the American Society of Hypertension* 2017 June 2017;11(6):385-391.
- (25) Girardin E, Caverzasio J, Iwai J, Bonjour JP, Muller AF, Grandchamp A. Pressure natriuresis in isolated kidneys from hypertension-prone and hypertension-resistant rats (Dahl rats). *Kidney Int* 1980 Jul;18(1):10-19.

- (26) Shimamoto H, Shimamoto Y. Time course of hemodynamic responses to sodium in elderly hypertensive patients. *Hypertension* 1990 Oct;16(4):387-397.
- (27) Coffman TM. The inextricable role of the kidney in hypertension. *J Clin Invest* 2014 Jun;124(6):2341-2347.
- (28) Carey RM. The intrarenal renin-angiotensin system in hypertension. *Adv Chronic Kidney Dis* 2015 May;22(3):204-210.
- (29) Chun T, Chander PN, Kim J, Pratt JH, Stier CT. Aldosterone, but not angiotensin II, increases profibrotic factors in kidney of adrenalectomized stroke-prone spontaneously hypertensive rats. *American Journal of Physiology - Endocrinology and Metabolism* 2008;295(2):E305-E312.
- (30) Dinh QN, Drummond GR, Sobey CG, Chrissobolis S. Roles of Inflammation, Oxidative Stress, and Vascular Dysfunction in Hypertension. *Biomed Res Int* 2014;2014:10.1155/2014/406960.
- (31) Matchar DB, McCrory DC, Orlando LA, Patel MR, Patel UD, Patwardhan MB, et al. Systematic review: comparative effectiveness of angiotensin-converting enzyme inhibitors and angiotensin II receptor blockers for treating essential hypertension. *Ann Intern Med* 2008 Jan 1;148(1):16-29.
- (32) Zheng Y, Cai GY, Chen XM, Fu P, Chen JH, Ding XQ, et al. Prevalence, awareness, treatment, and control of hypertension in the non-dialysis chronic kidney disease patients. *Chin Med J (Engl)* 2013 Jun;126(12):2276-2280.
- (33) Cain A, Khalil R. Pathophysiology of essential hypertension: role of the pump, the vessel, and the kidney. *Semin Nephrology* 2002;22(1):3-16.
- (34) Kremer PH, Jolink WM, Kappelle LJ, Algra A, Klijn CJ, SMART and ESPRIT Study Groups. Risk Factors for Lobar and Non-Lobar Intracerebral Hemorrhage in Patients with Vascular Disease. *PLoS One* 2015 Nov 5;10(11):e0142338.
- (35) Nechikkat S, Chandni R, Sasidharan PK. Hypertension as a Risk Factor for Haemorrhagic Stroke in Females. *J Assoc Physicians India* 2014 Nov;62(11):24-28.
- (36) Li W, Jin C, Vaidya A, Wu Y, Rexrode K, Zheng X, et al. Blood Pressure Trajectories and the Risk of Intracerebral Hemorrhage and Cerebral Infarction: A Prospective Study. *Hypertension* 2017 Sep;70(3):508-514.
- (37) Brandts A, Westenberg JJ, van Elderen SG, Kroft LJ, Roes SD, Tamsma JT, et al. Site-specific coupling between vascular wall thickness and function: an observational MRI study of vessel wall thickening and stiffening in hypertension. *Invest Radiol* 2013 Feb;48(2):86-91.

- (38) Oberleithner H, Riethmuller C, Schillers H, MacGregor GA, de Wardener HE, Hausberg M. Plasma sodium stiffens vascular endothelium and reduces nitric oxide release. *Proc Natl Acad Sci U S A* 2007 Oct 9;104(41):16281-16286.
- (39) Cohen JD. Overview of physiology, vascular biology, and mechanisms of hypertension. *J Manag Care Pharm* 2007 Jun;13(5 Suppl):S6-8.
- (40) Faraco G, Iadecola C. Hypertension: a harbinger of stroke and dementia. *Hypertension* 2013 08/26;62(5):10.1161/HYPERTENSIONAHA.113.01063.
- (41) Scuteri A, Nilsson PM, Tzourio C, Redon J, Laurent S. Microvascular brain damage with aging and hypertension: pathophysiological consideration and clinical implications. *J Hypertens* 2011 Aug;29(8):1469-1477.
- (42) Girouard H, Iadecola C. Neurovascular coupling in the normal brain and in hypertension, stroke, and Alzheimer disease. *J Appl Physiol (1985)* 2006 Jan;100(1):328-335.
- (43) Uller W, Alomari AI, Richter GT. Arteriovenous malformations. *Semin Pediatr Surg* 2014 Aug;23(4):203-207.
- (44) Lawton MT, Rutledge WC, Kim H, Stapf C, Whitehead KJ, Li DY, et al. Brain arteriovenous malformations. *Nat Rev Dis Primers* 2015 May 28;1:15008.
- (45) Liao KH, Sung CW, Huang YN, Li WJ, Yu PC, Wang JY. Therapeutic Potential of Drugs Targeting Pathophysiology of Intracerebral Hemorrhage: From Animal Models to Clinical Applications. *Curr Pharm Des* 2017;23(15):2212-2225.
- (46) Balami JS, Buchan AM. Complications of intracerebral haemorrhage. *The Lancet Neurology* 2012 January 2012;11(1):101-118.
- (47) Charidimou A, Imaizumi T, Moulin S, Biffi A, Samarasekera N, Yakushiji Y, et al. Brain hemorrhage recurrence, small vessel disease type, and cerebral microbleeds: A meta-analysis. *Neurology* 2017 Aug 22;89(8):820-829.
- (48) Lin CY, Chen Y, Tseng SH. Chronic encapsulated intracerebral haematoma. *J Clin Neurosci* 2007 Jan;14(1):58-61.
- (49) Thiex R, Tsirka SE. Brain edema after intracerebral hemorrhage: mechanisms, treatment options, management strategies, and operative indications. *Neurosurg Focus* 2007 May 15;22(5):E6.
- (50) Chen S, Zeng L, Hu Z. Progressing haemorrhagic stroke: categories, causes, mechanisms and managements. *J Neurol* 2014 Nov;261(11):2061-2078.
- (51) Hu X, Tao C, Gan Q, Zheng J, Li H, You C. Oxidative Stress in Intracerebral Hemorrhage: Sources, Mechanisms, and Therapeutic Targets. *Oxid Med Cell Longev* 2016;2016:3215391.

- (52) Misarkova E, Behuliak M, Bencze M, Zicha J. Excitation-contraction coupling and excitation-transcription coupling in blood vessels: their possible interactions in hypertensive vascular remodeling. *Physiol Res* 2016 Jun 20;65(2):173-191.
- (53) Paulson OB, Strandgaard S, Edvinsson L. Cerebral autoregulation. *Cerebrovasc Brain Metab Rev* 1990 Summer;2(2):161-192.
- (54) Cipolla MJ. *The Cerebral Circulation*. San Rafael (CA): Morgan & Claypool Life Science 2009.
- (55) Lampe R, Botkin N, Turova V, Blumenstein T, Alves-Pinto A. Mathematical modelling of cerebral blood circulation and cerebral autoregulation: towards preventing intracranial hemorrhages in preterm newborns. *Comput Math Methods Med* 2014;2014:965275.
- (56) Kunz A, Iadecola C. Cerebral vascular dysregulation in the ischemic brain. *Handb Clin Neurol* 2009;92:283-305.
- (57) Osol G, Brekke JF, McElroy-Yaggy K, Gokina NI. Myogenic tone, reactivity, and forced dilatation: a three-phase model of in vitro arterial myogenic behavior. *Am J Physiol Heart Circ Physiol* 2002 Dec;283(6):H2260-7.
- (58) Kontos HA, Wei EP, Navari RM, Levasseur JE, Rosenblum WI, Patterson JL, Jr. Responses of cerebral arteries and arterioles to acute hypotension and hypertension. *Am J Physiol* 1978 Apr;234(4):H371-83.
- (59) Izzard AS, Heagerty AM. Myogenic properties of brain and cardiac vessels and their relation to disease. *Curr Vasc Pharmacol* 2014;12(6):829-835.
- (60) Xu TY, Staessen JA, Wei FF, Xu J, Li FH, Fan WX, et al. Blood flow pattern in the middle cerebral artery in relation to indices of arterial stiffness in the systemic circulation. *Am J Hypertens* 2012 Mar;25(3):319-324.
- (61) Chrissobolis S, Miller AA, Drummond GR, Kemp-Harper BK, Sobey CG. Oxidative stress and endothelial dysfunction in cerebrovascular disease. *Front Biosci (Landmark Ed)* 2011 Jan 1;16:1733-1745.
- (62) Koliass AG, Sen J, Belli A. Pathogenesis of cerebral vasospasm following aneurysmal subarachnoid hemorrhage: putative mechanisms and novel approaches. *J Neurosci Res* 2009 Jan;87(1):1-11.
- (63) Salamanca D, Khalil R. Protein Kinase C Isoforms as Specific Targets for Modulation of Vascular Smooth Muscle Function in Hypertension. *Biochem Pharmacol* 2005;70(11):1537-1547.
- (64) Hartshome DJ, Persechini AJ. Phosphorylation of myosin as a regulatory component in smooth muscle\*. *Ann N Y Acad Sci* 1980;356(1):130-141.

- (65) Gunst SJ, Zhang W. Actin cytoskeletal dynamics in smooth muscle: a new paradigm for the regulation of smooth muscle contraction. *American Journal of Physiology - Cell Physiology* 2008 06/30;295(3):C576-C587.
- (66) Takeya K, Wang X, Kathol I, Loutzenhiser K, Loutzenhiser R, Walsh MP. Endothelin-1, but not angiotensin II, induces afferent arteriolar myosin diphosphorylation as a potential contributor to prolonged vasoconstriction. *Kidney Int* 2015 Feb;87(2):370-381.
- (67) Walsh MP. Vascular smooth muscle myosin light chain diphosphorylation: mechanism, function, and pathological implications. *IUBMB Life* 2011 Nov;63(11):987-1000.
- (68) Somlyo AP, Somlyo AV. Ca<sup>2+</sup> sensitivity of smooth muscle and nonmuscle myosin II: modulated by G proteins, kinases, and myosin phosphatase. *Physiol Rev* 2003;83(4):1325-58.
- (69) Somlyo AP SA. Signal transduction by G-proteins, Rho-kinase and protein phosphatase to smooth muscle and non-muscle myosin II. *The Journal of Physiology*. 2000;522(- 0022-3751 (Print); - 0022-3751 (Linking)):177-185.
- (70) Somlyo AP SA. Signal transduction and regulation in smooth muscle. *Nature* 1994;372(6503)((6503)):231-6.
- (71) Goyal R, Mittal A, Chu N, Shi L, Zhang L, Longo LD. Maturation and the role of PKC-mediated contractility in ovine cerebral arteries. *Am J Physiol Heart Circ Physiol* 2009 American Physiological Society;297(6):H2242-H2252.
- (72) Liu WS, Heckman CA. The Sevenfold Way of PKC Regulation. *Cellular Signalling* 1998 September 1998;10(8):529-542.
- (73) Ron D, Kazanietz MG. New insights into the regulation of protein kinase C and novel phorbol ester receptors. *The FASEB Journal* 1999;13(13):1658-1676.
- (74) Marquez VE, Blumberg PM. Synthetic diacylglycerols (DAG) and DAG-lactones as activators of protein kinase C (PK-C). *Acc Chem Res* 2003 Jun;36(6):434-443.
- (75) Hughes-Darden CA, Wachira SJ, Denaro FJ, Taylor CV, Brunson KJ, Ochillo R, et al. Expression and distribution of protein kinase C isozymes in brain tissue of spontaneous hypertensive rats. *Cell Mol Biol* 2001;47(6):1077-88.
- (76) Soloviev AI, Parshikov AV, Stefanov AV. Evidence for the involvement of protein kinase C in depression of endothelium-dependent vascular responses in spontaneously hypertensive rats. *Journal of Vascular Research* 1998;35(5):325-31.
- (77) Schiffrin EL. Endothelin: potential role in hypertension and vascular hypertrophy. *Hypertension* 1995;25(6):1135-43.

- (78) Gamard CJ, Blobel GC, Hannun YA, Obeid LM. Specific role for protein kinase C beta in cell differentiation. *Cell Growth Differ* 1994 Apr;5(4):405-409.
- (79) McCarty MF. Up-regulation of intracellular signalling pathways may play a central pathogenic role in hypertension, atherogenesis, insulin resistance, and cancer promotion--the 'PKC syndrome'. *Med Hypotheses* 1996;46(3):191-221.
- (80) Gurusamy N, Watanabe K, Ma M, Zhang S, Muslin AJ, Kodama M, et al. Inactivation of 14-3-3 protein exacerbates cardiac hypertrophy and fibrosis through enhanced expression of protein kinase C beta 2 in experimental diabetes. *Biol Pharm Bull* 2005 Jun;28(6):957-962.
- (81) Qiao X, Khalil RA. *Role of Protein Kinase C and Related Pathways in Vascular Smooth Muscle Contraction and Hypertension*. Neurovascular Medicine New York: Oxford University Press; 2009.
- (82) Adapala RK, Talasila PK, Bratz IN, Zhang DX, Suzuki M, Meszaros JG, et al. PKC $\alpha$  mediates acetylcholine-induced activation of TRPV4-dependent calcium influx in endothelial cells. *Am J Physiol Heart Circ Physiol* 2011 Sep;301(3):H757-65.
- (83) Clapham DE. TRP channels as cellular sensors. *Nature* 2003 12/04;426:517.
- (84) Yue Z, Xie J, Albert SY, Stock J, Du J, Yue L. Role of TRP channels in the cardiovascular system. *American Journal of Physiology-Heart and Circulatory Physiology* 2015 02/01; 2017/12;308(3):H157-H182.
- (85) Sullivan MN, Earley S. TRP channel Ca<sup>2+</sup> sparklets: fundamental signals underlying endothelium-dependent hyperpolarization. *American Journal of Physiology-Cell Physiology* 2013 11/15; 2017/12;305(10):C999-C1008.
- (86) Sukumaran SV, Singh TU, Parida S, Narasimha Reddy C, Thangamalai R, Kandasamy K, et al. TRPV4 channel activation leads to endothelium-dependent relaxation mediated by nitric oxide and endothelium-derived hyperpolarizing factor in rat pulmonary artery. *Pharmacol Res* 2013 Dec;78:18-27.
- (87) Marrelli SP, Roger G. O'Neil, Brown RC, Bryan RM. PLA<sub>2</sub> and TRPV4 channels regulate endothelial calcium in cerebral arteries. *American Journal of Physiology-Heart and Circulatory Physiology* 2007 03/01; 2017/12;292(3):H1390-H1397.
- (88) Willette RN, Bao W, Nerurkar S, Yue T, Doe CP, Stankus G, et al. Systemic Activation of the Transient Receptor Potential Vanilloid Subtype 4 Channel Causes Endothelial Failure and Circulatory Collapse: Part 2. *J Pharmacol Exp Ther* 2008 American Society for Pharmacology and Experimental Therapeutics;326(2):443-452.
- (89) Earley S, Heppner TJ, Nelson MT, Brayden JE. TRPV4 Forms a Novel Ca<sup>2+</sup> Signaling Complex With Ryanodine Receptors and BK<sub>Ca</sub> Channels. *Circ Res* 2005 Lippincott Williams & Wilkins;97(12):1270-1279.

- (90) Song S, Yamamura A, Yamamura H, Ayon RJ, Smith KA, Tang H, et al. Flow shear stress enhances intracellular Ca<sup>2+</sup> signaling in pulmonary artery smooth muscle cells from patients with pulmonary arterial hypertension. *American Journal of Physiology-Cell Physiology* 2014 08/15; 2017/12;307(4):C373-C383.
- (91) Dietrich A, Chubanov V, Kalwa H, Rost BR, Gudermann T. Cation channels of the transient receptor potential superfamily: Their role in physiological and pathophysiological processes of smooth muscle cells. *Pharmacology & Therapeutics* 2006 December 2006;112(3):744-760.
- (92) Sullivan MN, Earley S. TRP channel Ca(2+) sparklets: fundamental signals underlying endothelium-dependent hyperpolarization. *Am J Physiol Cell Physiol* 2013 Nov 15;305(10):C999-C1008.
- (93) Sonkusare SK, Bonev AD, Ledoux J, Liedtke W, Kotlikoff MI, Heppner TJ, et al. Elementary Ca<sup>2+</sup> signals through endothelial TRPV4 channels regulate vascular function. *Science* 2012 May 4;336(6081):597-601.
- (94) Hatano N, Suzuki H, Itoh Y, Muraki K. TRPV4 partially participates in proliferation of human brain capillary endothelial cells. *Life Sci* 2013 Mar 12;92(4-5):317-324.
- (95) Durand MJ, Gutterman DD. Diversity in mechanisms of endothelium-dependent vasodilation in health and disease. *Microcirculation* 2013 Apr;20(3):239-247.
- (96) Rajendran P, Rengarajan T, Thangavel J, Nishigaki Y, Sakthisekaran D, Sethi G, et al. The Vascular Endothelium and Human Diseases. *Int J Biol Sci* 2013;9(10):1057-1069.
- (97) Dong Z, N JE. Transcriptional targeting of tumor endothelial cells for gene therapy. *Adv Drug Deliv Rev* 2009 Jul 2;61(7-8):542-553.
- (98) Lüscher TF. Endothelial Control of Vascular Tone and Growth. *Clinical and Experimental Hypertension Part A: Theory and Practice* 1990 01/01;12(5):897-902.
- (99) Barton M, Baretella O, Meyer MR. Obesity and risk of vascular disease: importance of endothelium-dependent vasoconstriction. *Br J Pharmacol* 2012 Feb;165(3):591-602.
- (100) Hill MA, Meininger GA. Arteriolar vascular smooth muscle cells: mechanotransducers in a complex environment. *Int J Biochem Cell Biol* 2012 Sep;44(9):1505-1510.
- (101) Carvalho C, Moreira PI. Oxidative Stress: A Major Player in Cerebrovascular Alterations Associated to Neurodegenerative Events. *Front Physiol* 2018;9:10.3389/fphys.2018.00806.
- (102) Touyz RM, Briones AM. Reactive oxygen species and vascular biology: implications in human hypertension. *Hypertens Res* 2011 Jan;34(1):5-14.

- (103) Bachschmid MM, Schildknecht S, Matsui R, Zee R, Haeussler D, Cohen RA, et al. Vascular aging: chronic oxidative stress and impairment of redox signaling-consequences for vascular homeostasis and disease. *Ann Med* 2013 Feb;45(1):17-36.
- (104) Yu YP, Chi XL, Liu LJ. A hypothesis: hydrogen sulfide might be neuroprotective against subarachnoid hemorrhage induced brain injury. *ScientificWorldJournal* 2014 Feb 23;2014:432318.
- (105) Xiong X, Liu L, Yang Q. Functions and mechanisms of microglia/macrophages in neuroinflammation and neurogenesis after stroke. *Progress in Neurobiology* 2016 July 2016;142(Supplement C):23-44.
- (106) Li Q, Pogwizd SM, Prabhu SD, Zhou L. Inhibiting Na<sup>+</sup>/K<sup>+</sup> ATPase can impair mitochondrial energetics and induce abnormal Ca<sup>2+</sup> cycling and automaticity in guinea pig cardiomyocytes. *PLoS One* 2014 Apr 10;9(4):e93928.
- (107) Khaper N, Bryan S, Dhingra S, Singal R, Bajaj A, Pathak CM, et al. Targeting the vicious inflammation-oxidative stress cycle for the management of heart failure. *Antioxid Redox Signal* 2010 Oct 1;13(7):1033-1049.
- (108) Mracsko E, Veltkamp R. Neuroinflammation after intracerebral hemorrhage. *Front Cell Neurosci* 2014 Nov 20;8:388.
- (109) Sprague AH, Khalil RA. Inflammatory Cytokines in Vascular Dysfunction and Vascular Disease. *Biochem Pharmacol* 2009 05/04;78(6):539-552.
- (110) Szmítko PE, Wang CH, Weisel RD, de Almeida JR, Anderson TJ, Verma S. New markers of inflammation and endothelial cell activation: Part I. *Circulation* 2003 Oct 21;108(16):1917-1923.
- (111) Griendling KK, Sorescu D, Lassegue B, Ushio-Fukai M. Modulation of protein kinase activity and gene expression by reactive oxygen species and their role in vascular physiology and pathophysiology. *Arterioscler Thromb Vasc Biol* 2000 Oct;20(10):2175-2183.
- (112) Kofler S, Nickel T, Weis M. Role of cytokines in cardiovascular diseases: a focus on endothelial responses to inflammation. *Clin Sci (Lond)* 2005 Mar;108(3):205-213.
- (113) Sanchez A, Tripathy D, Yin X, Desobry K, Martinez J, Riley J, et al. p38 MAPK: a mediator of hypoxia-induced cerebrovascular inflammation. *J Alzheimers Dis* 2012;32(3):587-597.
- (114) Barone FC, Feuerstein GZ. Inflammatory mediators and stroke: new opportunities for novel therapeutics. *J Cereb Blood Flow Metab* 1999 Aug;19(8):819-834.
- (115) Sun J, Nan G. The Mitogen-Activated Protein Kinase (MAPK) Signaling Pathway as a Discovery Target in Stroke. *J Mol Neurosci* 2016 May;59(1):90-98.

- (116) Hommes DW, Peppelenbosch MP, van Deventer, S.J.H. Mitogen activated protein (MAP) kinase signal transduction pathways and novel anti-inflammatory targets. *Gut* 2003 01/01;52(1):144.
- (117) Culbert AA, Skaper SD, Howlett DR, Evans NA, Facci L, Soden PE, et al. MAPK-activated protein kinase 2 deficiency in microglia inhibits pro-inflammatory mediator release and resultant neurotoxicity. Relevance to neuroinflammation in a transgenic mouse model of Alzheimer disease. *J Biol Chem* 2006 Aug 18;281(33):23658-23667.
- (118) Shaul YD, Seger R. The MEK/ERK cascade: From signaling specificity to diverse functions. *Biochimica et Biophysica Acta (BBA) - Molecular Cell Research; Mitogen-Activated Protein Kinases: New Insights on Regulation, Function and Role in Human Disease* 2007 08/01;1773(8):1213-1226.
- (119) Goetze S, Xi XP, Kawano Y, Kawano H, Fleck E, Hsueh WA, et al. TNF-alpha-induced migration of vascular smooth muscle cells is MAPK dependent. *Hypertension* 1999 Jan;33(1 Pt 2):183-189.
- (120) Sugino T, Nozaki K, Takagi Y, Hattori I, Hashimoto N, Moriguchi T, et al. Activation of mitogen-activated protein kinases after transient forebrain ischemia in gerbil hippocampus. *J Neurosci* 2000 Jun 15;20(12):4506-4514.
- (121) KOLCH W. Meaningful relationships: the regulation of the Ras/Raf/MEK/ERK pathway by protein interactions. *Biochem J* 2000 Portland Press Ltd;351(2):289-305.
- (122) Ruhul Amin AR, Senga T, Oo ML, Thant AA, Hamaguchi M. Secretion of matrix metalloproteinase-9 by the proinflammatory cytokine, IL-1beta: a role for the dual signalling pathways, Akt and Erk. *Genes Cells* 2003 Jun;8(6):515-523.
- (123) Wortzel I, Seger R. The ERK Cascade: Distinct Functions within Various Subcellular Organelles. *Genes & Cancer* 2011 03;2(3):195-209.
- (124) Brozovich FV, Nicholson CJ, Degen CV, Gao YZ, Aggarwal M, Morgan KG. Mechanisms of Vascular Smooth Muscle Contraction and the Basis for Pharmacologic Treatment of Smooth Muscle Disorders. *Pharmacol Rev* 2016 Apr;68(2):476-532.
- (125) Klemke RL, Cai S, Giannini AL, Gallagher PJ, de Lanerolle P, Cheresch DA. Regulation of Cell Motility by Mitogen-activated Protein Kinase. *J Cell Biol* 1997 Apr 21;137(2):481-492.
- (126) Fujimoto S, Katsuki H, Ohnishi M, Takagi M, Kume T, Akaike A. Thrombin induces striatal neurotoxicity depending on mitogen-activated protein kinase pathways in vivo. *Neuroscience* 2007 Jan 19;144(2):694-701.
- (127) Ohnishi M, Monda A, Takemoto R, Matsuoka Y, Kitamura C, Ohashi K, et al. Sesamin suppresses activation of microglia and p44/42 MAPK pathway, which confers neuroprotection in rat intracerebral hemorrhage. *Neuroscience* 2013 Mar 1;232:45-52.

- (128) Burda JE, Sofroniew MV. Reactive gliosis and the multicellular response to CNS damage and disease. *Neuron* 2014 01/22;81(2):229-248.
- (129) Kohman RA, Rhodes JS. Neurogenesis, inflammation and behavior. *Brain Behav Immun* 2013 Jan;27(1):22-32.
- (130) Skaper SD, Giusti P, Facci L. Microglia and mast cells: two tracks on the road to neuroinflammation. *FASEB J* 2012 Aug;26(8):3103-3117.
- (131) Ransohoff RM, Brown MA. Innate immunity in the central nervous system. *J Clin Invest* 2012 Apr;122(4):1164-1171.
- (132) Zhang D, Hu X, Qian L, O'Callaghan JP, Hong JS. Astroglia in CNS pathologies: is there a role for microglia? *Mol Neurobiol* 2010 Jun;41(2-3):232-241.
- (133) Kim JY, Kawabori M, Yenari MA. Innate inflammatory responses in stroke: mechanisms and potential therapeutic targets. *Curr Med Chem* 2014;21(18):2076-2097.
- (134) Kirkley KS, Popichak KA, Afzali MF, Legare ME, Tjalkens RB. Microglia amplify inflammatory activation of astrocytes in manganese neurotoxicity. *Journal of Neuroinflammation* 2017 05/05;14(1):99.
- (135) Cekanaviciute E, Buckwalter MS. Astrocytes: Integrative Regulators of Neuroinflammation in Stroke and Other Neurological Diseases. *Neurotherapeutics* 2016 Oct;13(4):685-701.
- (136) Anderson CM, Swanson RA. Astrocyte glutamate transport: review of properties, regulation, and physiological functions. *Glia* 2000 Oct;32(1):1-14.
- (137) Bao Y, Qin L, Kim E, Bhosle S, Guo H, Febbraio M, et al. CD36 is involved in astrocyte activation and astroglial scar formation. *J Cereb Blood Flow Metab* 2012 Aug;32(8):1567-1577.
- (138) Wanner IB, Anderson MA, Song B, Levine J, Fernandez A, Gray-Thompson Z, et al. Glial scar borders are formed by newly proliferated, elongated astrocytes that interact to corral inflammatory and fibrotic cells via STAT3-dependent mechanisms after spinal cord injury. *J Neurosci* 2013 Jul 31;33(31):12870-12886.
- (139) Vyas P, Kalidindi S, Chibrikova L, Igamberdiev AU, Weber JT. Chemical analysis and effect of blueberry and lingonberry fruits and leaves against glutamate-mediated excitotoxicity. *J Agric Food Chem* 2013 Aug 14;61(32):7769-7776.
- (140) Sergeeva SP, Shishkina LV, Litvitskiy PF, Breslavich ID, Vinogradov EV. Structure changes of human brain gray matter neurons and astrocytes in acute local ischemic injury. *Patol Fiziol Eksp Ter* 2016 Oct-Dec;60(4):4-8.

- (141) Khudoerkov RM, Voronkov DN, Yamshchikova NG. Immunohistochemical and morphological changes in neurons and neuroglia in the cerebral nigrostriatal structures under conditions of experimental nigral neurodegeneration. *Bull Exp Biol Med* 2012 Oct;153(6):893-897.
- (142) Zlokovic BV, Griffin JH. Cytoprotective Protein C Pathways and Implications for Stroke and Neurological Disorders. *Trends Neurosci* 2011 Apr;34(4):198-209.
- (143) Viscomi MT, Molinari M. Remote neurodegeneration: multiple actors for one play. *Mol Neurobiol* 2014 Oct;50(2):368-389.
- (144) Pinching AJ, Powell TP. Ultrastructural features of transneuronal cell degeneration in the olfactory system. *J Cell Sci* 1971 Jan;8(1):253-287.
- (145) Buffo A, Fronte M, Oestreicher AB, Rossi F. Degenerative phenomena and reactive modifications of the adult rat inferior olivary neurons following axotomy and disconnection from their targets. *Neuroscience* 1998 Jul;85(2):587-604.
- (146) Florenzano F, Viscomi MT, Cavaliere F, Volonte C, Molinari M. Cerebellar lesion up-regulates P2X1 and P2X2 purinergic receptors in precerebellar nuclei. *Neuroscience* 2002;115(2):425-434.
- (147) Galluzzi L, Kepp O, Kroemer G. Mitochondria: master regulators of danger signalling. *Nat Rev Mol Cell Biol* 2012 Dec;13(12):780-788.
- (148) Klionsky DJ, Emr SD. Autophagy as a regulated pathway of cellular degradation. *Science* 2000 Dec 1;290(5497):1717-1721.
- (149) Shukla V, Shakya AK, Perez-Pinzon MA, Dave KR. Cerebral ischemic damage in diabetes: an inflammatory perspective. *J Neuroinflammation* 2017;14:10.1186/s12974-016-0774-5.
- (150) Fiumara E, Gambacorta M, D'Angelo V, Ferrara M, Corona C. Chronic encapsulated intracerebral haematoma: pathogenetic and diagnostic considerations. *J Neurol Neurosurg Psychiatry* 1989 Nov;52(11):1296-1299.
- (151) Zhao X, Aronowski J. Nrf2 to pre-condition the brain against injury caused by products of hemolysis after ICH. *Transl Stroke Res* 2013 Feb;4(1):71-75.
- (152) Aoyama M, Osuka K, Usuda N, Watanabe Y, Kawaguchi R, Nakura T, et al. Expression of Mitogen-Activated Protein Kinases in Chronic Subdural Hematoma Outer Membranes. *J Neurotrauma* 2015 Jul 15;32(14):1064-1070.
- (153) Henics T, Wheatley DN. Cytoplasmic vacuolation, adaptation and cell death: a view on new perspectives and features. *Biol Cell* 1999 Sep;91(7):485-498.

- (154) Michinaga S, Koyama Y. Pathogenesis of Brain Edema and Investigation into Anti-Edema Drugs. *Int J Mol Sci* 2015 May;16(5):9949-9975.
- (155) Yan T, Chopp M, Chen J. Experimental animal models and inflammatory cellular changes in cerebral ischemic and hemorrhagic stroke. *Neurosci Bull* 2015 Dec;31(6):717-734.
- (156) Krafft PR, Bailey EL, Lekic T, Rolland WB, Altay O, Tang J, et al. Etiology of Stroke and Choice of Models. *International Journal of Stroke* 2012 07/01; 2017/10;7(5):398-406.
- (157) Alharbi BM, Tso MK, Macdonald RL. Animal models of spontaneous intracerebral hemorrhage. *Neurol Res* 2016 05/03;38(5):448-455.
- (158) Belayev L, Saul I, Curbelo K, Busto R, Belayev A, Zhang Y, et al. Experimental intracerebral hemorrhage in the mouse: histological, behavioral, and hemodynamic characterization of a double-injection model. *Stroke* 2003 Sep;34(9):2221-2227.
- (159) Rosenberg GA, Mun-Bryce S, Wesley M, Kornfeld M. Collagenase-induced intracerebral hemorrhage in rats. *Stroke* 1990 May;21(5):801-807.
- (160) Bhasin RR, Xi G, Hua Y, Keep RF, Hoff JT. Experimental intracerebral hemorrhage: effect of lysed erythrocytes on brain edema and blood-brain barrier permeability. *Acta Neurochir Suppl* 2002;81:249-251.
- (161) Krafft PR, Rolland WB, Duris K, Lekic T, Campbell A, Tang J, et al. Modeling Intracerebral Hemorrhage in Mice: Injection of Autologous Blood or Bacterial Collagenase. *J Vis Exp* 2012;(67):4289. doi(67):10.3791/4289.
- (162) Lei B, Sheng H, Wang H, Lascola CD, Warner DS, Laskowitz DT, et al. Intraatrial Injection of Autologous Blood or Clostridial Collagenase as Murine Models of Intracerebral Hemorrhage. *J Vis Exp* 2014;(89):51439. doi(89):10.3791/51439.
- (163) Lopez Valdes E, Hernandez Lain A, Calandre L, Grau M, Cabello A, Gomez-Escalonilla C. Time window for clinical effectiveness of mass evacuation in a rat balloon model mimicking an intraparenchymatous hematoma. *J Neurol Sci* 2000 Mar 1;174(1):40-46.
- (164) Funnell WRJ, Maysinger D, Cuello AC. Three-dimensional reconstruction and quantitative evaluation of devascularizing cortical lesions in the rat. *J Neurosci Methods* 1990;35(2):147-156.
- (165) Sinar EJ, Mendelow AD, Graham DI, Teasdale GM. Experimental intracerebral hemorrhage: effects of a temporary mass lesion. *J Neurosurg* 1987 Apr;66(4):568-576.
- (166) Smeda JS. Hemorrhagic stroke development in spontaneously hypertensive rats fed a North American, Japanese-style diet. *Stroke* 1989 Sep;20(9):1212-1218.
- (167) Nabika T, Cui Z, Masuda J. The stroke-prone spontaneously hypertensive rat: how good is it as a model for cerebrovascular diseases? *Cell Mol Neurobiol* 2004 Oct;24(5):639-646.

- (168) Smeda JS. Cerebral vascular changes associated with hemorrhagic stroke in hypertension. *Can J Physiol Pharmacol* 1992 Apr;70(4):552-564.
- (169) Sadoshima S, Busija D, Brody M, Heistad D. Sympathetic nerves protect against stroke in stroke-prone hypertensive rats. A preliminary report. *Hypertension* 1981 May-Jun;3(3 Pt 2):I124-7.
- (170) Smeda JS, King S. Electromechanical alterations in the cerebrovasculature of stroke-prone rats. *Stroke* 2000 Mar;31(3):751-8; discussion 758-9.
- (171) Daneshtalab N, Smeda JS. Alterations in the modulation of cerebrovascular tone and blood flow by nitric oxide synthases in SHRsp with stroke. *Cardiovasc Res* 2010 Apr 1;86(1):160-168.
- (172) Smeda JS, VanVliet BN, King SR. Stroke-prone spontaneously hypertensive rats lose their ability to auto-regulate cerebral blood flow prior to stroke. *J Hypertens* 1999 Dec;17(12 Pt 1):1697-1705.
- (173) Lee JM, Zhai G, Liu Q, Gonzales ER, Yin K, Yan P, et al. Vascular permeability precedes spontaneous intracerebral hemorrhage in stroke-prone spontaneously hypertensive rats. *Stroke* 2007 Dec;38(12):3289-3291.
- (174) Bailey EL, Wardlaw JM, Graham D, Dominiczak AF, Sudlow CLM, Smith C. Cerebral small vessel endothelial structural changes predate hypertension in stroke-prone spontaneously hypertensive rats: a blinded, controlled immunohistochemical study of 5- to 21-week-old rats. *Neuropathol Appl Neurobiol* 2011;37(7):711-726.
- (175) Garosi L, McConnell JF, Platt SR, Barone G, Baron JC, de Lahunta A, et al. Clinical and topographic magnetic resonance characteristics of suspected brain infarction in 40 dogs. *J Vet Intern Med* 2006 Mar-Apr;20(2):311-321.
- (176) Fedchenko, Nickolay, Reifenrath, Janin. Different approaches for interpretation and reporting of immunohistochemistry analysis results in the bone tissue – a review.
- (177) Henics T, Wheatley DN. Cytoplasmic vacuolation, adaptation and cell death: A view on new perspectives and features. *Biology of the Cell* 1999;91(7):485-498.
- (178) Detre S, Saclani Jotti G, Dowsett M. A "quickscore" method for immunohistochemical semiquantitation: validation for oestrogen receptor in breast carcinomas. *J Clin Pathol* 1995 BMJ Publishing Group Ltd and Association of Clinical Pathologists;48(9):876-878.
- (179) Daneshtalab N, Smeda JS. Alterations in the modulation of cerebrovascular tone and blood flow by nitric oxide synthases in SHRsp with stroke. *Cardiovascular Research* 2010;86:160–168.
- (180) Kerrick WG, Hoar PE. Smooth muscle: regulation by calcium and phosphorylation. *Ciba Found Symp* 1986;122:183-196.

- (181) Gao N, Huang J, He W, Zhu M, Kamm KE, Stull JT. Signaling through myosin light chain kinase in smooth muscles. *J Biol Chem* 2013 Mar 15;288(11):7596-7605.
- (182) Sousa D, Cammarato A, Jang K, Graceffa P, Tobacman LS, Li X, et al. Electron Microscopy and Persistence Length Analysis of Semi-Rigid Smooth Muscle Tropomyosin Strands. *Biophys J* 2010 05/03;99(3):862-868.
- (183) Baumbach GL, Heistad DD. Remodeling of cerebral arterioles in chronic hypertension. *Hypertension* 1989 Jun;13(6 Pt 2):968-972.
- (184) Goulopoulou S, Webb RC. The symphony of vascular contraction: How smooth muscle cells lose harmony to signal increased vascular resistance in hypertension. *Hypertension* 2014 Mar;63(3):e33-9.
- (185) Policha A, Daneshtalab N, Chen L, Dale LB, Altier C, Khosravani H, et al. Role of Angiotensin II Type 1A Receptor Phosphorylation, Phospholipase D, and Extracellular Calcium in Isoform-specific Protein Kinase C Membrane Translocation Responses\*. *The Journal of Biological Chemistry* 2006:26340-26349.
- (186) Zhao Y, Zhang L, Longo LD. PKC-induced ERK1/2 interactions and downstream effectors in ovine cerebral arteries. *Am J Physiol Regul Integr Comp Physiol* 2005 Jul;289(1):R164-71.
- (187) Keranen LM, Dutil EM, Newton AC. Protein kinase C is regulated in vivo by three functionally distinct phosphorylations. *Curr Biol* 1995 Dec 1;5(12):1394-1403.
- (188) Huang KP. The mechanism of protein kinase C activation. *Trends Neurosci* 1989 Nov;12(11):425-432.
- (189) Tsuchiya A, Kanno T, Nishizaki T. Diacylglycerol promotes GLUT4 translocation to the cell surface in a PKCepsilon-dependent and PKClambda/iota and -zeta-independent manner. *Life Sci* 2013 Aug 14;93(5-6):240-246.
- (190) Kong L, Shen X, Lin L, Leitges M, Rosario R, Zou YS, et al. PKCbeta promotes vascular inflammation and acceleration of atherosclerosis in diabetic ApoE null mice. *Arterioscler Thromb Vasc Biol* 2013 Aug;33(8):1779-1787.
- (191) Mercado J, Baylie R, Navedo MF, Yuan C, Scott JD, Nelson MT, et al. Local control of TRPV4 channels by AKAP150-targeted PKC in arterial smooth muscle. *J Gen Physiol* 2014 May;143(5):559-575.
- (192) Li H, Kan H, Zhang X, Yang Z, Jin J, Zhang P, et al. TRPV4 activates cytosolic phospholipase A2 via Ca(2+) -dependent PKC/ERK1/2 signaling in controlling hypertensive contraction. *Clin Exp Pharmacol Physiol* 2018 Apr 27.

- (193) Peng H, Lewandrowski U, Muller B, Sickmann A, Walz G, Wegierski T. Identification of a Protein Kinase C-dependent phosphorylation site involved in sensitization of TRPV4 channel. *Biochem Biophys Res Commun* 2010 Jan 22;391(4):1721-1725.
- (194) Mamenko M, Zaika OL, Boukelmoune N, Berrou J, O'Neil RG, Pochynyuk O. Discrete control of TRPV4 channel function in the distal nephron by protein kinases A and C. *J Biol Chem* 2013 Jul 12;288(28):20306-20314.
- (195) Laurent S, Boutouyrie P. The structural factor of hypertension: large and small artery alterations. *Circ Res* 2015 Mar 13;116(6):1007-1021.
- (196) Filosa JA, Yao X, Rath G. TRPV4 and the regulation of vascular tone. *J Cardiovasc Pharmacol* 2013 Feb;61(2):113-119.
- (197) Sun J, Nan G. The Mitogen-Activated Protein Kinase (MAPK) Signaling Pathway as a Discovery Target in Stroke. *Journal of Molecular Neuroscience* 2016 05/01;59(1):90-98.
- (198) Cao L, Cao YX, Xu CB, Edvinsson L. Altered endothelin receptor expression and affinity in spontaneously hypertensive rat cerebral and coronary arteries. *PLoS One* 2013 Sep 2;8(9):e73761.
- (199) Lu D, Kassab GS. Role of shear stress and stretch in vascular mechanobiology. *J R Soc Interface* 2011 Oct 7;8(63):1379-1385.
- (200) Anwar MA, Shalhoub J, Lim CS, Gohel MS, Davies AH. The effect of pressure-induced mechanical stretch on vascular wall differential gene expression. *J Vasc Res* 2012;49(6):463-478.
- (201) Roberts RE. The role of Rho kinase and extracellular regulated kinase-mitogen-activated protein kinase in alpha2-adrenoceptor-mediated vasoconstriction in the porcine palmar lateral vein. *J Pharmacol Exp Ther* 2004 Nov;311(2):742-747.
- (202) Ohnishi M, Katsuki H, Izumi Y, Kume T, Takada-Takatori Y, Akaike A. Mitogen-activated protein kinases support survival of activated microglia that mediate thrombin-induced striatal injury in organotypic slice culture. *J Neurosci Res* 2010 Aug 1;88(10):2155-2164.
- (203) Zhang YH, Chen H, Chen Y, Wang L, Cai YH, Li M, et al. Activated microglia contribute to neuronal apoptosis in Toxoplasmic encephalitis. *Parasit Vectors* 2014 Aug 15;7:372-3305-7-372.
- (204) Jeong HK, Ji K, Min K, Joe EH. Brain Inflammation and Microglia: Facts and Misconceptions. *Exp Neurobiol* 2013 Jun;22(2):59-67.
- (205) Luo XG, Chen SD. The changing phenotype of microglia from homeostasis to disease. *Transl Neurodegener* 2012;1:9-9158-1-9.

- (206) Kaminska B, Gozdz A, Zawadzka M, Ellert-Miklaszewska A, Lipko M. MAPK signal transduction underlying brain inflammation and gliosis as therapeutic target. *Anat Rec (Hoboken)* 2009 Dec;292(12):1902-1913.
- (207) Liu Y, Wu X, Luo Q, Huang S, Yang QQ, Wang F, et al. CX3CL1/CX3CR1-mediated microglia activation plays a detrimental role in ischemic mice brain via p38MAPK/PKC pathway. *Journal of Cerebral Blood Flow & Metabolism* 2015 04/13;35(10):1623-1631.
- (208) Park S, Sapkota K, Kim S, Kim H, Kim S. Kaempferol acts through mitogen-activated protein kinases and protein kinase B/AKT to elicit protection in a model of neuroinflammation in BV2 microglial cells. *Br J Pharmacol* 2011 Oct;164(3):1008-1025.
- (209) Taylor RA, Sansing LH. Microglial Responses after Ischemic Stroke and Intracerebral Hemorrhage. *Clin Dev Immunol* 2013;2013:10.1155/2013/746068.
- (210) del Zoppo GJ, Frankowski H, Gu YH, Osada T, Kanazawa M, Milner R, et al. Microglial cell activation is a source of metalloproteinase generation during hemorrhagic transformation. *J Cereb Blood Flow Metab* 2012 May;32(5):919-932.
- (211) JÄkel S, Dimou L. Glial Cells and Their Function in the Adult Brain: A Journey through the History of Their Ablation. *Front Cell Neurosci* 2017;11:10.3389/fncel.2017.00024.
- (212) Rahimian R, Cordeau P, Kriz J. Brain Response to Injuries: When Microglia Go Sexist. *Neuroscience* 2018 Available online 8 March 2018.
- (213) Karthikeyan A, Patnala R, Jadhav SP, Eng-Ang L, Dheen ST. MicroRNAs: Key Players in Microglia and Astrocyte Mediated Inflammation in CNS Pathologies. *Curr Med Chem* 2016;23(30):3528-3546.
- (214) Wanner IB, Anderson MA, Song B, Levine J, Fernandez A, Gray-Thompson Z, et al. Glial scar borders are formed by newly proliferated, elongated astrocytes that interact to corral inflammatory and fibrotic cells via STAT3-dependent mechanisms after spinal cord injury. *J Neurosci* 2013 Jul 31;33(31):12870-12886.
- (215) Romero J, Muniz J, Logica Tornatore T, Holubiec M, Gonzalez J, Barreto GE, et al. Dual role of astrocytes in perinatal asphyxia injury and neuroprotection. *Neurosci Lett* 2014 Apr 17;565:42-46.
- (216) Sofroniew MV. Astrocyte barriers to neurotoxic inflammation. *Nat Rev Neurosci* 2015 May;16(5):249-263.
- (217) Chen Z, Yao Y, Norris EH, Kruyer A, Jno-Charles O, Akhmerov A, et al. Ablation of astrocytic laminin impairs vascular smooth muscle cell function and leads to hemorrhagic stroke. *J Cell Biol* 2013 06/06;202(2):381-395.

- (218) Beihui L, Teschemacher AG, Sergey K. Astroglia as a cellular target for neuroprotection and treatment of neuro-psychiatric disorders. *Glia* 2017 08/01; 2018/07;65(8):1205-1226.
- (219) Xia CY, Zhang S, Gao Y, Wang ZZ, Chen NH. Selective modulation of microglia polarization to M2 phenotype for stroke treatment. *Int Immunopharmacol* 2015 Apr;25(2):377-382.
- (220) Scimemi A. Astrocytes and the Warning Signs of Intracerebral Hemorrhagic Stroke. *Neural Plast* 2018;2018:10.1155/2018/7301623.
- (221) Shackelford C, Long G, Wolf J, Okerberg C, Herbert R. Qualitative and Quantitative Analysis of Nonneoplastic Lesions in Toxicology Studies. *Toxicol Pathol* 2002 01/01; 2017/11;30(1):93-96.
- (222) Detre S, Saclani Jotti G, Dowsett M. A "quickscore" method for immunohistochemical semiquantitation: validation for oestrogen receptor in breast carcinomas. *J Clin Pathol* 1995 BMJ Publishing Group Ltd and Association of Clinical Pathologists;48(9):876-878.
- (223) Fedchenko N, Reifenrath J. Different approaches for interpretation and reporting of immunohistochemistry analysis results in the bone tissue: a review. *Diagnostic Pathology* 2014 11/29;9(1):221.
- (224) Wang JT, Medress ZA, Barres BA. Axon degeneration: Molecular mechanisms of a self-destruction pathway. *J Cell Biol* 2012 Jan 9;196(1):7-18.
- (225) Obermeier B, Daneman R, Ransohoff RM. Development, maintenance and disruption of the blood-brain barrier. *Nat Med* 2013 Dec;19(12):1584-1596.